# A rabbit phantom study to reduce neonatal radiation dose without compromising image quality.

Anita Erasmus

*Submitted in fulfilment of the requirements in respect of the M.Med.Sc degree qualification in the Department of Medical Physics*
*In the Faculty of Health Sciences*
*At the University of the Free State*

Supervisor: Prof C.P. Herbst

February 2015

# DEDICATION

This dissertation is dedicated to my parents; I honour you for your support and loving care.

# DECLARATION

1. I, Anita Erasmus declare that the master's research dissertation or publishable, interrelated articles that I herewith submit at the University of the Free State, is my independent work and that I have not previously submitted it for a qualification at another institution of higher education.

2. I, Anita Erasmus hereby declare that I am aware that the copyright is vested in the University of the Free State.

3. I, Anita Erasmus hereby declare that all royalties as regards intellectual property that was developed during the course of and/or in connection with the study at the University of the Free State, will accrue to the University.

4. I, Anita Erasmus hereby declare that I am aware that the research may only be published with the dean's approval.

…………………………………………………………….

Date: February 2015

# ACKNOWLEDGEMENTS

My supervisor Prof Herbst – thank you for the support, guidance and endless hours of input and discussion. I learned valuable lessons during this project.

I thank Universitas Hospital for allowing me to conduct the study in the hospital.

I thank the staff at the Department of Clinical Imaging Science for their assistance with the positioning and imaging of the phantoms and evaluation of images.

I thank the Head of the Department of Clinical Imaging Science for allowing me to use the equipment, together with the expert observers for the time spent evaluating the images.

I thank all my dear friends whom helped me with editorial matters and proof reading.

I thank my husband and family for their continuous support and motivation.

# PRESENTATIONS ARISING FROM THIS STUDY

| | | |
|---|---|---|
| A Phantom study to reduce neonatal dose without compromising image quality. | **European Congress of Radiology, Vienna, Austria** | 4 – 8 March 2014 |
| A Phantom study to reduce neonatal dose without compromising image quality. | **Faculty Research Forum, Medical Faculty, University of the Free State** | 28 - 29 August 2014 |

# TABLE OF CONTENTS

# LIST OF FIGURES

*The figures listed below were specifically drawn by the researcher for explanatory purposes. This was not the case for figures with references.*

# LIST OF TABLES

# Acronyms and Abbreviations

| | |
|---|---|
| 2-AFC | Two alternative forced choice |
| AEC | Automatic exposure control |
| Al | Aluminium |
| ALARA | As low as reasonably achievable |
| AP | Anterior-posterior |
| AUC | Area under the curve |
| CNR | Contrast to noise ratio |
| CR | Computed radiography |
| Cu | Copper |
| DAP | Dose area product |
| DQE | Detective quantum efficiency |
| DRLs | Diagnostic reference levels |
| EC | European Commission |
| ED | Effective dose |
| ESD | Entrance surface dose |
| ESE | Entrance surface exposure |
| FDD | Focus to detector distance |
| FSD | Focus to skin distance |
| GSDF | Grey scale display function |
| Gy | Gray, unit of absorbed dose |
| $H_T$ | Equivalent dose |

| | |
|---|---|
| HVS | Human visual system |
| ICC | Intra class correlation coefficient |
| IP | Imaging plate |
| ICRP | International Commission on Radiation Protection |
| ICRU | International commission on Radiological Units |
| IPEM | Institute of Physics and Engineering in Medicine |
| ISL | Inverse square law correction |
| KAP | Kerma air product |
| kV | Tube voltage setting |
| lp/mm | Line pairs per millimetre |
| mAs | milliampere-second |
| mR | milli-roentgen |
| MTF | Modulation transfer function |
| NICU | Neonatal intensive care unit |
| NPS | Noise power spectrum |
| PACS | Picture archive and communication system |
| QC | Quality control |
| RAP | Roentgen air product |
| ROC | Receiver operating characteristics |
| SF | Screen film |
| SFS | Spatial frequency spectrum |
| SNR | Signal to noise ratio |

| | |
|---|---|
| SSD | Source to surface distance |
| TLD | Thermoluminescent dosimeter |
| VGA | Visual grading analysis |
| WL | Window level |
| $W_R$ | Radiation weighting factor |
| $W_T$ | Tissue weighting factor |
| WW | Window width |

# *CHAPTER 1*

# *DOSE CONSIDERATONS IN NEONATAL RADIOGRAPHY*

---

## 1.1 INTRODUCTION

Neonates, especially those born prematurely, often suffer from respiratory and cardiovascular complications and therefore require intensive care and long periods of hospitalization.

Radiography plays an important role in diagnosis and management of hospitalized neonates. Radiographs of neonates who are ill at birth may be taken daily, for a few weeks after birth to assess the progress of disease, response to treatment, or in the case of respiratory illness to assess the placement of endotracheal tubes and intravenous lines.

X-rays fall into the category of ionizing radiation which has the potential to cause cell damage and therefore are associated with a radiation risk. The radiation risk to these neonates is higher than in adults as their cells are more radiosensitive and they have a longer life expectancy and thus a longer period for the expression of malignancies, such as leukaemia (Boice, 1998). Children have smaller body diameters compared to adults, thus less attenuation of x-rays are achieved by overlying tissue and therefore their internal organs will receive a higher dose than those of an adult (*UNSCEAR 2013 Report*).

Although there is a radiation risk associated with x-ray images, McParland et al. (1996) found that the calculated risk of childhood cancer from a single radiograph is low compared to the other medical risks these neonates face. According to Blencowe et al. (2012) premature births are regarded as the second largest cause of death in children younger than 5 years of age. Velaphi and Rhoda (2012) indicated that the South African neonatal mortality rate is 14/1000. The benefit of proper diagnosis and good disease management in neonatal radiography, that might improve the life expectancy of these ill neonates, outweighs the risk of receiving the radiation exposure. However, considering the number of radiographs that neonates might receive during their stay in the Neonatal Intensive Care Unit (NICU), dose optimization studies are necessary.

The number of radiographic examinations per neonate depends on the clinical judgement of the physician and can be influenced by various factors such as gestational age, birth weight and medical condition (Datz et al., 2008). A study by Ono et al. (2003) showed that neonates with a low gestational age and low birth weight (less than 1000g) require a longer NICU stay and often more frequent x-ray examinations.

Optimization refers to the process where radiological images of the highest quality are obtained at the lowest dose to the patient. This is in line with the As Low As Reasonably Achievable (ALARA) principle which describes a balance between patient dose and image quality (Willis, 2009). It should however be noted that there is a difference between the highest image quality that can be achieved and diagnostically acceptable image quality. Diagnostically acceptable image quality should be the aim.

Knowledge of the radiation dose received by the patient is the first step in a dose and image quality optimization process. Entrance surface dose (ESD) is often used as an indicator of patient dose. The selection of exposure parameters (also referred to as beam parameters) such as tube voltage (kV), tube current-time product (mAs) and filtration will affect the ESD. According to Honey et al. (2005) an optimization study should investigate kV selection and receptor dose required to achieve the minimum acceptable level of image quality. Adjusting the beam parameters will affect the image quality, therefore image quality and dose cannot be investigated in isolation.

Image quality can be affected by physical factors such as resolution, noise and contrast. Diagnostic image quality is to a large extent subjective and depends also on observer preference. This presents a difficult task when evaluating image quality in the clinical setting as both physical parameters and observer preference should be taken into consideration to determine diagnostically acceptable image quality.

Digital detectors, such as CR, allow the manipulation of the acquired image by adjusting the window width (WW) and level (WL) as well as mathematical histogram manipulation to change the gray scale appearance of the image. This gives an advantage over conventional screen film (SF) as image contrast is not solely related to subject contrast. The image can be acquired over a wide range of exposure levels without appearing overexposed or underexposed. This allows the use of beam parameter combinations not used with SF. With this advantage comes the difficult task of deciding which parameters should be used for a certain type of clinical examination.

The European Commission (EC) has given recommendations regarding the kV range and filter combinations for neonatal radiography (European Commission, 1996). A study by Frayre et al. (2012) indicated the wide variations in imaging parameter selection used for neonatal radiography within an institution, leading to a large variation in dose to the patient. This emphasizes the need for dose and image quality optimisation.

The aim of this phantom study was to reduce neonatal radiation dose while maintaining diagnostically adequate image quality for neonatal radiography. In an attempt to identify the most suitable parameters for clinical use the influence of different imaging parameter combinations on diagnostic image quality will be investigated.

# *CHAPTER 2*

# *BIOLOGICAL EFFECTS AND RADIATION DOSE*

## 2.1 INTRODUCTION

Radiography refers to the imaging of body parts using x-rays and plays an important role in the diagnosis and follow-up of patients suffering from various medical conditions. X-rays interact with tissue and may cause biological changes and are therefore associated with a radiation risk. According to the International Commission for Radiological Protection (ICRP), the radiation risk can be classified into deterministic and stochastic effects (ICRP, 2007).

Deterministic effects are harmful tissue effects such as skin erythema, hair loss and cataracts caused by cell malfunction or death. These effects occur after a certain threshold value has been reached. Deterministic effects are associated with a threshold value since radiation damage to a number of cells needs to occur before a clinically relevant injury is observed. The severity of these effects that may include cell malfunction or cell death, increases with increased radiation dose above the threshold.

Skin effects, such as early transient erythema, will be seen within a few hours after the threshold dose has been reached. According to Koenig et al. (2001), no skin effects are expected below the threshold value of 2 Gy i.e. 2000 mGy.  Furthermore, the ICRP reports that in the absorbed dose range up to 100 mGy no clinical relevant functional impairment of tissue is expected (ICRP, 2007). Therefore deterministic effects are not expected in general neonatal radiography, with recommended skin doses below 80 µGy (European Commission, 1996).

Stochastic effects, unlike deterministic effects can occur at any radiation dose. Radiation has the ability to cause complex DNA damage (DNA double strand breaks) which cells struggle to repair. This leads to mutation of cells which can present as cancer (mutation of somatic cells) or hereditary effects (mutation of reproductive cells). The radiation protection recommendations of the ICRP are based on the linear-non-threshold dose-response mode. According to this model, the assumption is made that even at doses below 100 mSv the probability of stochastic effects are proportional to the radiation dose (ICRP, 2007).

Although the dose per neonatal x-ray examination is low, neonates are often exposed to a large number of radiographic examinations. Therefore although we are not concerned about deterministic effects in neonatal radiography, the possibility of stochastic effects remains. As pointed out earlier neonates have rapidly dividing cells and they have a longer life expectancy, once cured, therefore a longer period for the expression of stochastic effects such as cancer to occur. It is thus important to keep the radiation dose per x-ray examination as low as reasonably achievable.

Although there is a risk associated with radiation, according to Lawn et al. 2005, neonatal mortality accounts for 40 % of deaths in children under the age of 5, therefore the benefit of receiving medical treatment and the possibility of surviving the medical complications greatly outweighs the risk of radiation exposure. However, to be able to adhere to the ALARA principle and compare the dose per x-ray examination to guidelines, the radiation dose per x-ray examination should be known.

The dose per examination is dependent on beam parameter selection as well as patient and geometrical factors such as position of x-ray field on the patient, the size of the x-ray field and the thickness and composition of the tissue in the area of interest.

Various dose metrics have been used to estimate the radiation dose to the patient. Detailed discussion of these dose metrics can be found in a number of handbooks (IAEA, 2014; Bushberg et al., 2011; Dendy & Heaton, 1999; Meredith and Massey, 1977). In the following section only the most relevant dose related quantities, of importance in this investigation will be discussed, namely absorbed dose, effective dose (ED) and ESD, see figure 2-1.

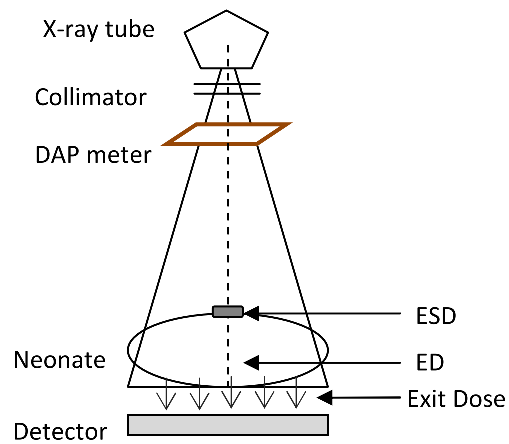


***Figure 2-1: Schematic representation of the dose related quantities.***

Absorbed dose, in units of joule/kg or gray (Gy), is defined as the ratio of the imparted energy (Joule) per mass (kg) of any material. The absorbed dose therefore gives an indication of the amount of energy deposited in matter. Absorbed dose however, does not give an indication of the amount of tissue exposed. The absorbed dose will remain the same regardless of the x-ray field size selected (if the imaging parameters do not change).

It can be difficult to calculate the absorbed dose, without the use of specialized computer programs, taking into consideration that tissue is not homogeneous and organs are located at different depths. The absorbed also dose does not take into consideration that the biological damage varies according to the radiation type as well as the tissue sensitivity. Therefore other dose metrics are needed.

The equivalent dose ($H_T$) takes into account that different types of radiation produce different biological damage per unit absorbed dose. $H_T$ can be obtained by multiplying the absorbed dose with a radiation weighting factor ($w_R$) which takes into account the relative biological effectiveness of the radiation type to that of x-ray photons. This is most applicable in the case of radiation by charged particles. In radiology the equivalent dose will be the same as the absorbed dose, as $w_R = 1$, for photons of all energies.

The ED gives a complete description of the stochastic risk to a generic patient, taking into consideration that tissue varies in sensitivity to radiation. This is achieved using organ specific tissue weighting factors ($w_T$) listed in the ICRP report (ICRP, 2007). ED from x-ray exposure can be determined using equation 2-1 (Bushberg et al., 2011).

$$E(Sv) = \sum_{T} w_T \times H_T(Sv) \qquad [2\text{-}1]$$

ED can be used for risk estimation as the ED gives an indication of organ doses. However the ICRP report recommends that the ED should be used with caution, it should be noted that ED is aimed at comparing doses received by a population (ICRP, 2007). ED gives an indication of the dose to a reference person and not an individual. ED is not age, anatomical or physiologically specific and ED should only be used to compare diagnostic procedures if the patients are similar regarding age and gender. Although ED can sufficiently estimate the risk of radiological exams in adult patients, according to Wall (1996) it can underestimate the risk to paediatric patients by up to a factor of two.

The ESD defined as the absorbed dose at the point of intersection of the x-ray beam axis with the entrance surface of the patient, including backscattered radiation (Smans et al., 2008) can be used as input value for ED calculations in the place of the absorbed dose. If the risk needs to be calculated the ESD can be multiplied by the appropriate conversion factor to obtain the ED. These conversion factors can be obtained from Monte Carlo simulations. The commercially available PCMXC software developed by Servomaa and Tapiovaara (1998) can be used to calculate organ and effective doses in neonatal radiography. More information regarding this method can be found in the studies by Olgar et al. 2008, Smans et al. 2008 and Dabin et al. 2014.

The ESD is relatively easy to measure in routine practice and is often used in dose optimization studies to compare x-ray exposures for a certain type of examination when the beam area and the part of the patient being exposed are assumed to remain constant. The ESD, similar to absorbed dose, does however not give an indication of the biological risk associated with radiation field size used. The larger the radiation field size, the larger the number of cells included in the radiation field, thus the larger the possibility of a biological effect occurring due to radiation interacting with a single cell. The Dose Area Product (DAP) is useful in this regard, as it gives an indication of the radiation dose to a specific area.

The beam area is determined by the collimation applied by the radiographer. Collimation is of particular importance in neonatal imaging as the neonates are small and their organs are situated close together leading to an increase in effective dose. A study by Schneider et al. (1998) showed that an increase of 1 cm at upper- and lower field margins of 6 $cm^2$ field can increase the dose received by neonates with 33 %. Phantom simulations by Dabin et al. (2014) indicated that a field shift of 1 – 2 cm can lead to a seven-fold dose increase as organs supposed to be outside the field might be included. Collimation aids in the reduction of tissue volume exposed to radiation; it does not reduce the dose to the exposed volume. However as mentioned, keeping the beam area smaller can also aid to reduce the number of cells with which radiation can interact and cause biological damage.

Although collimation can indirectly influence the dose to the patient it is a variable that cannot easily be controlled and will not be considered in this study. The physical factors influencing the patient dose and which can easily be controlled, namely; time current product, tube potential and filtration will be discussed in more detail in the section to follow.

## 2.2 PHYSICAL FACTORS INFLUENCING RADIATION DOSE

### *2.2.1 Time Current Product*

A current is applied to the x-ray tube cathode, see Figure 2-2, allowing electrons to be released through thermionic emission. These electrons are accelerated towards the target and then interact with the target to produce x-rays. The tube current, measured in milli-amperes (mA), refers to the rate of electron flow from the cathode to the target. The product of the tube current and exposure time are considered an entity referred to as the time-current-product (mAs). For a more detailed discussion on x-ray generation refer to Bushberg et al. (2011).

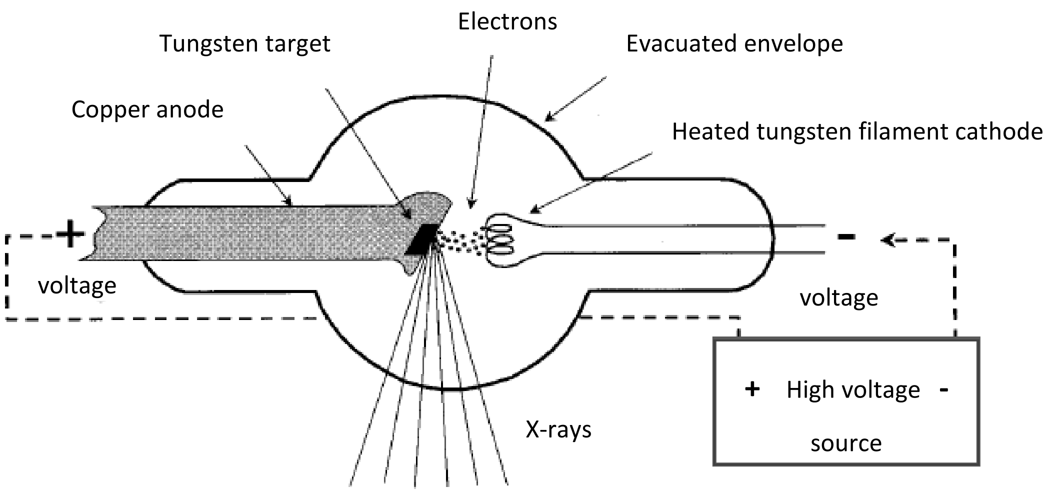


***Figure 2-2: Minimum components of an x-ray tube (Bushberg et al., 2001).***

Increasing the mAs will increase the number of electrons interacting with the target and thus increase the quantity of photons produced. The energy of the photons also referred to as the quality of the radiation is unaffected by the tube current.

The beam output typically measured in milli-roentgen (mR) is proportional to the mAs, keeping all other parameters constant. Increasing the tube current will proportionally increase the dose to the patient, unless other parameters are adjusted to compensate for the increase in photon quantity.

A certain quantity of photons is required to form an image of diagnostic quality. The quantity will depend on the attenuation of x-rays by the patient as well as the detector characteristics. If an inadequate number of photons are detected the image will appear grainy, this might influence the image quality to such an extent that the image is regarded as unacceptable for the diagnostic task. Therefore appropriate mAs selection is needed for each x-ray examination.

### *2.2.2 Tube Potential*

Tube potential, in units of kilovolt (kV), refers to the high voltage applied between the cathode and target of a glass vacuum tube used to produce x-rays. Electrons emitted from the heated filament are attracted to the target. These electrons acquire energy during their travel from the cathode to the target. The acquired energy is equal to the product of the charge of the electrons and the applied voltage difference between the filament and the target.

Electrons are brought to rest by the target and the acquired energy is converted into other forms of energy, such as heat and x-ray photons. The heat capacity of the anode limits both the current that can be selected and the total amount of x-rays generated. The x-ray spectrum, see Figure 2-3, has two distinct parts; the continuous spectrum, containing all the energies from the maximum energy (applied voltage) downwards and the characteristic spectrum, which depends on the anode material.

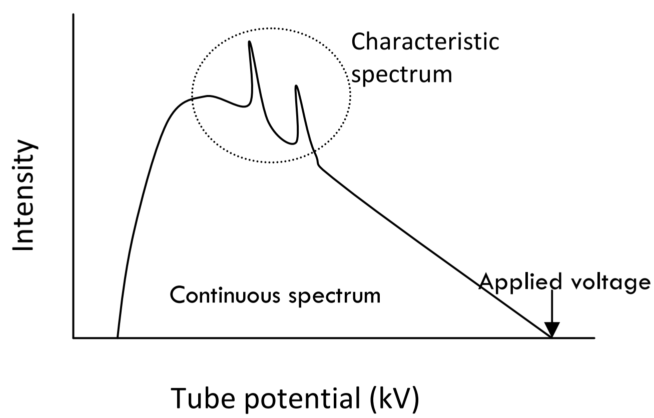


***Figure 2-3: Schematic of the X-ray spectrum produced by electron interactions with the target.***

Changes in the applied voltage will alter the spectrum. If a higher voltage is applied the maximum photon energy, determining the quality of the beam, will increase and the beam will become more penetrating. In addition the efficiency of photon production will increase and therefore the quantity (intensity) of photons will also increase. Therefore using a higher kV technique allows the mAs to be reduced, rendering a lower patient dose. According to Dendy and Heaton (1999) at 70 kV a 10 kV increase will allow the mAs to be approximately halved. The mAs, as mentioned in the previous section, is proportional to the patient dose and therefore the patient dose will approximately be halved with a 10 kV increase. It should however be kept in mind that an increase in kV might degrade image quality due to a loss in contrast (refer to Section 3.2.2 for a discussion on contrast).

### *2.2.3 Filtration*

Filtration refers to the removal of x-rays as the beam passes through a layer of material. Filtration can be categorised into either inherent filtration, usually the glass tube window, collimation assembly and housing oil that can remove x-rays below 15 keV (Bushberg et al., 2011) or additional filtration from metal sheets intentionally placed in the beam. Additional filtration can be installed on any system; however it is important that the tube output should be adequate otherwise exposure time will be too long, which can lead to patient motion artefacts.

The purpose of additional filtration is to attenuate the low energy x-rays in the spectrum unable to penetrate through the patient. A large portion of the diagnostic X-ray spectrum consists of radiation with energy of 20 keV or less with a linear attenuation coefficient in soft tissue of approximately 0.7 $cm^{-1}$, thus only 0.3 % of the photons will penetrate through 10 cm of tissue (Meredith and Massey, 1977). The energy from these low energy photons will be absorbed in the tissue and contribute to patient dose. An ideal filter should therefore remove the unwanted low energy radiation, whilst having a small effect on the high energy part of the spectrum, see Figure 2.4.

This is achieved through the photoelectric effect where the incident photon energy is absorbed within the filter material and transferred to an electron which is then ejected from the atom. A detailed description of the photoelectric effect is given by Bushberg et al. (2011). The probability of photoelectric absorption increases with atomic number. It is therefore important that the filter material should have an adequately high atomic number. The filter material should also not have an absorption edge close to that of the useful (desired) photon energies. Photons below the absorption edge are transmitted more readily than those with energies slightly higher than the absorption edge, which might cause unwanted energies to pass through the filter while desired energies are absorbed. This is not favourable as the purpose of the filter is to remove the unwanted low energies.

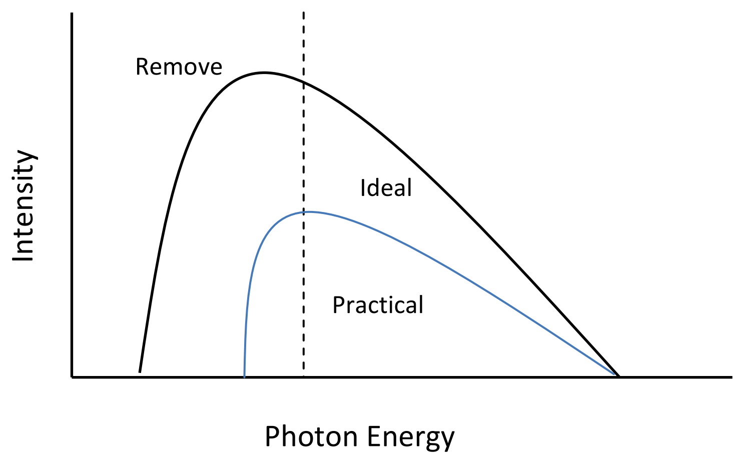


***Figure 2-4: Schematic representation of the ideal and practical filter.***

Aluminium (Al) and Copper (Cu) are regarded as suitable filter materials in the diagnostic X-ray energy range, especially when used in combination. Al (Z = 13) has a considerable photo electric effect below 50 keV with its K absorption edge at approximately 1.6 keV. No backing filter is required when using Al filtration as the characteristic radiation is readily absorbed in air. Al does however not provide full filtering at energies higher than 60 keV due to its low atomic number. Cu has a higher atomic number (Z = 29) compared to Al and a K edge at 9 keV. Cu is regarded as a suitable filter in the diagnostic energy range of 60 keV upward. Aluminium is often used in combination with Copper and acts as a backing filter to remove the unwanted low energy characteristic photons.

A filter will affect photons of all energies, by reducing the intensity of the beam and removing the unwanted low energy radiation. Beam filtration thus reduces the photon intensity and increases the beam quality, therefore making filtration an important factor to consider for dose reduction studies. Increasing the thickness of the filter material will increase the quality of the beam and decrease the intensity, however beyond a certain filtration thickness no increase in beam quality will occur, although the intensity will keep on decreasing. Highly filtered beams will require higher mAs settings compared to lightly filtered beams to achieve a particular x-ray intensity. This was demonstrated by Bushberg et al. (2011), using a 10 cm PMMA phantom with 2 mm Al and 0 mm Al filtration, and a selected 60 kV. 5 mAs was required compared to 3.8 mAs to achieve the same signal at 2 mm Al and 0 mm Al respectively with a dose reduction of approximately 30 % for the additional filtration, 2 mm Al, even though a higher mAs was used.

### *2.2.4 Combination of Effects*

The physical factors influencing radiation dose should not be investigated in isolation as these factors in combination have an effect on patient dose and image quality. Imaging parameters should be selected to keep the dose to the patient as low as possible without compromising the diagnostic value of the image. A reduction in mAs will reduce the dose proportionally; however a reduction in the number of photons reaching the detector will influence the image quality. As mentioned in Section 2.2.2 higher kV techniques can lead to a possible ESD reduction if the mAs is adjusted accordingly.

Similar to ESD used as a measure to quantify patient dose, exit dose is often used to describe optimal detector exposure. When using SF it was important to keep the exit dose constant in order to achieve optimal detector blackening everytime, ensuring that the film was not over- or under exposed. This was often achieved using automatic exposure control (AEC), detailed discussion is given by Bushberg et al. (2011). Mobile general x-ray units used for neonatal radiography are usually not equipped with AEC capabilities, therefore optimal manual beam parameters selection is required.

Various beam parameter combinations with the focus on dose reduction, have been recommended for neonatal radiography. Dougeni et al. (2007) suggested that the use of higher tube voltages could result in neonatal dose reduction without image quality degradation; they found the visibility of endotracheal tubes, catheters and long lines acceptable in the range between 44 – 66 kV and 0.5 – 2.5 mAs.

Smans et al. (2010a) showed a neonatal lung dose reduction of approximately 25 % when using 60 kV with additional filtration of 0.2 mm Cu + 1 mm Al. Seifert et al. (1998) found that at 66 kV with additional filter of 0.1mm Cu + 1mm Al the dose could be decreased by approximately 40 % with a minimal decrease in contrast. Wraith et al. (1995) found a similar dose reduction of 25 – 50 %, depending on the neonatal weight group, when using 60 kV and additional filtration of 2.5 – 3.5mm Al.

Hansson et al. (2005) recommended 90 kV when using Fuji FCR 5000 standard plates (Fuji Photo Film, Tokyo, Japan) as the optimal setting for digital neonatal chest radiography.

The large variation in proposed kV and mAs settings emphasizes the need for each institution to perform optimization of imaging parameters to fit their image requirements at the lowest possible dose to the patient. Different parameter combinations are selected for different anatomical areas based on the thickness of the anatomy and the image quality requirements, including factors such as contrast and noise which will be discussed in the next chapter.

The following examples illustrate the different beam parameters selected for different examinations. The beam parameters; 117 kV and 12.5 mAs and 109 kV and 3.2 mAs are used, at UAH, for a lateral and a PA adult chest x-ray examinations respectively. A higher kV is required to compensate for the larger thickness of the lateral chest compared to the PA chest and still render the same apparent contrast. A higher mAs is also required, to compensate for the increased attenuation of photons due to the increased tissue thickness to ensure that an adequate quantity of photons reach the detector.

A low kV technique is used for an AP hand to prevent over penetration of the tissue as well as increased scatter associated with higher kV techniques in order to maintain adequate contrast between the tissue and bone. The following beam parameters; 46 kV and 4.0 mAs, are used at UAH for an AP hand examination. Note that the mAs used for a AP hand, which is thinner than a PA chest examination, is almost the same as the mAs used for a PA chest, this can be explained by the kV that does not only influence the energy of the photons, but also the number of photons and therefore a higher kV can be used in combination with a lower mAs as discussed in Section 2.2.2. The mAs selection of the hand preserves the fine detail of the metacarpal and phalangeal bones by limiting the noise in the image.

The European Commission, (1996) recommends the use of 60 – 65 kV and 0.1 mm Cu + 1 mm Al additional filtration for neonatal AP chest examinations. The mAs should be determined by the institution. The patient radiation dose can be decreased by optimizing the beam parameters; kV, mAs and filtration. Dose measurements are required to evaluate and monitor the dose to the patient.

## 2.3 DOSE MEASUREMENT

There are several dose related quantities; however only ESD will be considered for dose comparison purpose of neonatal chest x-rays examinations. ESD can be determined by direct measurement using thermoluminescent dosimeters (TLDs) placed directly on the skin surface of the patient during radiographic examination, or by indirect measurement using the tube output measurements. These methods will be discussed in the following sections.

### *2.3.1 Dose Estimation using Tube Output Measurements*

Tube output measurements form part of routine quality control making this method a convenient indirect method to calculate ESD. As discussed by Wraith et al. (1995) the tube output at a constant mAs and known focal spot to detector distance can be measured using an ionization chamber, for a range of kV values. These measurements can then be used to calculate the ESD, using the following equation 2-2.

$$ESD = U\left(\mu Gy.mAs^{-1}\right) \times mAs \times BSF \times ISL \times \left(\frac{\mu_{en}}{\rho}\right)_{Air}^{Tis} \qquad [2\text{-}2]$$

Where U is the x-ray tube output measured with an ionization chamber at a constant focus to detector distance (FDD) for a range of kV values, mAs refers to the time-current-product used during the examination. BSF is the back scatter factor taking into account scatter radiation from the patient that will contribute to the dose at the surface. The International Commission on Radiation Units & Measurements (ICRU) listed BSF for a range of kV values at different filtration and field size options (ICRU, 2005). The recommended BSF 1.27, simulated for a 30 cm x 30 cm x 15 cm water phantom, at 60 kV, 2.5 mm Al and a 20 cm x 20 cm field is however not appropriate for neonatal imaging as this is an overestimation of the scatter contribution. A BSF of 1.1 estimated by Chapple et al. (1994) for a 5 cm thick phantom in the energy range 50 - 70 kV and used since for ESD calculations in neonatal radiography by McParland et al. (1996), Armpilia et al. (2002), Olgar et al. (2008) and Faghihi et al. (2012) was considered appropriate for use in this study as it closely approximate neonatal thickness and energy range.

The inverse square law (ISL) correction, takes into account that the distance at which the tube output was measured might differ from the clinically used focus to skin distance (FSD). The ratio of the mass energy absorption coefficient of tissue over air $\left(\frac{\mu_{en}}{\rho}\right)_{Air}^{Tis}$ is used to convert the exposure measurement in air to a measurement in tissue, Chapple et al. (1994) proposed a value of 1.05 used by various researchers such as McParland et al. (1996), Olgar et al. (2008) and Faghihi et al. (2012).

### *2.3.2 Dose Area Product Measurements*

DAP measurements is another indirect method that can be used to determine the ESD delivered during an x-ray procedure, a detailed description is given by Bushberg et al. (2011). DAP measurements are performed using an ionization chamber transparent to x-rays attached to the diaphragm of the x-ray tube. Various acronyms such as dose-area-product, kerma-area-product (KAP) and roentgen-area-product (RAP) have been used to describe these systems. The DAP meters typically reports tube output in units of mGy - cm$^2$. If the exposed skin area (in cm$^2$) is known the skin dose can be estimated by dividing the DAP meter reading with the known exposed skin area.

DAP meter readings are convenient to use in the calculation of ESD, if the field size is known, as the measurements are easily obtained and independant of the setup. It can also be used to compare studies, calculate effective dose and set up dose reference levels (DRLs).

DAP meter readings are not only dose dependant but also depends on the irradiated area, therefore variations in selected field size will be reflected in the DAP reading. Although DAP meters are required for fluoroscopic units, these meters are not a standard requirement for x-ray units especially mobile x-ray units.

ESD for neonatal radiography, using DAP meters have been performed by Lowe et al. (1999), Dougeni et al. (2007) as well as Smans et al. (2008) and Borisova et al. (2008).

In a study by Lowe et al. (1999) some of the neonatal patient doses could not be determined because the DAP meter was operating at its minimum limit. Dougeni et al. (2007) described a correction method used, in an effort to obtain better accuracy measuring neonatal doses at the lower level of detectability of the DAP meter.

### *2.3.3 Thermoluminescent Dosimeters*

TLDs are inorganic scintillation discs with a diameter of approximately 5 mm that can be placed onto the skin of the patients to measure ESD directly. These disks are transparent to x-rays and take the back scatter contribution to surface dose into account as it is placed directly onto the patient skin inside the x-ray field.

When exposed to ionising radiation electrons become trapped in the scintillator in an excited state. The scintillator can later be heated (in a TLD reader), causing the electrons to fall to their ground state with the emission of light proportional to the energy absorbed by the TLD. After the light information from the TLD had been registered, the TLD could be annealed in a process that would empty the electron traps still populated by electrons. Subsequently the TLD may be reused.

TLDs are made from materials with an effective atomic number close to that of tissue, such as Lithium fluoride (LiF). Therefore dose to the TLD is closely related to the tissue dose. LiF TLD's have a wide dose response; ranging from 10 µSv - $10^3$ Sv (Bushberg et al., 2001). In a study to compare doses delivered from two radiographic techniques Jones et al. (2001) indicated that LiF TLDs were not suitable for neonatal dosimetry due to the minimum detectable dose of approximately 100 µGy.

LiF:Mg,Ti, also known as TLD-100 was used by Seifert et al. (1998), Borisova et al. (2008), Olgar et al. (2008) and Faghihi et al. (2012) to measure neonatal ESD. Although Seifert et al. (1998) indicated that they were able to measure doses below 50 µGy, Borisova et al. (2008) indicated that TLD-100 was found not to be sensitive enough for doses below 50 µGy.

LiF:Mg,Cu,P TLDs have been used and proved suitable for neonatal dosimetry, as these TLDs are more sensitive than conventional LiF TLDs in the dose range below 50 µGy. More information can be obtained from work done by Duggan et al. (1999), Armpilia et al. (2002) and Smans et al. (2008).

A disadvantage of TLDs is that the accumulated dose is not immediately indicated, but a lengthy readout process needs to be followed. Another disadvantage is the labour intensive calibration. The TLDs need to firstly be calibrated by exposure to a known dose and the light emitted during readout should be correlated to the given dose. This can be obtained by setting up a calibration curve. Care should be taken to minimize the error in these steps as this contributes to the sensitivity with which dose can be estimated. The TLDs are then grouped based on their response to ensure that all the disks in a group will have a comparable dose response.

Although dose measurements using TLDs are regarded as a good indication of clinical practice it is often not practical to use as the direct placement onto the skin can be in violation of the infection policies of the NICU. Also disturbance of neonates should be avoided if possible as this can cause an increase in heart rate and blood pressure.

### 2.3.4 *Gafchromic Film*

Gafchromic film, similar to TLDs, may be used for direct measurement of dose. Gafchromic film also referred to as radiochromic film, is a self-developing film sensitive to radiation in a specific energy and dose range. When exposed to radiation the film changes colour, the magnitude of colour change is proportional to the dose given to the film.

These films are convenient to use in dosimetry applications as the film is insensitive to ambient light, water resistant, do not require chemical processing which may be prone to artefacts, and the film can be cut into smaller pieces as needed. A disadvantage is that these films need to be calibrated every time a new batch is received, which can be a lengthy process.

Different radiochromic films have been developed for applications in Radiotherapy and Radiology. GAFCHROMIC® EBT film has been used to measure the dose distribution in paediatric head CT examinations (Gotanda, 2008). The EBT film, designed for dosimetry measurements in radiotherapy, is sensitive in the dose range 1 cGy to 800 cGy. This study highlighted the need to select the radiochromic film according to the appropriate dose range expected in a study.

The radiology based product line includes films specially designed for use in Computed Tomography, Mammography and Interventional Radiology. GAFCHROMIC® XRQA2 film designed for quality control in the radiology environment is recommended for use in the energy range 20 kV – 200 kV and dose range 0.1 cGy – 20 cGy. XRQA2 were found to be an effective dosimetry method in the fluoroscopic dose range by both Barrera-Rico et al. (2012) and Soliman and Alenezi (2013) in studies performed to estimate the ESD of patient undergoing fluoroscopic procedures. XRQA2 have also been used in CT dosimetry studies by Loader et al., (2012). Tomic et al. (2014) found XR-QA2 GafChromic™ film to be accompanied by a pronounced energy dependent response for beam qualities in the diagnostic x-ray range.

Radiochromic film, although used for various dosimetry applications in radiology, was regarded not sensitive enough for use in neonatal general radiography applications with an expected dose range below 0.01 cGy.

### *2.3.5 Preferred Method for Neonatal Dose Measurements*

Although ESD determined from direct TLD measurements are regarded as the gold standard, as mentioned in Section 2.3.3, the lowest detection limit of LiF:Mg,Ti TLDs are in the order of the expected ESD for neonatal radiography. LiF:Mg,Cu,P have however been used successfully in neonatal dosimetry. TLDs are not available at our institution and were not considered for ESD estimation. The high initial setup cost, laborious calibration process together with the infection risk from placement of TLDs on the skin surface of fragile neonates, was regarded unnecessary with alternative dosimetry methods available.

GAFCHROMIC® XRQA2 film recommended for use in the energy range 20 – 200 kV and dose range 0.1 – 20 cGy, although sensitive in the neonatal energy range of 50 – 66 kV was considered not sensitive enough in the neonatal dose range below 0.01 cGy.

ESD can also be determined through an indirect method making use of tube output measurements. A study by Ono et al. (2003) indicated no significant differences between ESD determined using TLDs and ESD determined using tube output measurements. Routine tube output measurements described in Section 2.3.1 as well as DAP readings (Section 2.3.2) are convenient ways to determine ESD. The mobile x-ray equipment at our institution was not fitted with DAP meters. The sensitivity of most commercial DAP meters are above the expected neonatal ESD and will thus require further adjustments to the DAP meter. It was therefore decided not to determine the ESD from DAP meter measurements.

Therefore the preferred method for neonatal ESD determination in this study was tube output measurement as described by Wraith et al. (1995).

# *CHAPTER 3*

# *IMAGE QUALITY*

## 3.1 INTRODUCTION

Image quality is a generic concept that applies to different imaging modalities such as television, photography and medical imaging. The required image quality depends on the function of the image. The image quality in radiography should be such that an accurate diagnosis can be made from the image.

Image quality is influenced by two main steps before the image is available for interpretation by the radiologist, namely; (1) image acquisition and formation, (2) processing and display.

Image acquisition and formation is influenced by the attenuation characteristics of the tissue being imaged; x-rays are attenuated differently depending on the type of tissue it interacts with, resulting in primary image contrast. This primary information is captured onto a detector, which can either be screen film or a digital detector. The physical characteristics of the system such as; noise, resolution, and detective quantum efficiency also influence the first step.

Step two is influenced by image processing including the features of the display system and viewing environment, as well as observer performance and image quality preference. The quality of step one influence step two and therefore these two steps should both be evaluated when describing image quality.

Although it is possible to control some of the factors discussed above, it is difficult to control the observer performance and image quality preference i.e. the human component in the image quality chain.

As pointed out by Tapiovaara (2008), there are many different tasks that require the assessment of image quality such as (a) ensuring new equipment meet specifications, (b) ensuring that clinical needs are fulfilled and (c) optimization attempts. The type of assessment method, whether physical- or subjective image quality evaluation, will depend on the task. Calculating only physical image quality parameters might be adequate when comparing equipment or ensuring that equipment meet specifications. However, when performing dose optimization both physical factors and the observer preference should be considered. The following paragraphs will elaborate on these considerations and methods used to evaluate image quality.

## 3.2 PHYSICAL FACTORS INFLUENCING IMAGE QUALITY

Image quality is influenced by all the components in the imaging chain including; the beam parameters, detector characteristics, processing and display. The physical factors influencing image quality of radiographic images will be discussed in more detail in the following section.

### *3.2.1 Signal Intensity and Noise*

A radiographic image is formed when x-rays interact with the tissue of the patient, penetrates the tissue, reaches the detector and is displayed, see figure.

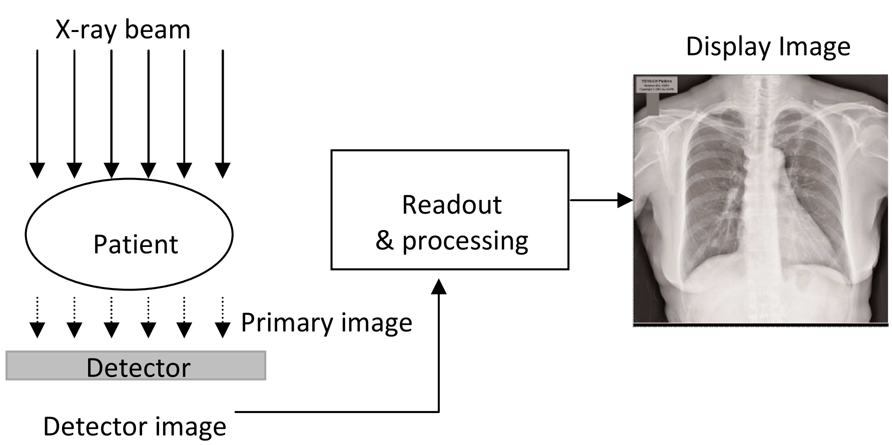


***Figure 3-1: Schematic representation of the image formation chain.***

The intensity of the x-ray beam falling onto the patient is decreased through a process called attenuation occurring within the tissue, the amount of attenuation depend on the tissue characteristics as well as the beam parameters (kV, mAs, filtration). The beam parameters are selected to take advantage of the attenuation characteristics of the tissue to form an image of varying gray scales. The intensity of the image will depend on the initial intensity of the beam falling onto the patient as well as the amount of attenuation in the body of the patient.

Noise in a radiographic image refers to information that is not useful for diagnosis of the patient's condition. According to Hendee and Ritenour (2003) noise refers to information that can interfere with the visualization of anatomical structures or pathology. Image noise can be described by the main causes of the noise that may include quantum noise, receptor noise, display noise and anatomical noise.

In general, the noise in an image will be related to the signal intensity of the image. The factors influencing the signal intensity and noise will therefore be discussed in the following section.

#### *3.2.1.1 Primary image*

The primary image refers to the information contained in the x-ray beam exiting the patient before reaching the detector. The signal intensity of the primary image is proportional to the number of photons penetrating the patient. If a large number of photons penetrate the patient the primary image will have a larger signal and less noise. This can either be achieved by increasing the mAs which is proportional to the number of photons in the x-ray beam or increasing the kV and /or using additional filtration and thereby increasing the penetrability of the x-ray beam.

Quantum noise is influenced by the number of photons in the primary beam that interacts with the detector and therefore the noise depends on the signal intensity of the primary image. The variation in the number of x-ray photons can be described by Poisson statistics. The noise can be obtained from the standard deviation ($\sigma$) of the mean number of photons per unit area (N).

The noise perceived by an observer is usually expressed as relative noise, given by equation 3-1.

$$\textit{Relative noise} = \frac{\sigma}{N} \qquad [3\text{-}1]$$

Using the formula it is possible to predict the noise in an image when the imaging parameters are adjusted. The noise is inversely related to the radiation dose. Thus as the dose decreases (N decreases) the noise increases. If less noise is present the image will have a smooth appearance.

As discussed in Section 2.2.4, if the energy of the x-ray photons is increased the mAs can be decreased to minimize the patient dose and still maintain images of acceptable quality. This is a direct result of the fact that more of the higher energy photons will penetrate through the patient to reach the film, as well as the fact that the image detector is often more sensitive for higher energy photons (see next paragraph). The reduction in mAs will lead to fewer photons reaching the detector, however the photons reaching the detector will be more energetic thus maintaining the total intensity in the beam notwithstanding a decrease in mAs. This decrease in the number of photons leads to more noise in the image. An increase in kV also increases the scatter contribution as the Compton Effect becomes the dominating process.

Although a theoretical increase in noise is postulated with dose reduction it does not necessarily mean that the increased noise will be visible to the radiologist. The amount of noise acceptable in an image will be determined by the function of the image as well as the preference of the radiologist.

In a study performed by Ravenel et al. (2001) investigating the possibility of CT dose reduction while maintaining diagnostically acceptable images, six observers were asked to rank CT images obtained at mAs values ranging between 40 – 280 mAs. Image quality deterioration caused by quantum noise was the main concern as the mAs was reduced. It was found that observers had difficulty to distinguish between the images generated at 160 mAs and 280 mAs. This shows the possibility of dose reduction. The above mentioned study demonstrated a certain level of noise in an image is acceptable as the aim is not to achieve the best quality image, but rather an image that is diagnostically acceptable. Keeping in line with the ALARA principle the dose must be reduced as low as reasonably achievable, while maintaining a confident diagnosis.

#### *3.2.1.2 Detector image*

The detector image, illustrated in Figure 3-1, is formed after the primary image falls onto the detector and the information is captured and stored within the detector. The information is then retrieved by chemical processing in SF or by laser light stimulation of the IP in CR. The information capture (i.e. the detection efficiency) depends on the detector thickness, density and composition. A thick detector will be able to absorb more information (attenuated x-ray photons) than a thin detector. A trade-off however exists between detection efficiency and resolution, see Section 3.2.3.

Detectors have different absorption characteristics depending on the composition, whether it is photo-stimulable phosphors (PSP) or rare-earth screens. The probability of an interaction increases just above the k-edge, an energy level characteristic to the detector material. Therefore the kV selection will have an influence on the detection efficiency. Plates with a k-edge at a higher energy will benefit from high kV techniques and vice versa. Figure 3-2 indicates the absorption fractions as a function of beam energy for different detector compositions. The Agfa CR plates currently used at UAH is made of BaF ($Br_{0.85}I_{0.15}$) with a characteristic k-edge at 37 keV compared to rare earth screens used in SF radiography, such as $Gd_2O_2S$ with a k-edge at 50 keV (Honey et al., 2005).

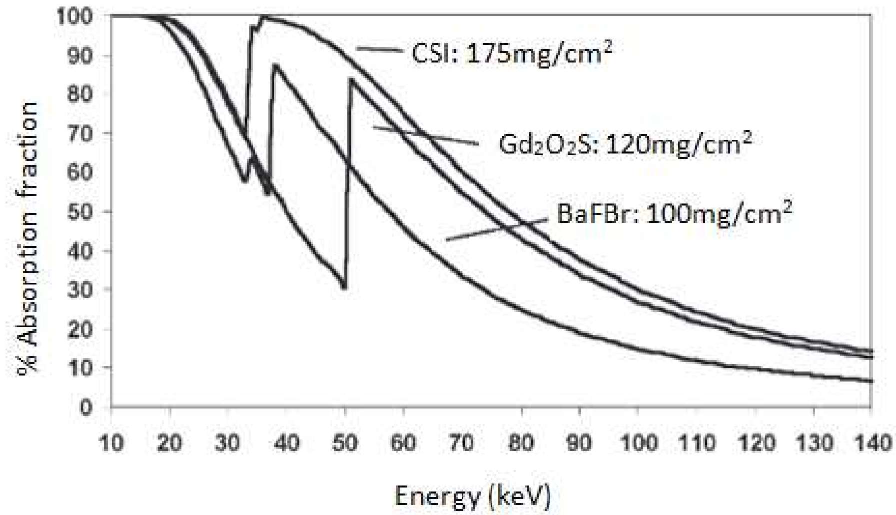


***Figure 3-2: Comparison of the absorption characteristics of BaFBr, CsI and $Gd_2O_2S_2$ phosphors of the "typical" thickness used for digital radiography*** **(Seibert, 2004).**

The higher k-edge of rare earth screens compared to CR plates indicates that lower kV techniques might be more favourable in CR, however lower kV techniques are often associated with increased ESD. This poses the question when referring to low kV techniques, which kV would be the most effective for neonatal imaging? The answer to this question is not generic and depends to a large extent on the detector used at an institution and the optimum kV to maintain a balance between dose and image quality should be established.

Receptor noise can be influenced by non-uniform sensitivity of the detector resulting from chemical processing of the SF or CR IP plate damage. Examples of IP plate damage include suction cup marks formed when IP is removed from cassette during the digitization process as well as scratches that may occur from repeated use and rough handling of the IP. Specs of dust and dirt on the imaging plate can be seen on the image after it has been readout. This type of noise can be difficult to correct for, it can however be minimized with good quality control procedures and regular cleaning of the imaging plates as prescribed by the supplier.

### *3.2.1.3 Display image*

The signal from the detector image will subsequently be influenced by the characteristics of the display system. When using SF the film fulfils both the function of the detector and the display system. The detector and display function in CR is performed by two independent components in the imaging chain.  This offers the advantage of manipulating the signal from the detector for display. There exists a linear relationship between the number of x-ray photons of the primary image and the signal of the detector image. This signal is then processed by software in a non-linear fashion to mimic the appearance of SF images which radiologists are familiar with. The images generated from the detector signal are then displayed on monitors for reporting.

The software processing is done through mathematical manipulation of the signal, including the use of lookup tables to relate the detector signal to an output signal displayed as a shade of gray on the display monitor. This process does not only amplify the image signal but also the noise present in the image.

Although a certain amount of noise might be acceptable, care should be taken that the noise does not negatively influence the observer's ability to distinguish objects of interest. According to Uffmann and Schaefer-Prokop (2009) the human visual system can tolerate a substantial amount of  noise. However, the way in which the observer was trained may also influence the acceptable amount of noise as familiarity has an influence on human perception according to Mansilla et al. (2009).  Observers used to report on high dose images (low noise), might be reluctant to accept images acquired at a lower dose with an increase in noise even though this might not influence the diagnostic task.

Another type of noise that might influence image quality is caused by structures in the patient that is not needed for diagnosis e.g. the shadow of the ribs in radiographs requested to investigate the lung parenchyma. These structures are disturbing and can hide small lesions or certain pathology. This type of noise is often referred to as anatomical noise or structural noise.

The signal intensity and acceptable noise level required to produce an adequate final image will therefore depend on the clinical reason for generating the image.

### *3.2.2 Contrast*

Contrast can be described as the signal difference between closely adjacent regions in the image. Contrast is thus a function of signal intensity. If the signal in the image is too low, image information may be lost due to a lack of contrast. Contrast in images is therefore attributed to the different steps in the imaging acquisition and is influenced in both SF and digital imaging by the subject contrast as well as detector sensitivity.

Contrast in a digital image is expressed as the relative gray scale difference between the areas of interest on the display monitor. Two types of contrast can be defined in medical imaging (IAEA, 2014);

The local contrast or Weber contrast given by equation 3.2;

$$C_W = \frac{(S_o - S_b)}{S_b} \qquad [3\text{-}2]$$

where $S_o$ and $S_b$ denotes signal values in object and background respectively. The Weber contrast is used when small features are present on a large uniform background. The Michelson or modulation contrast given by equation 3-3;

$$C_M = \frac{(S_{\max} - S_{\min})}{(S_{\max} + S_{\min})} \qquad [3\text{-}3]$$

where $S_{max}$ and $S_{min}$ represents the highest and lowest signal respectively. The modulation contrast is used when both dark and bright features take up similar fractions of the image.

The effect of the different sections in the imaging chain on image contrast will be discussed in the following paragraphs.

### *3.2.2.1 Subject contrast*

Subject contrast gives an indication of the interaction between the x-ray beam and the object being imaged before reaching the detector. The subject contrast can be explained by the difference in x-ray beam intensity in different areas of the beam as a result of the attenuation properties of the tissue being imaged. Attenuation, as mentioned previously, depends on the x-ray spectrum and the patient's anatomy. As discussed in Section 2.2 the x-ray spectrum depends on the target material, tube potential and filtration.

The kV selected during acquisition determines the penetrating power of an x-ray beam which in turn influences the interaction processes responsible for image formation. If the applied voltage is increased, the x-ray beam will be attenuated more by the Compton process resulting in the beam to become more penetrating. There will also be a loss in contrast as the penetration differences between dense materials e.g. bone and less dense material e.g. lung tissue will decrease.

In the diagnostic energy range the Photoelectric Effect and Compton Scattering Effect are the dominant interaction processes between x-ray photons and soft tissue. The Photoelectric Effect is the domination interaction process when x-rays with energies below 50 keV interacts with high atomic number materials. The Compton Effect becomes the dominating effect at x-ray energies above 26 keV and is responsible for deflection of x-ray photons from their original path, a process known as scattering. Aside from the decrease in contrast with increased applied voltage the image will also include more scatter as the Compton Effect becomes dominant at higher diagnostic energies.

Scattered photons reduce subject contrast as the true position of the signal from the x-ray photon is miss-registered by the detector. Anti-scatter grids are often used in general radiography to remove the unwanted scattered radiation. The grid is placed between the patient and the detector. The use of grids is recommended for CR because of the increased scatter sensitivity of barium halide due to the lower k-absorption edge, which makes the detector more sensitive to the low energy scattered radiation.

Grids are however not recommended for use in neonatal radiography as these grids may lead to increased radiation dose in order to compensate for the loss of primary radiation that would have contributed to the image signal. Another reason for grids not being recommended for use in neonatal radiography is the unwanted artefacts that may be caused by the misalignment of grids in mobile radiographic examinations requiring a repeat of the examination, leading to an increase in dose.

Although scatter are present in neonatal radiography, the effect is less than in adults due to the lesser thickness of tissue through which the x-ray beam should pass compared to adults. Lower kV techniques of approximately 60 kV are also used for neonatal chest radiography resulting in a decrease of scattered radiation compared to adult chest radiography with techniques performed at approximately of 109 kV.

#### *3.2.2.2 Detector and display contrast*

The detector relates input signal to output signal with different levels of contrast amplification, depending on the required mathematical relationships used, e.g. linear or logarithmic translation.

In SF the detector contrast as well as the display contrast depends on the slope of the film characteristic curve (Figure 3-3). Only input signals falling in the linear section of the S-shaped curve (i.e. within the dynamic range) will display adequate contrast. Input signal outside the dynamic range will result in display images with poor contrast which cannot be adjusted post-acquisition since no post-processing is performed when using SF.

Due to the linear relationship between exposure and signal, the CR detector has a greater dynamic range compared to SF; the detector contrast can be altered after acquisition using mathematical manipulation. The relationship between the detector contrast and display contrast (image gray-scale value) in digital radiography are usually established by proprietary image processing software that is not under the control of the radiologist.

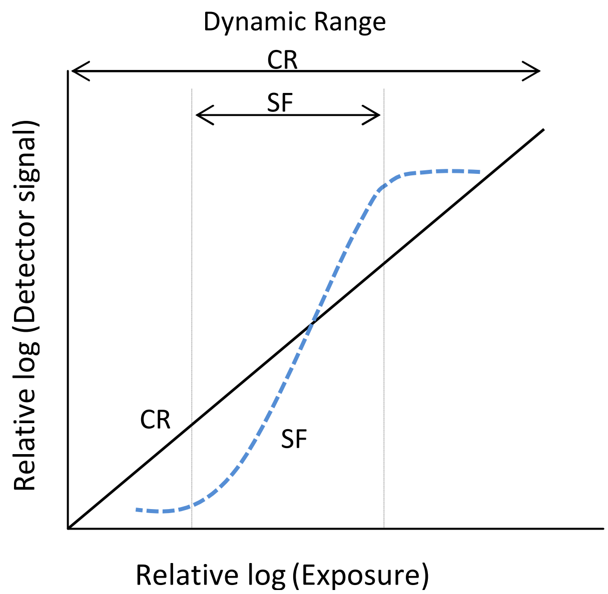


***Figure 3-3: Comparison of the characteristic curves for screen film and digital detectors.***

The radiologists can change the display appearance (contrast) of a digital image by windowing and levelling, which is one of the advantages of digital images. By changing the WW/WL the slope op the translation curve is either increased or decreased, resulting in a higher or lower contrast. A look-up-table can also be used to convert the detector image into the image displayed on a monitor. Image contrast can be changed by changing the slope of the look-up-table for example in histogram equalization. Due to the above mentioned reasons display contrast can be a misleading indicator of digital image quality.

Changing the look-up-table may be an arbitrary process and depends on the manufacturer specific processing algorithms used. This makes it difficult to describe contrast of a digital system.

The ambient light in the viewing room will also influence the perceived image contrast. Therefore to ensure that the ambient room illuminance does not influence visual contrast perception it is recommended that the ambient room illuminance should be below 15 lux (IPEM, 2005).

### *3.2.3 Resolution*

The spatial resolution describes the ability of an imaging system to accurately depict objects as separate when they become smaller and closer together. Spatial resolution is often expressed in line pairs per millimetre (lp/mm) indicating the frequency dependence of resolution. Spatial resolution is influenced by geometrical factors as well as the detector and display system.

The primary resolution is influenced by factors not relating to the detector including the x-ray field penumbra caused by the size of the focal spot, the magnification between the object of interest and the detector as well as patient motion. Detector resolution is influenced by light spread in the detector and the size of the sampling intervals between measurements and the active picture element (pixel) area.

There exists a trade - off between detector efficiency and resolution. As the detector (screen/film combination or IP) thickness increases so does the detector efficiency but on the down side the light released by the interaction process of the X-ray photon spreads and therefore degrades resolution, see figure.

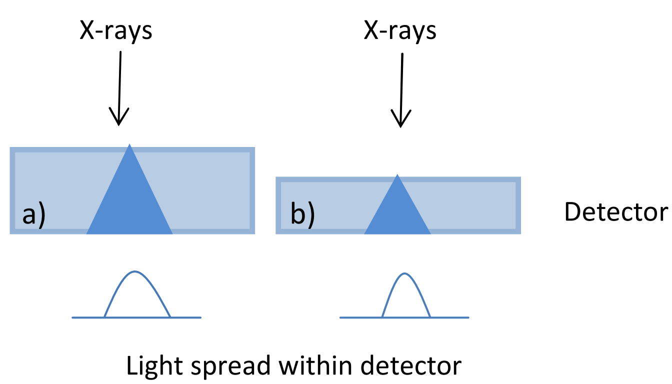


***Figure 3-4: Schematic illustrating that X-rays incident on (a) a thick detector are absorbed more effectively but with a larger spread of light within the thick detector when compared to (b) a thin detector.***

Spatial resolution in SF is mainly limited by the screen thickness as the display resolution associated with the film itself has a high resolution due to the small granule sizes used. In CR detector resolution is mostly lost during the readout process. This loss is caused by the scattering of laser light in the IP which in turn releases electrons in a larger area than intended, causing a blurring of the image. The display resolution in CR is further influenced by the pixel size of the monitor used for display purpose.  Reporting monitors used for general radiology should be at least 3 mega pixels to ensure that the display resolution is not the limiting factor for image quality.

Although SF has superior resolution over CR and DR the loss in spatial resolution is outweighed by the gain in contrast resolution obtained by post processing. As pointed out by Yaffe and Rowlands, (1997) high resolution is not as important as the ability to maintain image contrast over a wide range of x-ray exposures. This might be attributed to the limitations by the human visual system (HVS) which operates with a variable resolution in order to deal with the large amount of information it receives. Very high resolution is obtained only in a small part and the acuity of the eye with which this high resolution can be perceived drops off dramatically further into the periphery of the retina. The HVS is however very sensitive to contrast changes (EUSIPCO, 1998).  Therefore calculating the resolution, contrast and noise properties of an imaging system separately does not give an indication of the possible influence on the HVS. Other image quality metric should also be considered.

### *3.2.4 Combined Parameters*

#### *3.2.4.1 Contrast to Noise Ratio*

The contrast to noise ratio (CNR) gives an indication of how well an object can be distinguished from the background in the presence of noise. The CNR can be obtained by dividing the average difference in signal from a region of interest drawn on the object and the background by the noise in the background, see equation 3-4.

$$CNR = \frac{\left(\bar{x}_s - \bar{x}_{bkg}\right)}{\sigma_{bkg}} \qquad [3\text{-}4]$$

CNR can be used to optimize the kV used in a study, since kV influence contrast, or to determine the minimum concentration of contrast agent required when the dose is kept constant. The CNR gives a better indication of the quality of the digital image than the subject contrast alone as digital images are noise limited rather than contrast limited (Hansson et al., 2005).

### *3.2.4.2 Signal to Noise Ratio*

The signal to noise ratio (SNR) describes how clearly an object can be visualized in the presence of noise. If the SNR ≥ 5 an object will most likely be detected by the observer (Bushberg et al., 2011)

The SNR can be obtained from the ratio of the mean signal value of the object of interest and the noise, see equation 3.5.

$$SNR = \frac{S_O}{\sigma_O} \qquad [3\text{-}5]$$

where $S_O$ is the mean signal from a region of interest (ROI) drawn on the object of interest and $\sigma_O$ is the standard deviation (the noise).

A higher patient dose will give a larger signal to the primary image and include less noise in the image thus rendering higher SNR. This often is the motivation for using imaging parameters delivering a higher dose to the patient as these images might be preferred by the radiologist.

In a study aimed at determining the optimal kV setting for neonatal imaging Hansson et al. (2005) pointed out that digital images was not limited in contrast visualization but only in SNR of the original image.

### *3.2.4.3 Modulation Transfer Function*

The signal from an object being imaged can be expressed as a spectrum of spatial frequencies. An imaging system detecting a signal from a particular size object (at a specific frequency) will produce an image of the object often with reduced intensity (amplitude). The modulation transfer function (MTF) gives the relationship between the intensity (amplitude) of the input- and output signals for different object sizes (frequencies) i.e. how well the imaging system modulated the output signal in terms of the input signal. Fourier analysis is used to relate the object in real space to its image in frequency space.

The system has to transmit every frequency with 100 % efficiency to obtain an exact image of the object of interest. This does however not happen in practice. A signal of a certain frequency will fall onto the detector and an image of the same frequency but at lower signal amplitude compared to the input signal will be produced, see Figure 3.5. This reduction in signal amplitude is due to resolution limitations in the system. No imager can have a MTF of unity at all spatial frequencies. Each of the different components in an imaging component of the imaging chain will have an associated MTF that modifies the spatial frequency spectrum (SFS) of the object transferred as an image.

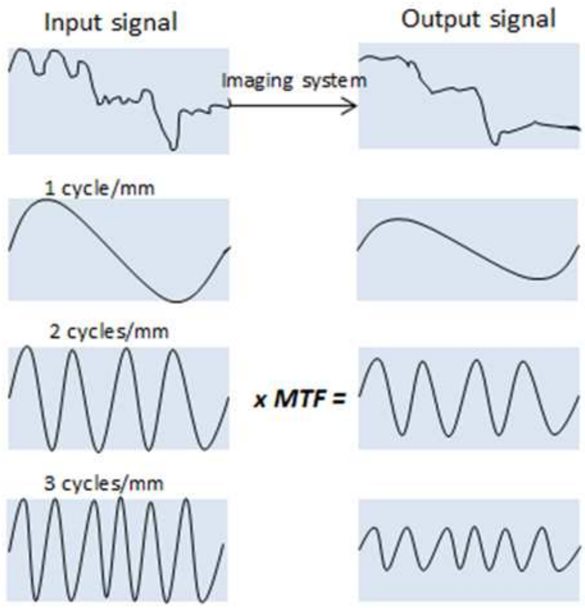


***Figure 3-5: Schematic depiction of the input signal and modulated output signal at the different frequency components of the image.***

The MTF is often expressed as a plot of the resolution properties of a system as a function of the spatial frequency of the input signal, see Figure 3-6. The total system MTF is given by the product of the MTF's of each component in the imaging chain.

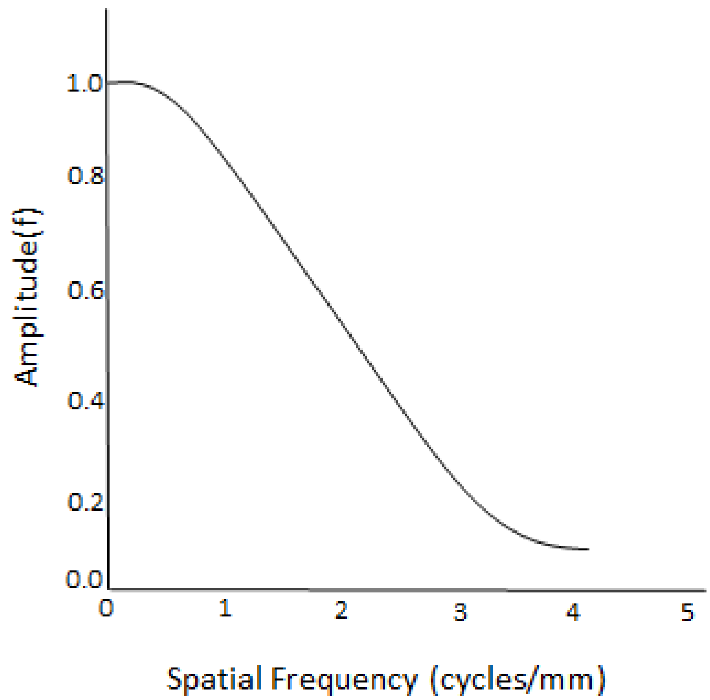


***Figure 3-6: Modulation transfer function of an imaging system***

An input signal with low spatial frequency results in an output signal amplitude with little modulation compared to the input signal amplitude i.e. an MTF value of approximately 1. Fine detail or high resolution, i.e. sharper edges in real space, are associated with higher frequencies in the spatial frequency spectrum (SFS). The reduction in amplitude of the output signal compared to the input signal is greater for higher frequency signals (Figure 3.5).

A practical example of this principle can be seen when imaging the Artinis CDMAM 3.4 phantom used for contrast detail measurements in mammography. The phantom consists of 24 carat gold discs of varying thickness and diameter encased in Perspex, Figure 3-7.

***Figure 3-7: Artinis CDMAM 3.4***

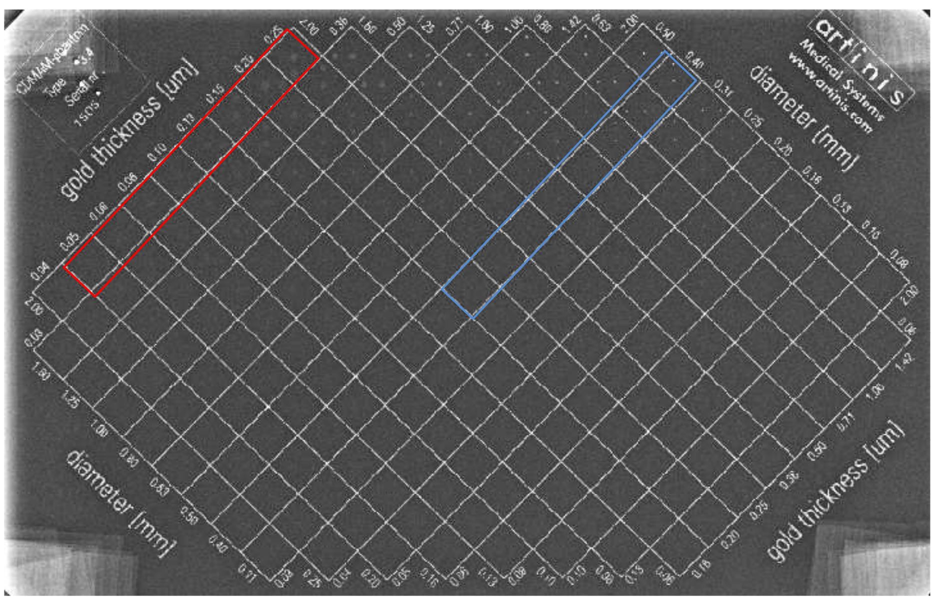


***Figure 3-8: Artinis CDMAM3.4 image obtained with mammography***

The larger diameter disks (indicated by the red rectangle in Figure 3.8) associated with lower frequencies will have a higher intensity, are more visible at decreasing thickness (indicating decreasing contrast), compared to the small diameter disks associated with higher frequencies (blue rectangle Figure 3.8). All diameter disks are not equally visible due to the effect of the modulation transfer function of the system, especially on smaller objects.

Higher frequency signal is not only associated with fine detail, but also noise. This creates an uncertainty whether the higher frequency components of the MTF are an indication of fine detail or image noise. Therefore, estimating the MTF alone does not give a complete description of the signal transfer properties of an imaging system.

#### *3.2.4.4 Noise Power Spectrum*

The noise in an image, similar to signal, is constituted of different frequency components. Therefore only calculating the variance of the noise does not give a complete description on how the imaging system handles the noise input to the system. The noise appearance (texture) of two images might be different although the noise variance is the same due to the frequency dependence of the noise in the images.

The Weiner spectrum also referred to as the noise power spectrum (NPS), gives an indication of the total noise in an image i.e. the sum of the quantum noise and the inherent system noise, see Figure 3-9.

Similar to the MTF giving an indication of the frequency dependant input-signal modulation, the NPS gives an indication of the noise variance of an image as a function of the spatial frequency, see equation 3-6.

$$NPS(f_x, f_y) = \left| \int_x \int_y \left[ I(x,y) - \bar{I} \right] e^{-2\pi i (x f_x + y f_y)} dx dy \right|^2 \qquad [3\text{-}6]$$

where $f_x$ and $f_y$ is the frequency corresponding to the *x*-dimension and *y*-dimension respectively and $\bar{I}$ is the mean of the image I(*x,y*) (Bushberg et al., 2011).

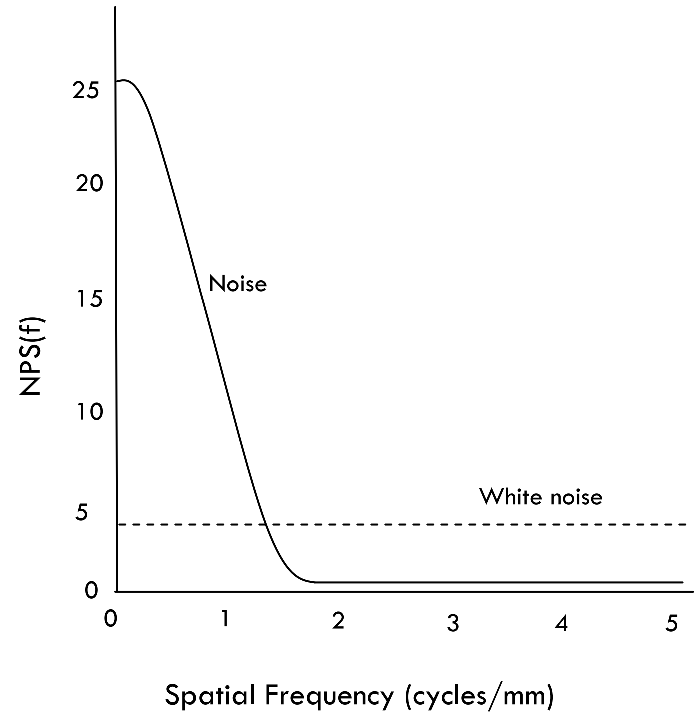


***Figure 3-9: Schematic representation of the noise power spectrum.***

Images also contain a random fluctuation in noise at all frequencies known as white noise, this type of noise is uncorrelated between image pixels and will appear as a flat line on the NPS, see Figure 3-9.

### *3.2.4.5 Detective Quantum Efficiency*

The Detective Quantum Efficiency (DQE) can be defined as the ratio of the output $SNR^2$ to the input $SNR^2$, given by equation 3-7.

$$DQE = \frac{SNR_{out}^2}{SNR_{in}^2} \qquad [3\text{-}7]$$

The input SNR is dependent on the SNR of the primary image which can be influenced by the number of photons as well as the scattered radiation. The output signal is mainly influenced by the detector system. According to Tapiovaara (2008) the DQE is considered as one of the best ways to describe the image detector.

The DQE gives a description of the imaging system by describing the overall signal and noise performance of the system. Both the MTF (f) and NPS (f) give an indication of how the output relates to the input and can be combined to estimate the $SNR^2_{out}$, see equation 3-8.

$$SNR^2_{out} = \frac{[MTF(f)]^2}{NPS(f)} \qquad [3\text{-}8]$$

The $SNR^2_{in}$ is given by the number of x-ray quanta, N, therefore the DQE can be calculated using equation 3-9.

$$DQE(f) = \frac{k[MTF(f)]^2}{NNPS(f)} \qquad [3\text{-}9]$$

where *k* is a constant to convert units. Detectors with a high DQE requires less exposure to maintain an adequate SNR.

### *3.2.4.6 Summary*

Estimating the MTF can be advantageous as it gives a pictorial representation of the signal transfer capabilities of the whole system. The MTF of each component can be determined separately to identify the weak link in the imaging system. The MTF can also be used to compare various imaging conditions as well as different systems with each other. The MTF however does not give any information regarding the dose used to obtain an image.

The NPS compliments the MTF by describing the frequency dependent noise in an image. Calculating the NPS is useful when evaluating different detector types or comparing x-ray units from different vendors. However, calculating the NPS in practice can be challenging as demonstrated by Hanson (1998). The NPS - although describing the noise characteristics of an image - does not give a measure of the impact the noise will have on diagnostic image quality and therefore the NPS will not be calculated in this study.

The MTF and NPS will not be determined in the study as it was not the aim to optimize the performance of the imaging system. The focus was rather to measure the effectiveness with which the image can be used for diagnostic purpose where signal needs to be detected by observers in the presence of noise. Also only one type of detector system was used in this study there is thus no need for calculating these parameters since no detector comparison will be performed. The DQE is dependent on both the MTF and NPS and will thus not be calculated either.

## 3.3 SUBJECTIVE EVALUATION OF IMAGE QUALITY

Månsson (2000) emphasized that image quality should agree with the radiologist's view of good quality images. It is important that the image quality should be such that the radiologist is able to: distinguish between disease states, accurately report on diagnostic relevant structures and classify different types of abnormalities.

In applications where images will be viewed by human observers subjective evaluation is thought to be the correct method to quantify visual image quality (Wang et al., 2004). Subjective evaluation requires human observers to directly give feedback regarding the visual information in an image. Some of the subjective methods used to evaluate image quality will be discussed in the following section.

### *3.3.1 Receiver Operating Characteristics Analysis*

Receiver operating characteristics (ROC) analysis tests the observer's ability to detect low contrast signal in a noisy background. This analysis is also often used in clinical settings to detect abnormal cases compared to normal cases in systems where differences are not easily distinguished. According to Månsson, (2000) this method is only applicable to a task that required a binary decision, "Is the image normal or abnormal" and where the answer to the question i.e. "the truth" is known. For example when radiologists reports on a mammogram of a patient with a visible lesion they have to decide if the lesion is benign (normal) or malignant (abnormal). If the radiologist reported the lesion to be abnormal and through a biopsy it is found abnormal it is known as a true positive, if the biopsy indicated the lesion to be normal it is referred to as a false positive. If the observer indicated the lesion to be normal and it is confirmed normal through the biopsy it is referred to as a true negative if the lesion was however found abnormal it is referred to as a false negative.

The experiment renders a curve of the true-positive fraction as a function of the false-positive fraction. The area under the curve (AUC), ranging between 0.5 – 1.0, serves as a quality index to compare different systems or methods. An AUC value of 0.5, illustrated by the dotted line in Figure 3.10, indicates pure guess work on the part of the observer. The larger the AUC, i.e. a value closer to 1, the better the diagnostic accuracy of the system or method being tested.

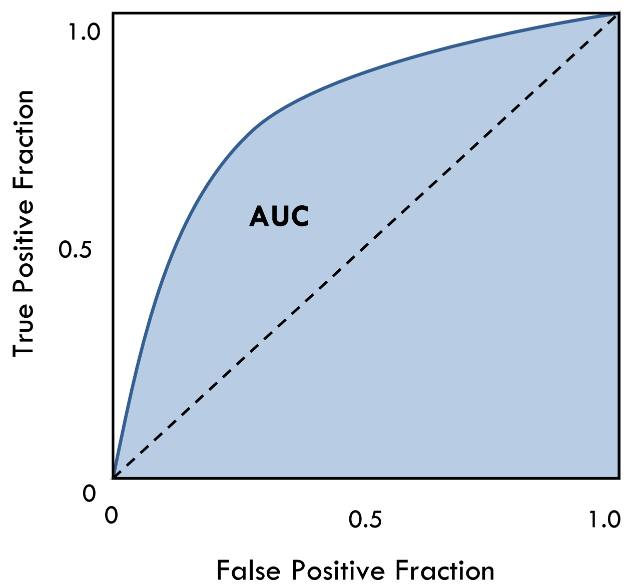


***Figure 3-10: Schematic representation of an ROC curve.***

Limitations of the ROC analysis are the large number of images required for statistical relevant results and only images with known structural abnormality can be used (Tingberg et al., 2000). Experts are required to perform the analysis and because this method is time consuming it is often difficult to implement in practice. For a more detailed discussion on ROC analysis refer to the textbooks by Bushberg et al. (2011) and Dendy and Heaton (1999).

### *3.3.2 Visual Grading Analysis*

Visual Grading Analysis (VGA) offers a method to quantify subjective opinions. This method has been described as attractively simplistic with powerful discrimination properties that can easily be implemented in clinical practice (Månsson, 2000). VGA results have also been found to be comparable to ROC analysis (Tingberg et al., 2000) and can be done in a fraction of the time.

There are two variations to VGA namely relative and absolute grading. Relative grading makes use of a reference image and observers are asked to compare anatomical landmarks between a given image and the reference image using a 3 -, 5 - or 7 - point-scale. Examples of such a scale are presented in Table 3.1. This method accepts that the reference image is of good image quality. More information on relative grading can be found in studies by Niemann et al. (2010), Tingberg et al. (2000).

Absolute grading does not make use of a reference image. An absolute grading scale is used to indicate the image quality of a given image based on anatomical landmarks. The guidelines on quality criteria for diagnostic images published by the European Commission (1996) can be used to give an indication of the anatomical landmarks that should be visualized for different exams e.g. neonatal anterior-posterior (AP) chest images.

**Table 3-1: The grading system for VGA. Comparison is made with the reference image; both images are selected from the same patient. (Tingberg et al., 2000)**

| Grading | Visibility of structure |
|---|---|
| -2 | Clearly inferior to |
| -1 | Slightly inferior to |
| 0 | Equal to |
| +1 | Slightly better than |
| +2 | Clearly better than |

### 3.3.3 Rank Order Method

In this relative visual grading derivative observers are presented with images in which factors influencing image quality has been varied. The observers are tasked to rank these images by arranging the images in order of preference. Experienced observers are able to identify images of good quality. The observers are however not always able to define the criteria on which the judgment was based. The ranking order method gives an indication on whether observers agree on image quality. If there is a preference towards a certain image a trend would be observed. If no clear trend in image ranking is observed it can be concluded that observers have no preference towards a certain image. If for example various parameters lowering the ESD, with the possibility of affecting image quality, was used a decision can be made on which parameters will have the least effect on image quality when compared to an accepted image quality standard. This can be useful in dose reduction studies, where it is known that a change in image parameters will influence image quality; however, the impact of these changes on observer interpretation of image quality is unknown.

In a study conducted by Ravenel et al. (2001) five interpreters were asked to rank ten sets of images, at six different dose levels, from best to worst based on image quality. This relative scale method was found efficient to identify small differences in image quality and make a recommendation for clinical practice.

### 3.3.4 Summary and Recommendations to Assess Clinical Image Quality

Physical parameters are useful to compare different imaging systems in a quantitative manner and to try and understand the effect that changing imaging parameters might have on perceived image quality. However, physical parameters alone have been shown to have poor correlation with clinical image quality (Månsson, 2000).

If a study is focused on optimizing equipment used to generate medical images, physical parameters alone might be acceptable. If the study is however focused on dose reduction using available equipment the effect of the dose reduction attempts on observer's perception of image quality should also be investigated.  This should be done using subjective image quality evaluation.

Subjective methods might be time consuming and recruiting observers willing to take part in the study might be challenging. However, using a simple method such as the ranking order method has been shown to be effective in establishing appropriate imaging parameters that will lead to a dose reduction while maintaining diagnostically acceptable image quality.

## 3.4 PHANTOMS USED FOR IMAGE QUALITY ASSESMENT

Image quality, whether referring to physical characteristics of the equipment or observer performance and judgment) are usually assessed using phantom measurements.  These phantoms vary from simple Perspex phantoms to detailed anthropomorphic phantoms and even mathematical phantoms developed for use in simulation, depending on the task. Phantom selection therefore forms an important part of image quality measurement.

Physical image quality is routinely measured in phantoms constructed of Perspex with inserts that depend on the intended use of the phantom; e.g. resolution line patterns or contrast discs added to a certain thickness of Perspex to represent the standard patient.  Subjective image quality evaluation to assess observer performance and judgment of image quality are mostly performed on anthropomorphic phantoms.  The phantoms used to measure image quality can be commercially obtained or manufactured in house. The following section will touch on different phantoms.

### *3.4.1 Anthropomorphic Phantoms*

According to Båth et al. (2005) the use of contrast detail- and homogeneous phantoms are recommended for and should be limited to constancy checks rather than optimization studies. A Perspex phantom such as used by Wraith et al. (1995) and Jones et al. (2001) to investigate the radiation dose delivered to neonates would therefore not be appropriate for this study as an indication of clinical image quality cannot be obtained.

Anatomical noise also referred to as structural noise have been found to have a large influence on observer judgment of image quality (Hansson et al., 2005). It is therefore appropriate to use a phantom that includes anatomical structures to simulate anatomical noise in the evaluation of image quality for a clinical application.

Tapiovaara (2008) pointed out that actual patient images or high quality anthropomorphic phantoms should be used in optimization studies. As multiple images at different dose values were obtained it were deemed more appropriate to use an anthropomorphic phantom and not clinical patient images.

#### *3.4.1.1 Commercial Neonatal Phantom*

The commercially available Gammex 610 neonatal chest phantom used in a study by Rattan and Cohen (2013) as well as the study by Smans et al. (2010a) may be considered. This phantom represents a 1000 – 2000g neonate in its anatomical structures and tissue attenuation (Gammex, 2008).

Using such a type of phantom has the advantage of producing reproducible images each time without positioning challenges such as rotation and motion. However it was decided that the structures in this phantom do not mimic the influence of anatomical noise satisfactory. Alternative options such as software-, chicken- and rabbit phantoms (at a much lower cost) may also be considered.

#### *3.4.1.2 Software Phantoms*

Computer modelling is often used in dose optimization studies, not only to estimate organ dose and risk as mentioned in Chapter 2, but also to simulate the image acquisition process and thereby create virtual x-ray images. Smans et al. (2010a) validated such a computer model using the Monte Carlo MCNPX code to simulate the neonatal chest for two different x-ray units. Smans et al. (2010b) used this model to investigate the influence of Cu filtration on patient dose and image quality. The virtual x-ray images obtained was compared to images the Gammex 610 neonatal chest phantom obtained using a standard x-ray exposure. These studies however did not use subjective evaluation of image quality which has been established to play an important role in image quality perception. Computer modelling also required special software packages and programming skills.

### *3.4.1.3 Chicken Phantom*

In a study to investigate the influence of a new screen film combination on dose reduction and image quality a 1820 g, 8.9 cm thick chicken was used as a phantom approximating the neonatal chest (Burton et al., 1988). This type of anthropomorphic phantom with ribcage and soft tissue mimic the neonatal chest more closely. It is however difficult to use living chickens and a chicken corpse has the limitation of not having the heart and lungs intact. As chicken corpses are readily available from local supermarkets and cost effective, it can be a consideration if the heart shadows and bronchi do not need to be evaluated.

### *3.4.1.4 Rabbit Phantom*

Living rabbits have been used as phantoms in studies were image quality was evaluated after a change in practice e.g. exposure parameters, imaging modality or procedure. In a study by Seifert et al. (1998) a rabbit approximating the thickness and length of an average neonate was sedated and imaged using different exposure parameters to determine the minimum acceptable dose that still produces a diagnostic adequate image in digital luminescence radiography. In a study to compare the ability of CR and screen film radiography in the detection of pulmonary oedema and to determine if the radiation exposure can be reduced when using CR while still maintaining diagnostic accuracy Don et al. (1999) used rabbits to simulate the opacity in the lungs of neonates. Hansson et al. (2005) conducted a study to determine the optimal tube potential settings for neonatal chest CR. In this study a rabbit of approximately 1000g, to ensure abdominal volume corresponds to that of a neonate, was sedated and imaged. The image quality of the images obtained at the different setting was then compared.

Images of rabbit radiographs obtained in previous studies were shown to the observers of the current study. In their opinion clinical structures such as the lungs and heart when compared to neonatal radiographs mimicked these structures satisfactory. Therefore using a rabbit phantom will allow the evaluation of structures present in neonatal radiographs. As mentioned in Section 3.4.1.1 motion and reproducible positioning can however be a limitation when using a living creature as a phantom.

### *3.4.2 Summary and Recommendation*

In this study image quality in terms of different aspects such as lung patterns, diaphragm as well as mediastinum and heart shadow will be evaluated. Rabbits are available at the institution where the study will be performed. It was therefore decided to use rabbits to simulate the neonatal chest.

# *CHAPTER 4*

# *OPTIMAL BEAM PARAMETERS FOR DOSE REDUCTION*

## 4.1 INTRODUCTION

Dose reduction, as discussed in Chapter 1, is very important in paediatric radiology. Paediatric patients are more radiosensitive due to the rapid dividing nature of their cells and the longer life expectancy compared to adults. Special attention should be given to neonatal radiography as neonates have tiny bodies resulting in organs within close proximity of each other. This often leads to tissue not of clinical interest to be included in the x-ray field. Therefore selecting beam parameters to ensure that the lowest possible dose is received by the patient, in an attempt to minimize stochastic effects, is especially important in neonatal radiography.

With the development of image detector technology and the change from SF to CR, the ALARA principle should be revisited and imaging protocols revised. Although the principles used in choosing the optimal relationship between kV and mAs for the primary image remains the same, the optimal beam parameter combination should be investigated when progressing from SF to CR as the image quality is also influenced by the detector and display characteristics.

Before dose reduction methods are implemented the dose obtained from current practice should first be estimated. The ESD, discussed in Section 2.2, gives an indication of patient entrance skin dose and can be used as a metric for patient dose evaluation. The ESD can conveniently be determined from routine quality control measurements (see Section 2.3.1) and will be used as a measure of patient dose in this study.

Dose reduction cannot be performed without investigating the effect it has on image quality. As mentioned in Section 3.3 images will be viewed by human observers and therefore a subjective approach to image quality evaluation where the observers give feedback regarding their perception of image quality is considered appropriate.

Although the ESD in neonatal x-ray examinations are mostly low and does not often exceed the European Commission (1996) dose reference level, studies by Dougeni et al. (2007), Smans et al. (2008) and Frayre et al. (2012) found large variation in neonatal ESD values per x-ray examination. This large variation can be attributed to difference in equipment, staff training and a lack of radiographic protocols.

Neonatal chest imaging have been performed with kV's ranging between 40 kV and 70 kV and mAs values as low as 0.5 mAs up to 4 mAs (Dougeni et al., 2007) (Azevedo et al., 2006) (Olgar et al., 2008) (Faghihi et al., 2012) (Frayre et al., 2012). The study by Dougeni et al., (2007) indicated that more than 70 % of the hospitals participating in their study used tube voltages below 60 kV. This will be associated with high ESD values.

There are no clear regulations on kV and mAs combinations to be used in neonatal imaging, except for the recommendations of kV and additional filtration given by the EC (European Commission, 1996).

As discussed in Section 2.2.4 the kV and mAs selection depends on various factors such as attenuating characteristics of anatomy being imaged, the detector composition and observer preference. Therefore a one-protocol-fits-all approach is not appropriate. Each institution should perform dose optimization studies and revise the protocols used for radiographic examinations to ensure that the dose received by the patient is as low as possible while still maintaining diagnostic adequate images.

Universitas Academic Hospital (UAH) has a fourteen bed NICU. Neonatal x-rays are done upon request from the referring doctor, with routine x-ray examinations often performed twice daily. Neonatal AP chest x-rays are the most common examination requested. The current protocol for neonatal AP chest examination uses beam parameters of 55 kV and 3.2 mAs with no additional filtration. These parameters are adjusted for different size patients according to the radiographer's professional judgement. The parameters currently used were optimised for SF and are still used even though the hospital is using CR.

The aim of this study was to determine the ESD of current neonatal CR, AP chest examinations and to determine beam parameter combinations that will reduce the radiation dose per examination without compromising image quality.

## 4.2 METHODS AND MATERIALS

Approval to perform the study was obtained from the Ethics Committee and the Radiation Control Committee of the Faculty of Health Sciences, University of the Free State, as well as the Head Clinical Service UAH and the Heads of the Departments Clinical Imaging Sciences and Medical Physics respectively.

### *4.2.1 Image Acquisition and Display*

Radiographic acquisitions were performed using a Philips Optimus 80 x-ray unit, with a half value layer of 3.2 mm Al at 81 kV and a nominal broad focal spot of 1.5 mm.

Neonatal imaging is mostly performed with mobile x-ray units, but the fixed x-ray unit was however more readily available and therefore convenient for multiple exposures performed during phase 1. To ensure correct functioning of the unit and reliability of the exposure parameters a complete quality check according to the requirements for licence holders by the Department of Health: Directorate Radiation Control (2014) was performed.

The neonatal chest was simulated using 5 cm of Perspex similar to the study by Mutch and Wentworth (2007). Perspex has attenuation characteristics similar to human skeletal muscle, making it a favourable phantom as the larger part of neonatal mass is composed of skeletal muscle (Jones et al., 2001).

Baseline ESD values were determined using the standard 55 kV and 3.2 mAs by imaging the above mentioned phantom. Dose measurements were performed using an 8000 Victoreen® NERO® mAx X-ray Test Device, with calibration traceable to a standards laboratory with an exposure uncertainty of ± 3.7 %. Exit dose measurements were performed at a focus to detector distance of 100 cm with 5 cm of Perspex placed on top of the detector to simulate the neonatal chest. The ESE, used to calculate the ESD, was measured at a focus to detector distance (FDD) of 95 cm, see Figure 4-1.

The ESD was determined according to equation 2-2, the measured entrance surface exposure was multiplied with the following constant factors, BSF = 1.1 and $\left(\frac{\mu_{en}}{\rho}\right)_{Air}^{Tis}$ = 1.05. No ISL corrections were performed as the measurements were performed at the FDD used clinically.

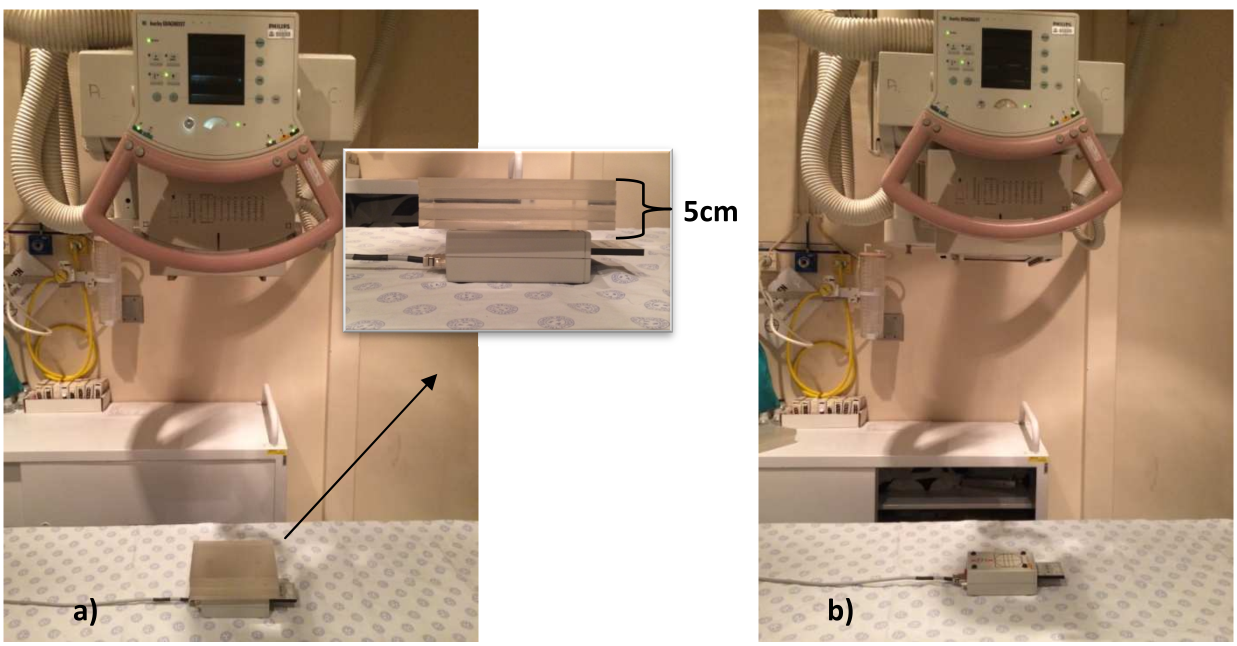


***Figure 4-1: Setup used to measure a) entrance surface exposure, b) exit dose***

#### 4.2.1.1 Parameter Selection

The following kV's were used in this study 60 kV, 66 kV and 70 kV. The kV selection was based on the recommendations of the EC (European Commission, 1996). Hansson et al. (2005) proposed 90 kV for neonatal chest x-rays. This was regarded as too high a kV for neonatal imaging since over penetration of structures might cause a loss in subject contrast. It was decided to use 70 kV as the highest kV value.

The European Commission, (1996) recommends the use of additional filtration of 0.1 mm Cu + 1.0 mm Al. This combination could not be obtained and therefore additional filtration of 2.0 mm Al, available at the institution, was used.

Keeping the selected kV and additional filtration constant, the mAs was varied to keep the exit dose as close as possible to 10 µGy (KCARE, 2005). The mAs values could however only be adjusted in fixed increments with a lower limit of 0.5 mAs. The exit dose gives an indication of the radiation dose to the IP. A constant exit dose should produce images with consistent image quality (Khotle et al., 2009).

### 4.2.2 Image Quality Evaluation

In an attempt to determine the effect of the imaging parameters determined above on image quality, a chicken corpse of approximately 1200 g was used to simulate the neonatal chest in the second phase of the study.

#### 4.2.2.1 Phantom image acquisition and display

The chicken phantom used for image quality evaluation was placed on top of an Agfa CR cassette at a FDD of 100 cm. The field size was set to ensure that the x-ray beam completely covered the phantom. The imaging parameters determined in the previous Section was used to obtain the images. The six images were obtained in a posterior-anterior orientation. The uniformity amongst the CR IP's used in this study was within the KCARE recommendations (KCARE, 2005).

The information from the IP's was obtained using the standard readout protocol at UAH, which automatically processes the image for display. The processing parameters cannot be changed by the user; the user can only adjust the image gray scales and apply digital collimation and annotation.

The subject contrast and CNR of the primary image was determined using equations 3-2 and 3-4 respectively. Figure 4.2 indicates the positions of the ROI used in the calculations. The contrast of the display image as mentioned in Section 3.2.2.2 can be manipulated by the observer through WW/WL adjustments. Although influencing the visual appearance of the image the display contrast does not influence the signal intensity of the primary image.

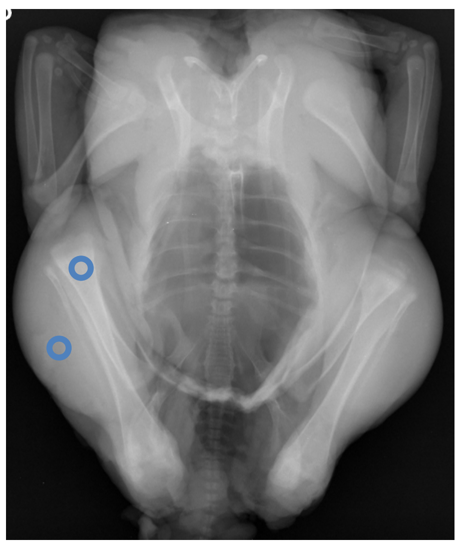

***Figure 4-2: ROI positions used in contrast and CNR calculations.***

The focus of this section was to eliminate beam parameters with noticeably poor image quality, observers were asked to rank the images from best to worst according to overall image quality. Ten observers including, five senior radiographers with at least five years of experience, four radiology registrars in their third year training and a senior medical physicist with more than twenty years of experience participated in the evaluation.

Image quality was evaluated using a variation of the multiple ranking order method described by Ravenel et al. (2001). The six chicken phantom images were displayed randomly withholding dose and imaging parameter information. Two reporting monitors were available at a reporting station; therefore two images (from the six) were displayed simultaneously, one per monitor. Using the forced choice method observers had to select the image with the best overall image quality, in their opinion, amongst the two displayed images. The image regarded as having poorer image quality amongst the two images was replaced by one of the remaining 5 images. Again the observer had to indicate the image with best overall image quality. The process was repeated until one image remained. The image regarded as having the best overall image quality was ranked number 1. The process was then repeated with the remaining 5 images to determine the second best image, which was then ranked number 2. This process was followed until all six images obtained a rank from 1 to 6.

All the images were viewed on Barco 3MP reporting monitors complying with the grey scale display function (GSDF) and other requirements from the Department of Health: Directorate Radiation Control (2014). Room illuminance was kept < 15 lux, no viewing distance restrictions were given and observers were allowed to adjust the displayed image using the WW/WL.

### *4.2.3 Statistical Analysis*

Error analysis of the ESD was performed as the quadrature sum of the estimated uncertainties; in test device calibration (± 4 %), variation in output with field size (± 2 %) and the BSF (± 5 %). The average rank position and standard deviation for each beam parameter combination was determined and graphically presented as 95 % confidence intervals. The intra-class correlation coefficient (ICC) was determined, with Excel according to the method described by Zaiontz, C, (n.d.), to assess observer agreement. No further statistical analysis were performed as only an indication of beam parameters rendering obvious poor visual image quality was needed.

## 4.3 RESULTS

### *4.3.1 Image Acquisition and Display*

#### *4.3.1.1 Parameter Selection*

Table 4.1 gives the beam parameters determined during phase 1 together with the associated ESD and exit dose measurements.

**Table 4-1: Beam parameters, ESD and Exit Dose values ordered by decreasing ESD.**

| *Beam reference | kV | mAs | Additional Filtration (2mm Al) | ESD (µGy) | Exit Dose (µGy) |
|---|---|---|---|---|---|
| BP5532 | 55 | 3.2 | No | 88.9 ± 0.5 | 24.0 ± 0.8 |
| BP6025F | 60 | 2.5 | Yes | 41.6 ± 1.3 | 14.0 ± 0.5 |
| BP6620F | 66 | 2.0 | Yes | 41.6 ± 0.0 | 13.0 ± 0.4 |
| BP5516 | 55 | 1.6 | No | 40.4 ± 0.8 | 11.0± 0.0 |
| BP7016F | 70 | 1.6 | Yes | 40.4 ± 0.5 | 13.0 ± 0.7 |
| BP6020F | 60 | 2.0 | Yes | 32.3 ± 0.4 | 10.0 ± 1.0 |

** For ease of reference in the text, the beam parameters are included in the reference names of the beam settings used in the rest of the document.*

The estimated uncertainty in the ESD is ± 7 %, correlating with the ± 8 % reported by McParland et al. (1996) and Armpilia et al. (2002). It should be noted that beam BP5532 currently used at UAH with an estimated ESD of 88.9 µGy delivered the highest ESD.

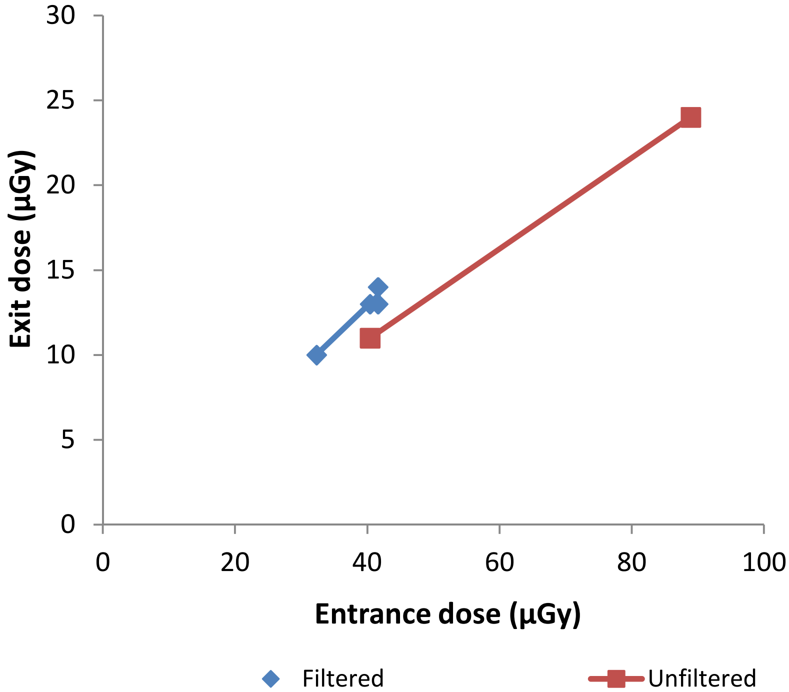


***Figure 4-3: Exit dose as a function of entrance dose for filtered and unfiltered beams.***

The trend lines in Figure 4-3 indicate that higher exit doses (and therefore better image quality) will be achieved with the use of filtered beams, using the same entrance doses compared to unfiltered beams. Limitations in the beam setting resulted in differences in the exit doses.

#### *4.3.1.2 Phantom image acquisition*

Image parameters given in Table 4.1 were used to obtain images of the chicken phantom. These images are displayed in Figure 4.4.


***Figure 4-4: Chicken phantom images obtained at the six selected beam parameters.***

Take note that the WW/WL of the images displayed in Figure 4-4 was adjusted to the preference of the researcher for display purposes, as it was also adjusted by the readers when ranking the images. (It is common practice for radiologists to adjust the perceived display of images using the WW/WL function).

### *4.3.2 Image Quality Evaluation*

No apparent contrast changes were observed with visual evaluation of the images in Figure 4-4. Quantitative analysis of the subject contrast together with the CNR is given in order of decreasing ESD in Table 4-2.

**Table 4-2: Contrast and CNR for the different beam parameters.**

| *Beam reference | ESD (µGy) | Subject Contrast | CNR |
|---|---|---|---|
| BP5532 | 88.9 ± 0. 5 | 0.055 ± 0.004 | 9.6 ± 1.5 |
| BP6025F | 41.6 ± 1.3 | 0.055 ± 0.006 | 9.9 ± 1.6 |
| BP6620F | 41.6 ± 0.0 | 0.052 ± 0.002 | 9.6 ± 0.8 |
| BP5516 | 40.4 ± 0.8 | 0.080 ± 0.003 | 10.3 ± 1.0 |
| BP7016F | 40.4 ± 0.5 | 0.048 ± 0.001 | 8.3 ± 0.7 |
| BP6020F | 32.3 ± 0.4 | 0.060 ± 0.002 | 8.0 ± 0.4 |

The estimated contrast together with the CNR is displayed as a function of kV, see Figure 4-5.

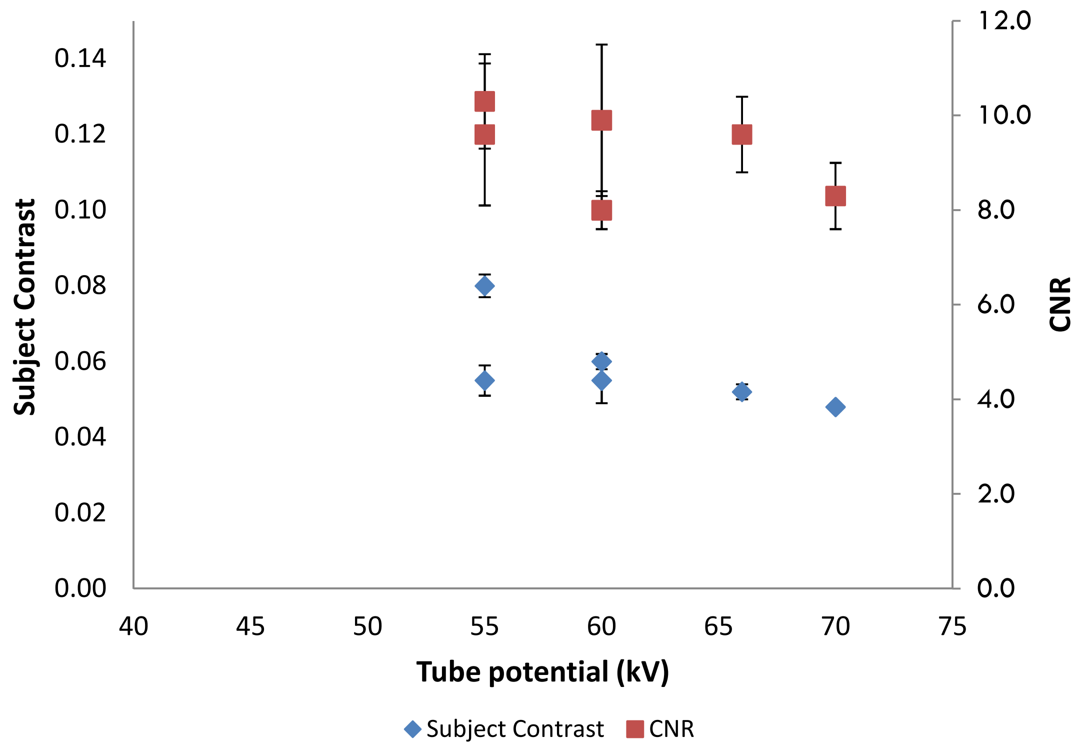


***Figure 4-5: Subject contrast and CNR as a function of tube potential.***

The subject contrast appears to remain fairly constant in the range 55 – 66 kV with a slight decrease above 66kV. The highest subject contrast was obtained with BP5516 and the lowest at BP7016F. The large contrast difference between BP5532 and BP5516 is however unexpected. The CNR also slightly decreased with an increase in kV. The lowest CNR occurred at BP6020F with the second lowest CNR at BP7016F.

The contrast together with the CNR is also displayed as a function of ESD; see Figures 4-6 and 4.7.

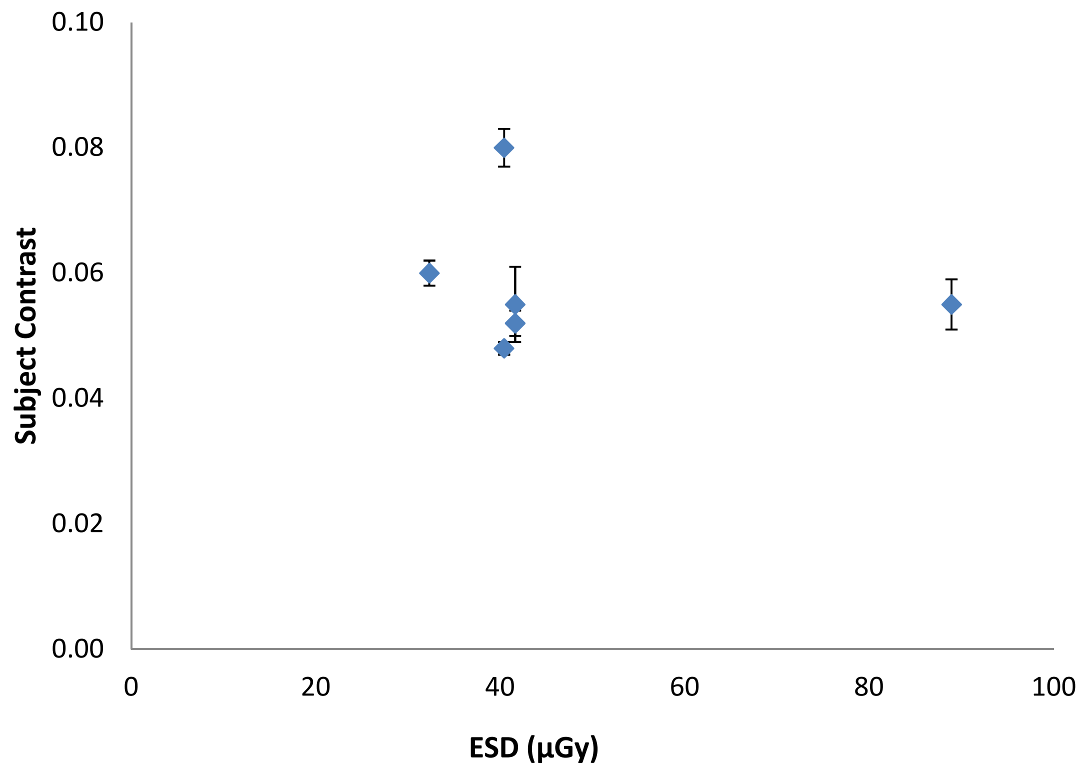


***Figure 4-6: Subject contrast as a function of ESD.***

The subject contrast appears fairly constant even with an approximate doubling of ESD; however an exception was seen at BP5516 having the highest estimated contrast. The highest and lowest contrast was obtained at an ESD of 40.4 µGy.

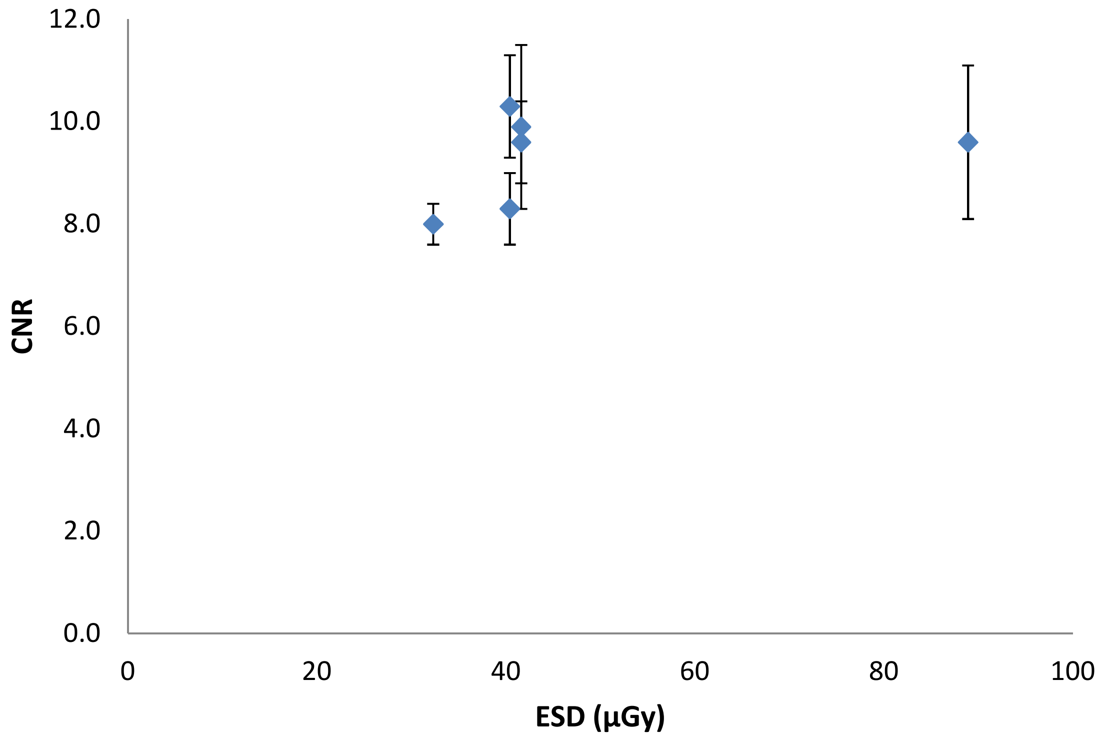


***Figure 4-7: CNR as a function of ESD.***

The CNR slightly increased with increasing ESD up to 40.4 µGy, increasing the ESD beyond this however appears not to improve the CNR. The lowest CNR was obtained at an ESD of 32.3 µGy and the highest CNR at ESD of 40.4 µGy.

The individual image rank positions assigned to each of the six images, by each of the ten observers are given in Table 4-3. This data is represented graphically in Figure 4-8.

**Table 4-3: Observer rank assigned to each image.**

| Beam Parameters | Observers 1 | 2 | 3 | 4 | 5 | 6 | 7 | 8 | 9 | 10 | Average | 95% Confidence Interval |
|---|---|---|---|---|---|---|---|---|---|---|---|---|
| BP5532 | 1 | 1 | 1 | 1 | 1 | 1 | 1 | 1 | 1 | 1 | 1.0 | 1.0 – 1.0 |
| BP6620F | 5 | 6 | 3 | 6 | 3 | 5 | 5 | 3 | 6 | 3 | 4.5 | 3.5 – 5.5 |
| BP6025F | 3 | 5 | 5 | 5 | 5 | 2 | 2 | 5 | 4 | 5 | 4.1 | 3.2 – 5.0 |
| BP7016F | 4 | 3 | 2 | 3 | 6 | 6 | 6 | 6 | 5 | 6 | 4.7 | 3.6 – 5.8 |
| BP5516 | 2 | 4 | 6 | 2 | 4 | 4 | 3 | 2 | 2 | 2 | 3.1 | 2.2 – 4.2 |
| BP6020F | 6 | 2 | 4 | 4 | 2 | 3 | 4 | 4 | 3 | 4 | 3.6 | 2.8 – 4 .4 |

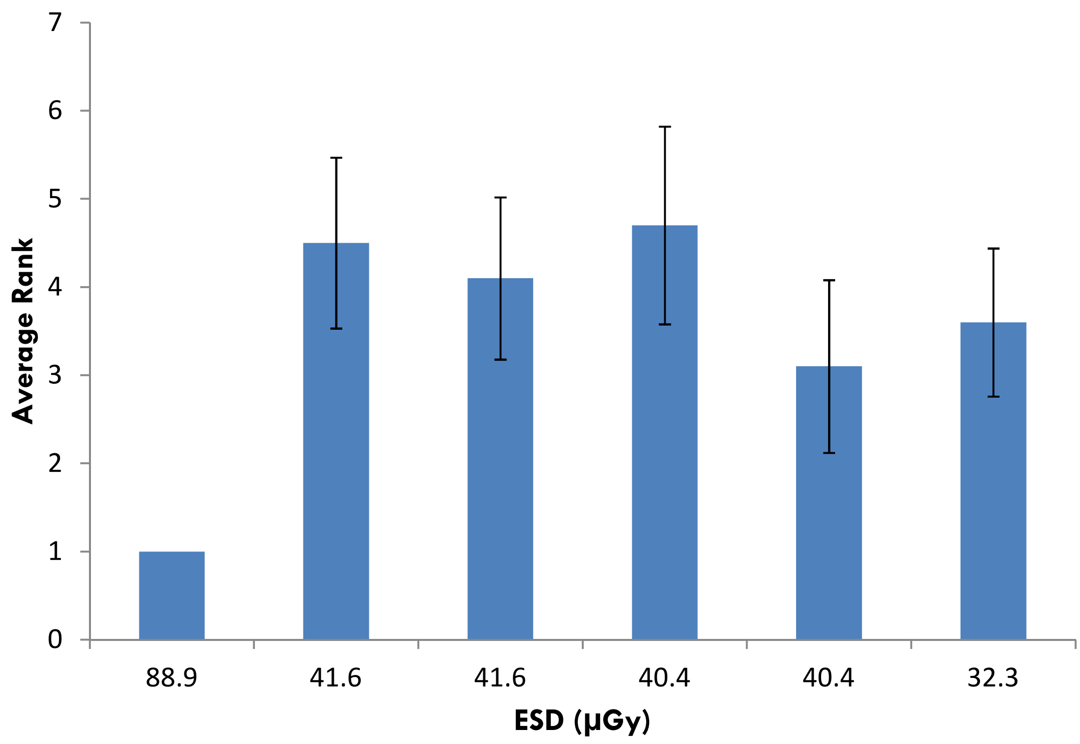


***Figure 4-8: Average image rank per ESD.***

The image quality of the highest dose option 88.9 µGy was ranked best (rank = 1) according to all ten observers. The observers had difficulty to distinguish between the image qualities of the remaining images. The poor observer agreement is confirmed by the ICC = 0.1. The ICC was calculated excluding observer ratings for the highest dose image as it was clear that there were good agreement between observers regarding the image quality of this image, indicated by the lack of error bars.

## 4.4 DISCUSSION

### *4.4.1 Quality Verification of Equipment used*

The x-ray unit, CR plates and reporting monitors all complied with the requirements by the Department of Health Directorate Radiation Control (2014) and were considered to function correctly. Therefore variations in image quality were expected not to be caused by inconsistent equipment performance.

### *4.4.2 Determination of Imaging Parameters*

#### *4.4.2.1 Parameter Selection*

The estimated ESD of the technique currently used for neonatal chest radiography at UAH (BP5532) exceeds the recommended reference values of the European Commission (1996) and the National Radiological Protection Board (NRPB) (2000). This was however not unexpected as lower kV techniques are often associated with higher ESD.

Smans et al. (2010a) indicated that the noise level for evaluation of respiratory distress syndrome at an exit dose of 7 µGy was not distracting when using similar CR plates than the HD 5.0 CR plates (Afga HealthCare) used at UAH. This shows that the exit dose of 24 µGy currently used for neonatal imaging is unnecessarily high and that there is room for improvement of radiographic practice.

The beam parameters 66 kV, 2 mAs (BP6620F) - although similar to those used by Seifert et al. (1998) - had a higher estimated ESD of 41.6 µGy and exit dose of 13 µGy compared to the ESD of 25 µGy and exit dose of 9 µGy measured by Seifert et al. This may be attributed to the use of a different filter combination (1.0 mm Al + 0.1 mm Cu) than the 2 mm Al used in the present study, or a variation in tube output between different x-ray units. BP6020F gave more comparable results. This was expected as the additional Cu, with a higher atomic number, will harden the x-ray beam more than the 2 mm Al used in this study and this will result in a lower ESD when keeping the beam parameters the same. Therefore to achieve a similar ESD than Seifert et al. (1998) a lower kV is needed.

The higher exit dose of filtered beams compared to unfiltered beams at the same ESD is beneficial for image quality. A higher exit dose might be associated with a larger number of photons reaching the detector, or more energetic photons reaching the detector. If a larger quantity of photons reached the detector the image will have less noise and therefore better image quality.

#### *4.4.2.2 Image Quality Evaluation*

The subject contrast stayed fairly constant with a slight decrease at 70 kV. Although lower kV techniques theoretically produce images with higher contrast the wide dynamic range together with the post processing capabilities of CR compared to SF allows the use of higher kV techniques without contrast loss. This is however only true up to the point where contrast loss due to over penetration of tissue cannot be compensated for by post processing. It is therefore important to identify the kV where primary contrast limitations start to play a role.

The large contrast difference between BP5516 and BP5532 could not be explained, as it is expected that the contrast of images at the same kV with different mAs values should remain constant.

The CNR (similar to the subject contrast) stayed fairly constant between 55 – 66 kV with a decrease at 70 kV. This is not unexpected as the lowest contrast was also seen at 70 kV. The

CNR difference at BP6025F and BP6020F both obtained at 60 kV was also not unexpected. Although the contrast stayed constant the increase in noise associated with the lower mAs, 2.0 mAs compared to 2.5 mAs, resulted in the lower CNR. The highest CNR, similar to the subject contrast, was obtained at BP5516. Although the 1.6 mAs might be regarded as low and contributing to more noise that the 2.0 mAs and higher used for the other image acquisitions the high contrast obtained at BP5516 could account for the high CNR at this beam parameter selection compared to the other.

The subject contrast was shown to be independent of ESD with the highest and lowest contrast obtained at the same ESD. This is not unexpected as the primary contrast is mainly influenced by the selected kV, which is then influenced by the post processing. The CNR however showed a slight dependence on ESD, the lowest CNR was obtained at the lowest ESD. This can be due to the increased noise associated with low dose images. This trend did not hold true for al ESD values above 40.4 µGy. Doubling the dose did not increase the CNR.

The highest dose image was ranked as having the best overall image quality. This does however not imply that the other images are of poor diagnostic quality. The observers indicated that in their opinion, all the images where of diagnostic image quality. The lack of a trend in ranking of the lower dose images did not indicate a preference towards a beam parameter selection. If the quality of a specific image was extremely good or poor a trend would have been observed. The poor observer agreement indicated that the ranking of image quality for the lower dose image was purely subjective and based on the personal preference of the observers. This is representative of the clinical setting where radiologists may have different opinions on image quality in spite of the fact that they are able to make a diagnosis.

Poor correlation between physical and subjective image quality evaluation was observed. Although BP6020F had the poorest CNR, this setting obtained the third best average rank. This can be attributed to the HVS being insensitive to small changes in image noise. This is in agreement with Månsson (2000) who also found poor correlation between physical image parameters and clinical image quality.

Out of the five beam parameter settings resulting in an exit dose less than or equal to 14 µGy, two sets had the same ESD. These beam parameter selections were included to investigate whether a preference towards a lower or higher kV technique rendering the same ESD existed. It was decided not to use the beam parameter BP7016F in further investigations since no dose gain was observed and the lowest contrast and second lowest CNR were calculated at this setting. BP6025F will also not be used further in this dose optimization study as BP6620F had a more favourable average ranking at the same ESD.

The fact that not all observers adjusted the WW/WL might have influenced the rank assigned to an image. Although this practise is not preferable and might be considered as a limitation of the study, it is considered to be representative of clinical practice as not all clinicians adjust these parameters equally.

The chicken phantom contained anatomical noise, but did not include structures such as heart and lungs. Image quality criteria such as the reproduction of the heart shadow and bronchi as required by the European Commission (1996) could not be evaluated. Therefore only a crude judgement on the effect of the different beam parameters on image quality could be performed. An anthropomorphic phantom that includes a heart and respiratory system is needed to more thoroughly evaluate the effect of dose reduction, using various image parameter combinations.

## 4.5 CONCLUSION

The ESD of the protocol used for neonatal chest x-rays at UAH exceeds the dose reference levels recommended by the EC and the NRPB. This study found that higher kV techniques up to 66kV with additional 2mm Al filtration offer potential dose reduction, compared to the current low kV technique.

Techniques higher than 66kV is not recommended due to a decrease in subject contrast and CNR without a gain in dose reduction compared to other beam parameters.

Although the additional filtration differed from that recommended by the EC it proved effective for ESD reduction.

The chicken phantom reproduced anatomical noise satisfactorily and is considered a cost-effective phantom for use when investigating the crude effect of different beam parameters on subjective image quality.

Further studies are required to ensure that beam parameters giving a lower ESD do not negatively affect the diagnostic image quality of clinical features such as the reproduction of the vascular lung pattern, the sharp representation of the heart border and diaphragm.

# *CHAPTER 5*

# *BEAM PARAMETER OPTIMIZATION DEPENDING ON ANATOMICAL FEATURES AND OBSERVER PREFERENCE*

## 5.1 INTRODUCTION

The focus on paediatric dose reduction has increased over the past decade. This can be attributed to dose optimization campaigns, such as Image Gently® by the Alliance for Radiation Safety in Paediatric Imaging creating awareness, as well as popular media articles informing the public about radiation. A good example is an article in The New York Times published in 2011 titled: "X-rays and Unshielded Infants", underlining bad practice and urging practitioners using ionizing radiation to re-evaluate their imaging protocols (Bogdanich and Rebelo, 2011).

Although the radiation dose associated with general x-ray examinations are very low and the medical benefit largely outweighs the risk, there is always a possibility of stochastic effects, such as cancer induction. Therefore it is important to ensure that the dose from these examinations is kept as low as possible to limit stochastic effects, but at the same time maintain images with adequate quality to fulfil the diagnostic requirements. To aid in achieving this goal, dose reference levels was recommended for neonatal AP chest x-ray examinations by the European Commission (1996) (ESD ≤ 80 μGy) and the NRPB (2000) (ESD ≤ 50 μGy).

The European Commission (1996) recommends the use of a higher kV radiographic technique, 60 – 65 kV, for neonatal AP chest examinations which is different than the 55 kV and 3.2 mAs with no additional filtration used for neonatal AP chest examinations at UAH hospital. However, changing the beam parameters to the recommended values will influence the image quality.

Image quality is characterized by physical parameters during the primary image formation stage such as contrast, noise and resolution as well as image display parameters and observer perception of image quality as pointed out in Chapter 3. Månsson (2000) indicated that the investigation of physical image parameters alone showed poor correlation to clinical image quality. This may be due to the patient anatomical detail (referred to as structural noise) that influences observer judgement of image quality. According to Hansson et al. (2005) structural noise has a large influence on observer's image quality preference. It is therefore important to not only evaluate physical image quality, but also subjective image quality as discussed in Chapter 3.

Subjective evaluation of image quality can be challenging. Unlike contrast and resolution requirements, no specific value is associated with subjective image quality evaluation. The only requirement is that the images should be diagnostically acceptable and therefore it is dependent on the preference of the observer, unless the truth is known e.g. a diagnosis has been confirmed and the observer has agreed with this fact in reading the image. It is therefore important to select appropriate phantoms that will mimic the clinical scenario as was pointed out in Chapter 3.

The aim of this study was to evaluate the effect of different beam parameter combinations on image quality using a live rabbit phantom (sedated) to simulate the neonatal chest in an attempt to decrease the ESD compared to our current practises.

## 5.2 METHODS AND MATERIALS

Approval to perform the study was obtained from the Ethics Committee, Animal Research Committee and the Radiation Control Committee of the Faculty of Health Sciences University of the Free State, as well as the Head Clinical Service UAH and the Heads of the Departments Clinical Imaging Sciences and Medical Physics respectively.

### *5.2.1 Image Acquisition and Display*

Five living sedated rabbits were used to simulate the neonatal chest. The anatomical features such as heart, lungs and diaphragm contributed to structural noise imitating the clinical situation. The weights of the rabbits were approximately the same as that of the average neonate in the ICU (1960 g, 2050 g, 2210 g, 2220 g and 2120 g). Six images were obtained for each of the five rabbits i.e. an image at each of the six imaging parameter combinations determined in the previous chapter, see Table 5-1.

Radiographic acquisitions were performed using a Siemens Mobilett XP mobile x-ray unit, exclusively used for neonatal radiography at UAH. The routine QC tests performed prior to the measurement were all within the limits set by DOH Directorate Radiation Control (2014). The exit dose and ESD values of this particular x-ray machine was determined using the same method and setup described in the previous chapter.

**Table 5-1: Beam parameters in order of decreasing ESD.**

| *Beam reference | kV | mAs | Additional Filtration (2mm Al) | ESD (µGy) | Exit Dose (µGy) |
|---|---|---|---|---|---|
| BP5532 | 55 | 3.2 | No | 90.9 ± 0.6 | 25.0 ± 0.0 |
| BP5516 | 55 | 1.6 | No | 44.7 ± 2.9 | 17.7 ± 0.6 |
| BP5532F | 55 | 3.2 | Yes | 42.4 ± 1.5 | 15.3 ± 1.2 |
| BP6020F | 60 | 2.0 | Yes | 40.4 ± 1.7 | 11.7 ± 0.6 |
| BP6620F | 66 | 2.0 | Yes | 32.7 ± 1.2 | 12.7 ± 0.6 |
| BP6610F | 66 | 1.0 | Yes | 20.4 ± 0.6 | 8.7 ± 0.6 |

** For ease of reference in the text, the beam parameters are included in the reference names of the beam settings used in the rest of the document.*

Although neonatal chest x-rays are routinely performed in the AP orientation, it was difficult to position the sedated rabbits in a reproducible manner in this orientation. Therefore the PA orientation was used. Acquisitions were done at a FDD of 100 cm simulating clinical practice.

The rabbit was positioned on top of the CR cassette with the field centred at the middle of the shoulder blades and the collimation set to include the entire chest area, Figure 5-1.

The IP was readout within five minutes of image acquisition using the standard mobile chest x-ray protocol (CXR Mobile) at UAH. The images were sent to the picture archive and communication system (PACS) for evaluation.

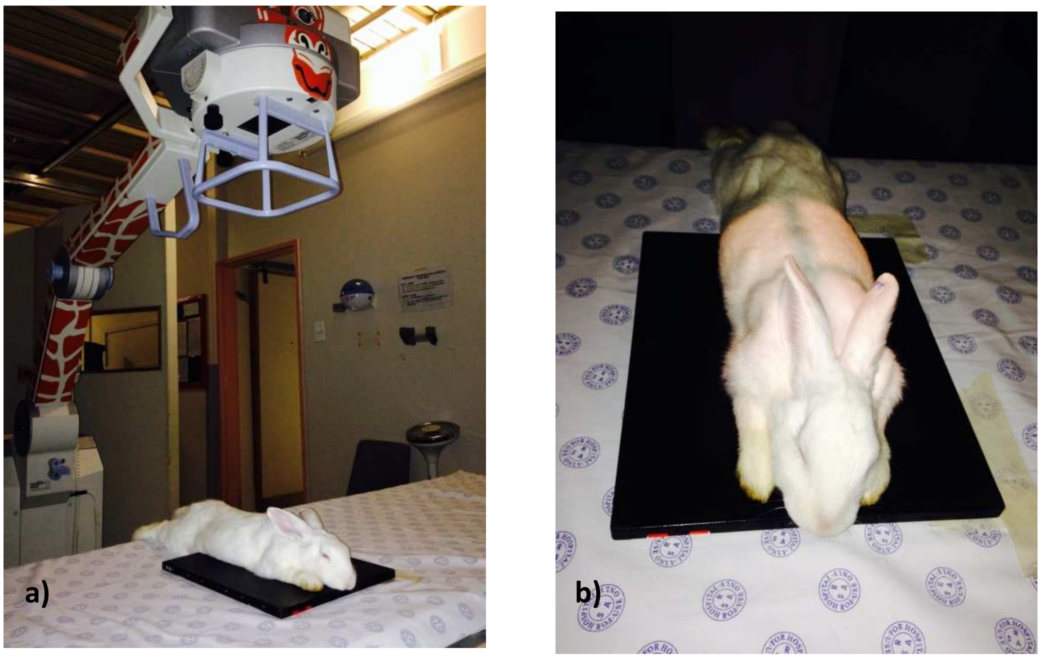


***Figure 5-1: a) Rabbit positioned on top of the CR cassette b) light field indicating collimation.***

### *5.2.2 Image quality evaluation*

Observers were first of all asked to rate the images using the five point scale in Table 5-2 to ensure that all images were of diagnostic quality. Observers were asked to ignore problems with positioning when considering the quality of an image as this study was designed to determine the effect of varying ESD on image quality.

**Table 5-2: Image quality scoring criteria (5-point scale)**

| Score | Diagnostic Quality | Explanation |
|---|---|---|
| 1. | Non-diagnostic quality with high level of noise | Recommend that the examination should be repeated |
| 2. | Borderline diagnostic quality with high level of noise | Study considered barely passable, might recommend a higher dose next time |
| 3. | Acceptable diagnostic quality with moderate noise level | The image is adequate and the dose could possibly be reduced without compromising image quality |
| 4. | Good diagnostic quality with moderate to low noise level | The dose should be reduced |
| 5. | Excellent diagnostic quality with low level of noise | The dose should definitely be reduced |

#### *5.2.2.1 Image features selected for evaluation*

Based on the image criteria for newborn AP chest according to the European guidelines on quality criteria for diagnostic radiographic images in paediatrics (European Commission, 1996) three main categories were identified and used in this study, namely; vascular lung pattern (will be referred to as lung pattern), mediastinum including borders of the heart (will be referred to as mediastinum) and diaphragm together with the costophrenic angles (will be referred to as diaphragm), see Figure 5-2.

Image quality evaluation was done using a variation of the multiple rank order method described by Ravenel et al. (2001) and discussed in more detail in the previous chapter.

Eight radiology registrars (3rd to final year of training), blinded to the dose parameter information, ranked the images of each rabbit from best (rank = 1) to worst (rank = 6) according to their professional judgement and individual preference. During each scoring session observers were asked to evaluate all three anatomical features mentioned above.

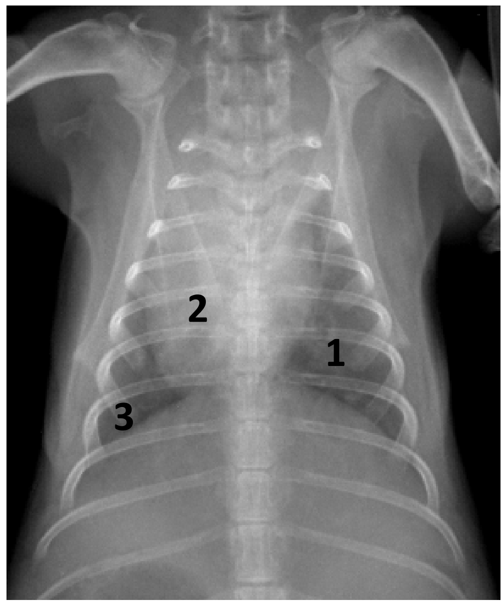


***Figure 5-2: Anatomical features evaluated 1) lung pattern 2) mediastinum 3) diaphragm.***

### *5.2.3 Statistical analysis*

In order to determine if images were regarded as diagnostically acceptable the mode was calculated for each observer's score, based on the overall image quality, according to the five point scale in Table 5-2 and represented graphically (see Figure 5-4).

The average rank position and standard deviation of all five rabbits were calculated for each observer, clinical task and beam setting. Because of the small number of observations per observer, this information is represented graphically as 95 % confidence intervals with no further statistical analysis. The average value of all observers and all rabbits were compared using multiple t - tests. The calculated p-values are used as an indication of the confidence that two averages differ from each other. (The usual 95 % confidence cut-off for an indication of a difference is not applicable in this investigation).

This was repeated for the three anatomical areas, namely (1) lung pattern, (2) mediastinum and (3) diaphragm. Images were also ranked for the clinical tasks combined as an indication of the effect if a clinical task not included in the current investigation may be requested.

The ICC was determined, for all eight observers at each beam parameter setting, using the method described by Zaiontz, C. (n.d.). To assess observer agreement the ICC was calculated for the three anatomical areas as mentioned above. An ICC of less than 0.5 is indicative of poor agreement amongst observers.

## 5.3 RESULTS

### *5.3.1 Image Quality Evaluation*

Image parameters given in Table 5.1 were used to obtain PA chest x-ray images of the rabbit phantom. The images for a rabbit data set are displayed in Figure 5.3.

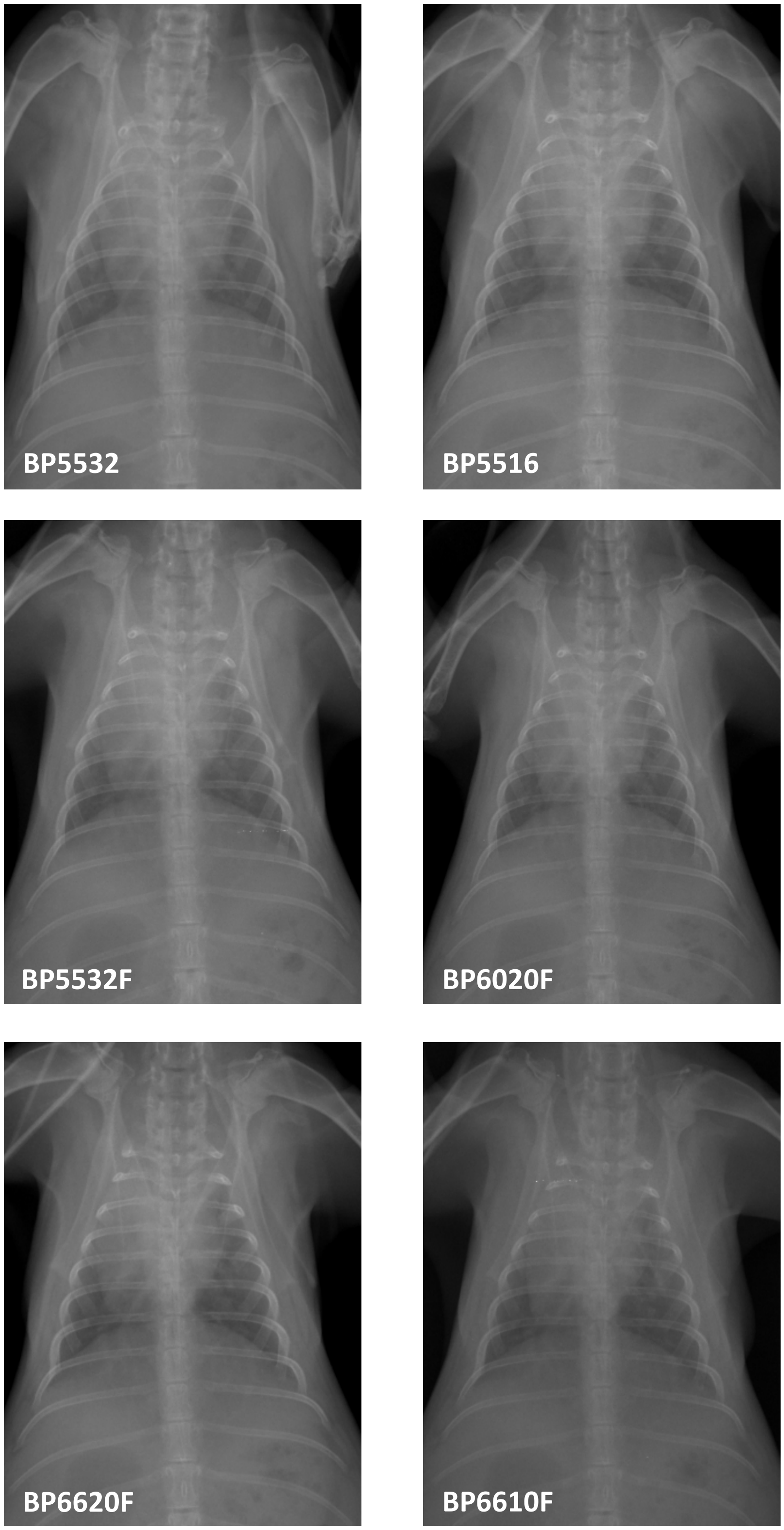


***Figure 5-3: Rabbit phantom images obtained at the beam parameter options given in table 5.1***

The images in Figure 5.3 appear to have the same apparent display contrast after adjustment of the WW/WL. The overall image quality scores assigned by each of the observers to an image obtained with the beam parameter given in Table 5.1 were calculated using the mode. The scores given by the observers were found to be in good agreement, see Figure 5-4.

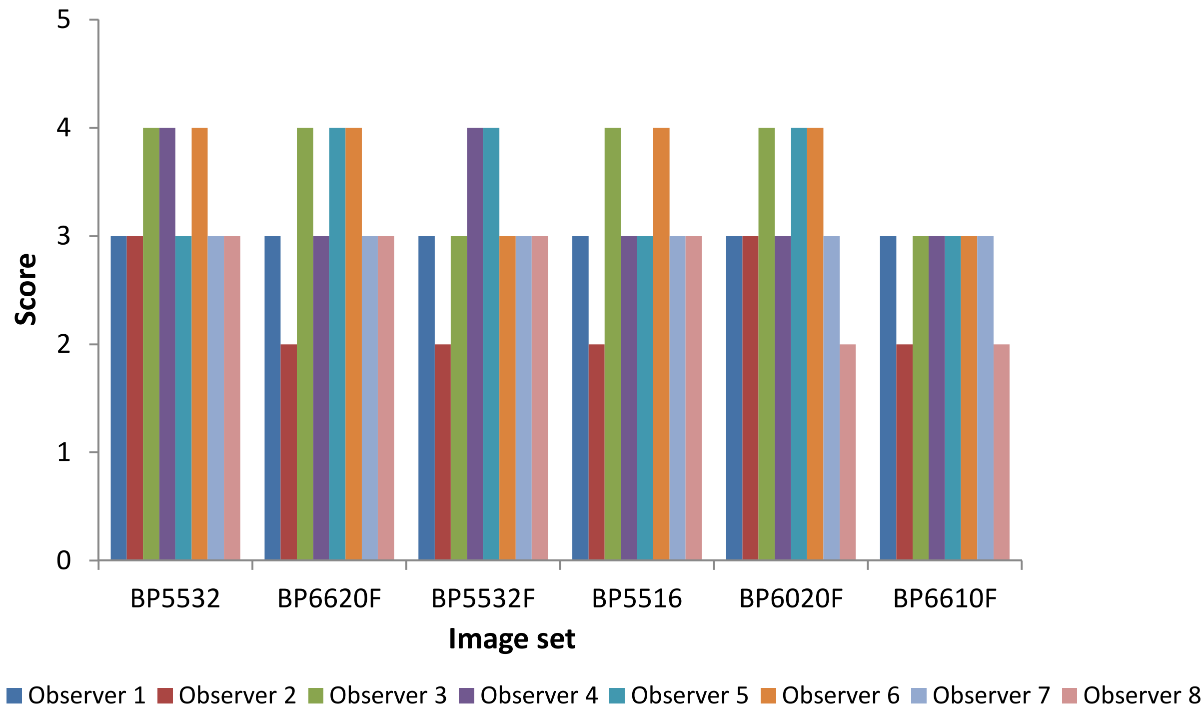


***Figure 5-4: Image quality evaluation based on a 5-point score for each observer at the six beam parameters used to obtain images of the five rabbits.***

From the figure it can be seen that all the images were regarded diagnostically acceptable, although observer two regarded all the images except at BP5532 and BP6020F as barely passable (score = 2).  On the other hand, observers three, four, five and six indicated that the dose can be reduced according to the criteria in Table 5.2  All the observers except for observer eight regarded the images at BP6020F and BP6610F to be acceptable with a moderate level of noise (score = 3)

The rank positions assigned by the observers gave similar results. Large variation between average assigned rank positions by the observers at a single ESD was however observed for the evaluation of the lung pattern, see Figure 5-5.

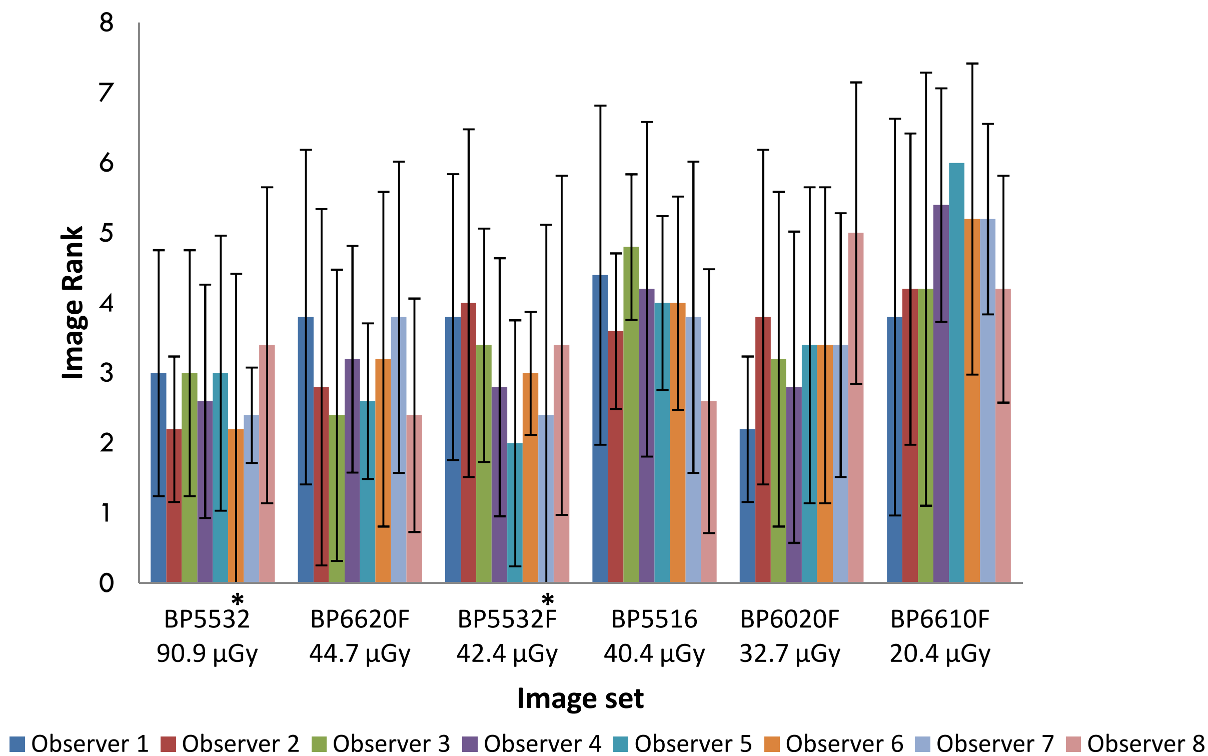


***Figure 5-5: Average image quality ranking, of the 5 rabbit image sets, of the lung pattern vs. ESD.*** ** Indicates error bars clipped at zero. Error bars going negative implies that the image was assigned a negative rank and does not make sense.*

The maximum difference was 2.8 rank positions (observer one and observer eight at BP6020F). The poor observer agreement was quantitatively confirmed with an ICC ≤ 0.4, except at BP6020F and BP6610F where observers had slightly better agreement (Table 5-3).

**Table 5-3: ICC for the lung pattern calculated using the average score of the five rabbit image sets at each beam parameter.**

| Settings | ICC |
|---|---|
| BP5532 | 0.30 |
| BP6620F | 0.40 |
| BP5532F | <0.01 |
| BP5516 | 0.04 |
| BP6020F | 0.60 |
| BP6610F | 0.46 |

Per observer a large variation in opinion was observed when evaluating the images of five rabbits at a fixed ESD. The maximum assigned rank difference for a single observer was 3.1 (observer three at BP6610F). The smallest variation for a single observer was achieved by observer five for the image set BP6610F. Observer five constantly ranked this beam setting at number six indicating the poorest image quality in the opinion of the observer.

The average rank assigned at each ESD, by the eight observers, for the lung pattern is given in Figure 5-6.

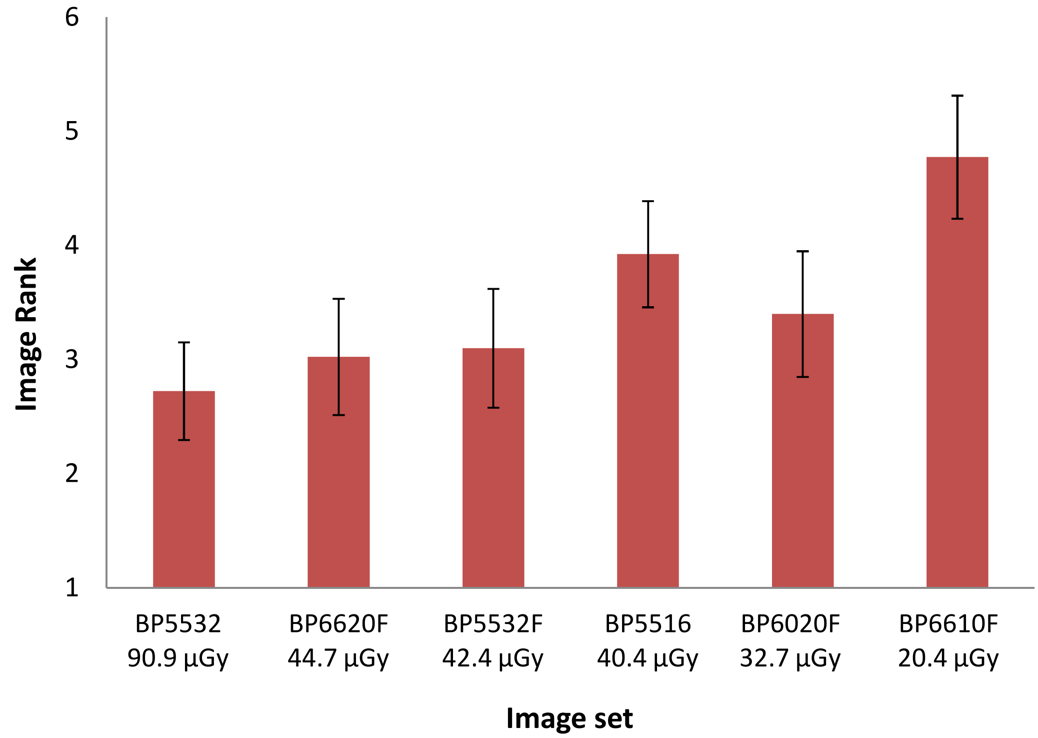


***Figure 5-6: Average rank position of the lung pattern for all eight observers and five rabbits at different ESD values.***

BP5532 had the lowest average rank of 2.7 compared to 3.0 the second lowest rank at BP6620F. A difference in rank position at a dose reduction of approximately 50 % can only be accepted at a 65 % confidence level; however a difference in rank position at a dose reduction up to 80 % (between 55.6 % and 77.6 % ) can be accepted at the standard 95 % confidence level (Table 5-4).

**Table 5-4: Confidence (p-value) required to verify that different dose values will result in different rank positions for the evaluation of the lung pattern.**

| Setting | BP5532 | BP6620F | BP5532F | BP5516 | BP6020F | BP6610F |
|---|---|---|---|---|---|---|
| BP5532 | | 0.35 | 0.23 | 0.01 | 0.05 | < 0.01 |
| BP6620F | | | 0.82 | 0.01 | 0.42 | < 0.01 |
| BP5532F | | | | 0.05 | 0.44 | 0.01 |
| BP5516 | | | | | 0.33 | 0.04 |
| BP6020F | | | | | | 0.01 |
| BP6610F | | | | | | |

The average assigned rank for each observer at different ESD for the mediastinum is given in figure 5-7.

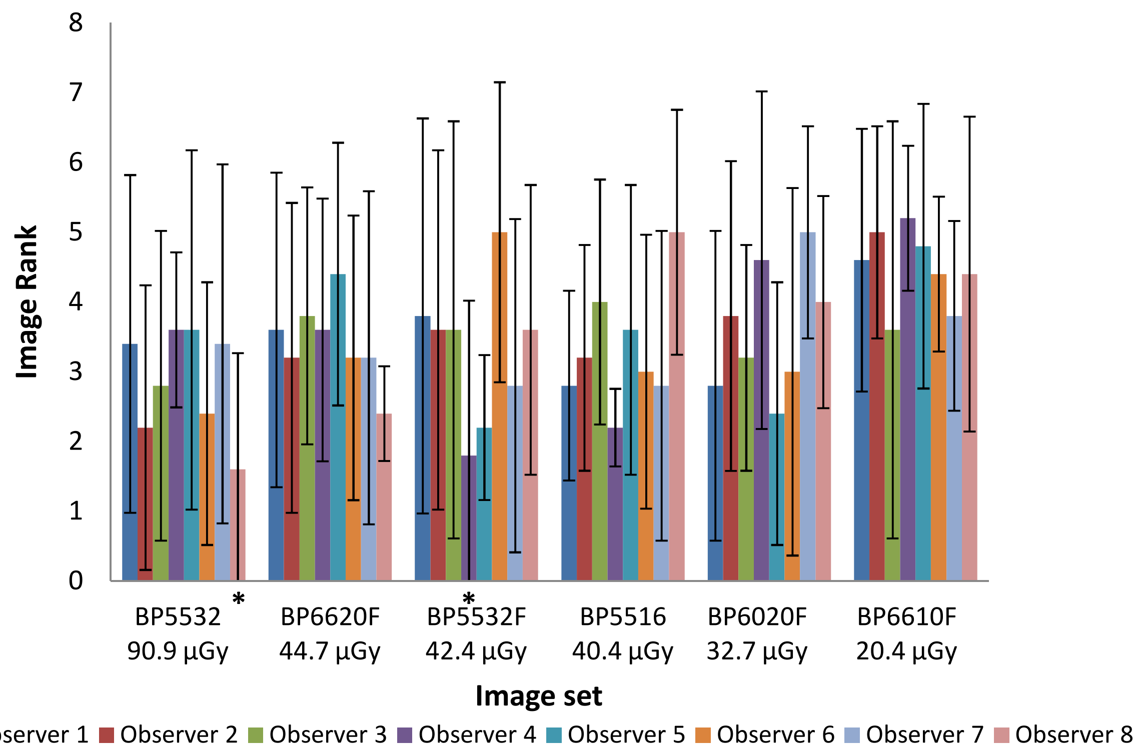


***Figure 5-7: Average observer image quality ranking, of the 5 rabbit image sets, of the mediastinum vs. ESD.***

The maximum difference in assigned rank between two observers at the same ESD was 3.2 (observer four and observer six at BP5532F). The poor overall observer agreement was quantitatively confirmed with an ICC ≤ 0.3 (The smallest variation for a single observer was achieved by observer four for image acquired with BP5516.).

**Table 5-5: ICC for the mediastinum calculated using the average score of the five rabbit image sets at each beam parameter.**

| Settings | ICC |
|---|---|
| BP5532 | 0.05 |
| BP6620F | 0.32 |
| BP5532F | 0.14 |
| BP5516 | 0.11 |
| BP6020F | 0.14 |
| BP6610F | 0.02 |

Similar to the lung pattern large variations in the opinion of a single observer at a fixed ESD was noted when evaluating the five rabbit images. The maximum assigned rank difference for a single observed was 3.0 (observer three at BP5532F). The smallest variation for a single observer was achieved by observer four for image acquired with BP5516.

The average rank of all the observers and rabbits for the mediastinum at the different ESD is given in Figure 5-8.

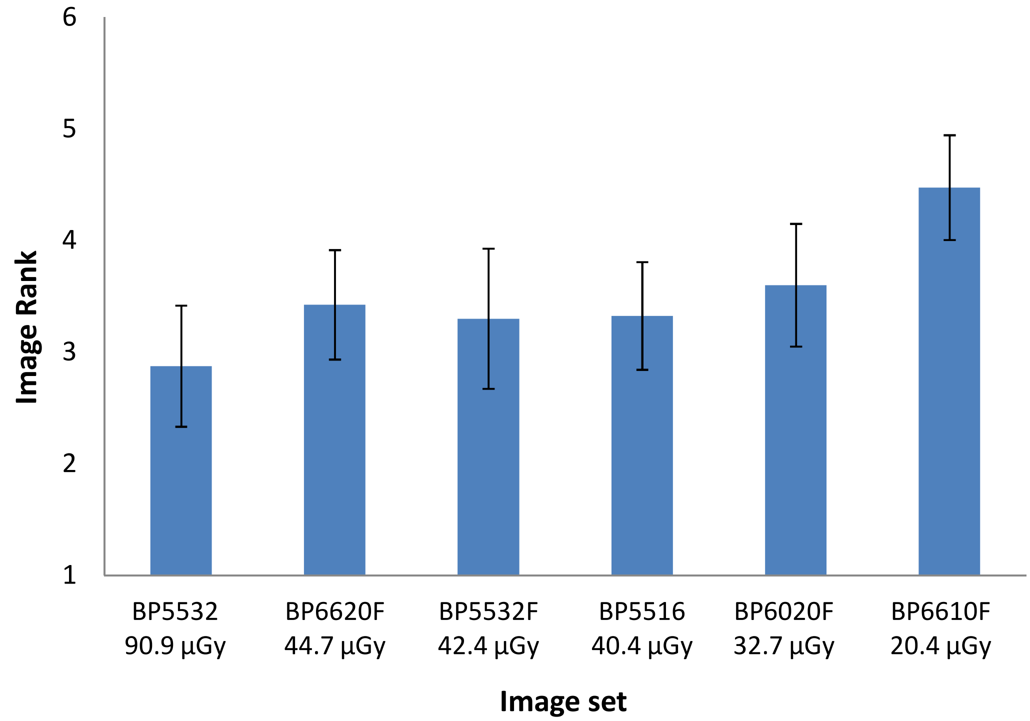


***Figure 5-8: Average rank position of the mediastinum for all observers and rabbits at different ESD.***

The average rank position is slightly better for BP5532 with an average rank of 2.9 compared to 3.3 at BP5532F and BP5516. A difference in rank position for the mediastinum at a dose reduction of approximately 50 % as well as 80 % can be accepted at a 95 % confidence level. However a difference in rank position at a dose reduction of approximately 55 % (between 53.4 % and 55.6 %) can only be accepted at a 53 % - 58 % confidence level (Table 5-6).

**Table 5-6: Confidence (p-value) required to verify that different dose values will result in different rank positions for the mediastinum.**

| Setting | BP5532 | BP6620F | BP5532F | BP5516 | BP6020F | BP6610F |
|---|---|---|---|---|---|---|
| BP5532 | | 0.01 | 0.47 | 0.42 | 0.13 | < 0.01 |
| BP6620F | | | 0.80 | 0.82 | 0.72 | 0.01 |
| BP5532F | | | | 0.95 | 0.61 | 0.04 |
| BP5516 | | | | | 0.59 | 0.03 |
| BP6020F | | | | | | 0.06 |
| BP6610F | | | | | | |

The average image quality rank for the diaphragm for all observers at different ESD is given in Figure 5-9.

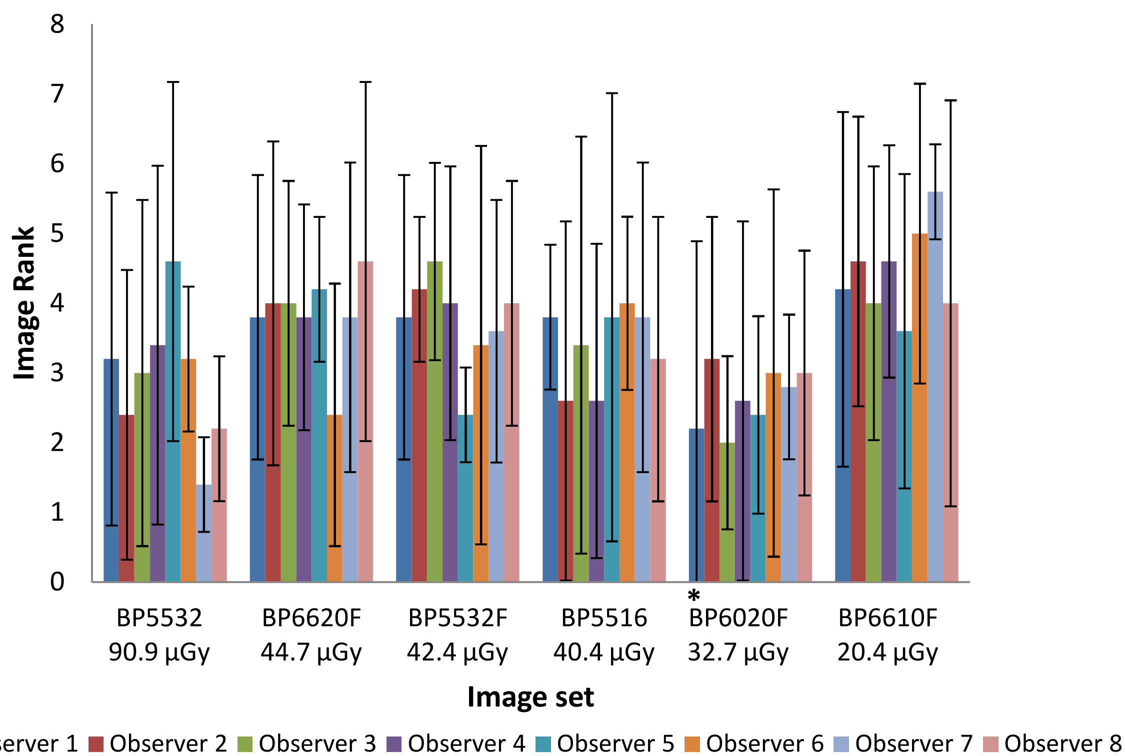


***Figure 5-9: Average observer image quality ranking, of the 5 rabbit image sets, for the diaphragm vs. ESD.***

The maximum difference between observers was 3.2 rank positions (observer five and observer seven for BP5532). The poor observer agreement was quantitatively confirmed with an ICC ≤ 0.4 (Table 5-7).

**Table 5-7: ICC for the diaphragm calculated using the average score of the five rabbit image sets at each beam parameter.**

| Settings | ICC |
|---|---|
| BP5532 | 0.04 |
| BP6620F | 0.38 |
| BP5532F | 0.09 |
| BP5516 | 0.11 |
| BP6020F | 0.12 |
| BP6610F | 0.30 |

The largest variation in rank for a single observer at a fixed ESD, when evaluating five rabbits, was 3.2 (observer five at BP5516). The smallest variation for a single observer is also seen at BP5532 as well as BP6610F (observer seven) and BP5532F (observer five).

The average rank of the diaphragm for all observers and rabbits for different ESD is given in Figure 5-10.

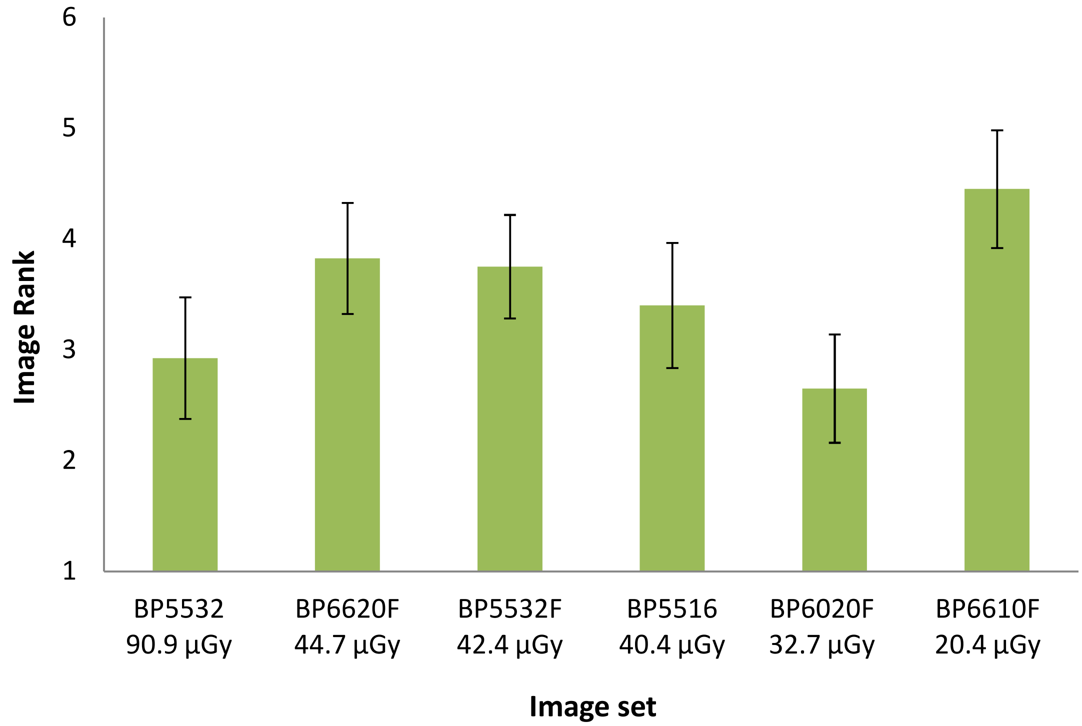


***Figure 5-10: Average rank position of the diaphragm for all observers and rabbits at different ESD.***

The lowest average rank (2.7) was obtained at BP6020F and the second lowest rank at BP5532 (2.9). A difference in rank position of the diaphragm at a dose reduction of approximately 50 % as well as 80 % can be accepted at a 95 % confidence level. However a difference in rank position at a dose reduction of approximately 64 % can only be accepted at a 46 % confidence level (Table 5-8).

**Table 5-8: Confidence (p-value) required to verify that different dose values will result in different rank positions for the diaphragm.**

| Setting | BP5532 | BP6620F | BP5532F | BP5516 | BP6020F | BP6610F |
|---|---|---|---|---|---|---|
| BP5532 | | 0.07 | 0.14 | 0.23 | 0.54 | 0.02 |
| BP6620F | | | 0.81 | 0.27 | <0.01 | 0.16 |
| BP5532F | | | | 0.38 | 0.01 | 0.05 |
| BP5516 | | | | | 0.03 | 0.01 |
| BP6020F | | | | | | <0.01 |
| BP6610F | | | | | | |

The overall observer ranking of the average general image quality as a function of ESD is given in Figure 5-11.

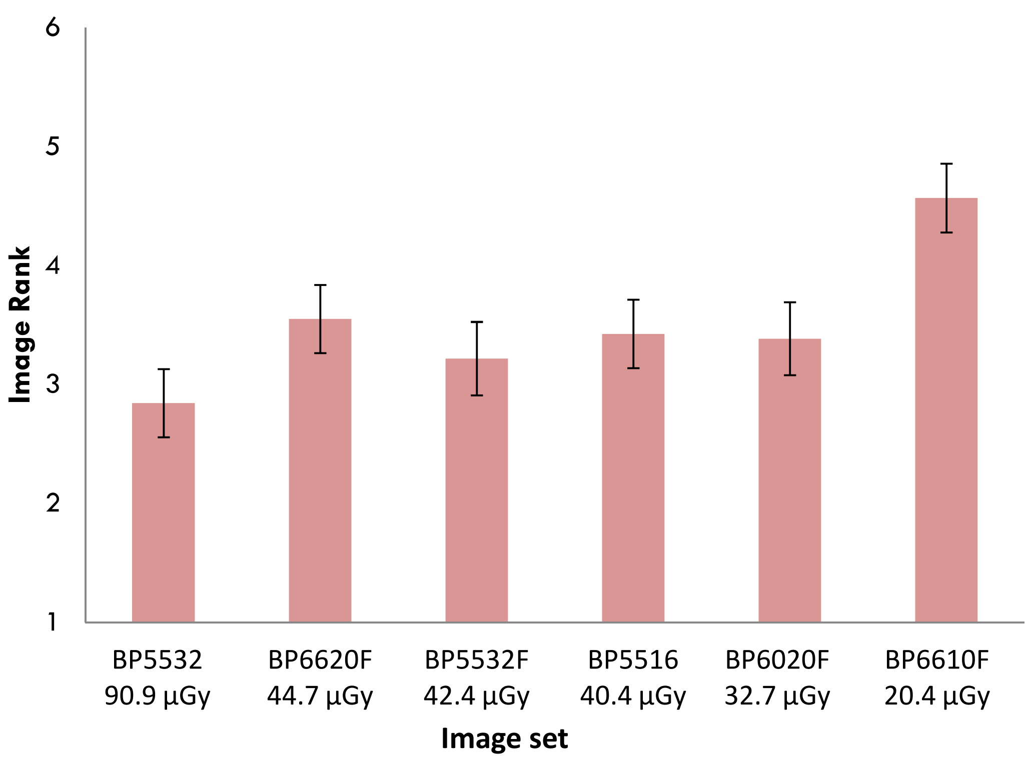


***Figure 5-11: Comparison of the overall image quality at varying ESD.***

The image obtained at BP5532 had the lowest average rank of 2.8 and the second lowest average rank was 3.2 at BP6020F. However the difference in rank position of the overall image quality between BP5532 and BP6020F, at a dose reduction of approximately 64%, cannot be accepted at a 95% confidence level.

**Table 5-9: Confidence (p-value) required to verify that different dose values will result in different rank positions for overall image quality.**

| Setting | BP5532 | BP6620F | BP5532F | BP5516 | BP6020F | BP6610F |
|---|---|---|---|---|---|---|
| BP5532 | | <0.01 | 0.18 | 0.01 | 0.32 | <0.01 |
| BP6620F | | | 0.89 | 0.46 | 0.44 | <0.01 |
| BP5532F | | | | 0.52 | 0.58 | 0.01 |
| BP5516 | | | | | 0.27 | <0.01 |
| BP6020F | | | | | | <0.01 |
| BP6610F | | | | | | |

## 5.4 DISCUSSION

Visual evaluation of the rabbit images obtained with different beam parameters shows very little perceived quality differences, Figure 5.3, even though there is an ESD reduction of 50.8 % - 77.6 % amongst some images. As mentioned previously this can be attributed to the digital image manipulation performed on the primary image. This is an advantage of CR over SF, where previously the display contrast could not be manipulated with post processing or by the observer. A negative feature of the digital image manipulation is that the observer is seldom aware how the manipulation is performed i.e. what happens in the steps from primary image to display image. It is therefore difficult to predict the effect of kV increase on contrast as the decrease of contrast in the primary image can be manipulated up to a certain level before it becomes visible. The manipulation is mostly performed by company specific software and companies are only prepared to make limited information known. Therefore it was not possible to adjust any image manipulation parameters in this study except for the WW/WL which is a standard manual adjustment performed by the observers when interpreting and reporting on radiographic images. The WW/WL adjustment performed by the observer has a large influence on the display image quality. However it is standard practise in clinical image evaluation to adjust the display image and thus the use was not restricted in this study.

The image quality of the images obtained at all six beam parameters (Table 5.1) was regarded as diagnostically acceptable. The larger number of observers gave the images a score of 3 according to the five-point scale (Table 5.2) demonstrating acceptable diagnostic quality with a moderate noise level indicating that the dose could possibly be reduced. According to observer two, however, all the images except the image obtained at BP5532 was of borderline diagnostic quality with a high level of noise indicated by a score of 2 (Figure 5-4). Observer eight also indicated that images obtained at BP6020F and BP6610F was of borderline diagnostic image quality, the clinician would not necessarily repeat the study but the image is considered barely passable. Although most observers regarded images as being diagnostically acceptable (score = 3), three out the eight observers however indicated that the images obtained at BP6020F was of good diagnostic quality with low to moderate levels of noise (score = 4) recommending that the dose could possibly be reduced even further. Three out of the eight observers also indicated that images obtained at BP5532 and BP6620F was of good diagnostic quality (score = 4), these were observers three, four and six and observers three, five and six respectively. Two out of the eight observers also indicated that BP5532F and BP5516 gave images of good diagnostic quality. These were observers four and five and observers three and six respectively. This indicates that it was not always the same observers giving a certain score to images at the different beam parameter settings, indicating the variation in individual preference towards image quality.

Although the images in general were considered diagnostically acceptable it was necessary to evaluate different anatomical regions to establish whether these images would fulfil the diagnostic requirements for neonatal imaging set out by the European Commission (1996).

Large variation in observers' opinion of image quality was observed at a fixed ESD (see Figure 5-5, Figure 5-7 and Figure 5-9). This variation was however not ESD specific, but occurred at each of the six different ESD options investigated. The variation was also observed in the evaluation of all three anatomical areas. The variation in observer opinion of image quality was also seen for the same observer when evaluating images of the five different rabbits at a single ESD. Although some observers seem to agree in their perception of image quality i.e. observers two, six and seven closely agreed on the image quality of the BP6620F (44.7 µGy) image (Figure 5-7), observer two and six did not agree on the image rank of the BP5532F (42.4 µGy) image however observers two, three and eight were in agreement. For the BP6020F (32.7 µGy) image observers one and six agreed on image rank while the other observers varied in opinion. The observer agreement also varied from image to image i.e. observer two and six did not always agree on the image quality at different ESDs. Observer five constantly ranked the image obtained with BP6610F (20.4 µGy) as having the poorest image quality for the evaluation of the lung pattern (Figure 5-5). This was due to rotation in the image obscuring a part of the structure to be evaluated. Although observers were asked not to take positioning into consideration when evaluating image quality, since this will differ from one acquisition to the next in the clinical environment, the observer indicated that it was difficult in his opinion to rank the image without being influenced by the positioning. The other observers did not complain about the positioning. This emphasizes the important role individual preference plays on image quality perception. The variation amongst observers could possibly be explained by their level of experience, as some of the radiology registrars where in their third year of training while others were towards the end of their five year period. However the registrars who were in agreement were in different phases of training.

As discussed in Chapter 3 and seen from the results, human observers have different opinions / preferences regarding image quality. This can sometimes complicate the image quality evaluation as physical parameters alone do not give the entire answer to the question of acceptable image quality. Some observers might accept more noise in an image and still regard the image as complying with the diagnostic task, where other observer might find the image unacceptable. It is therefore important to involve the radiologists at the institution where optimization is performed in the process of image quality evaluation to ensure that the diagnostic requirements will be fulfilled and that the future users will be convinced in this regard.

The rationale for this image quality evaluation method was that if images of the same phantom at different ESD values were evaluated by the observers and a trend was seen from which it could be assumed that a preference towards an image obtained at a certain ESD existed. This may show a preference towards a specific parameter combination, since the ESD is determined by different beam parameters. If the observers do not demonstrate a trend in their ranking of image quality, it can be concluded that they are unable to clearly distinguish a certain image as having better image quality than another image. In other words no preference towards a specific image exists.

BP5532 had the lowest average rank for the evaluation of the lung patterns and was therefore regarded as having the best image quality for the purpose of evaluating the vascular lung pattern. It should be noted that BP5532 is the highest dose option with an estimated ESD of 90.9 µGy and was used as the image quality reference throughout the study. BP5532 was used as a reference for image quality because that was the protocol currently used. Thus with dose reduction the image quality should preferably not be reduced compared to current practice when evaluating lung patterns. When evaluating the lung pattern (Figure 5-6) it could be shown with a 95 % confidence that the observers would assign a different image rank only between the highest dose option BP5532 and options BP5516, BP6620F and BP6610F. The large dose reduction effect of the additional filter should also be noted. Keeping all other parameters constant and by adding only 2 mm Al the ESD was reduced by 53.4 %.

A similar trend was observed when evaluating the mediastinum. BP5532 was regarded as having the best image quality. It could however not be shown with a 95 % confidence that observers would assign a different rank to image obtained with BP5532F, BP5516 and BP6620F at an ESD reduction larger than 50 %. A difference in image rank with a 95 % could only be accepted at BP6610F and BP6620F with a reduced ESD of 64.0 – 77.6 %. It should be noted that although a difference in image quality is noticed it does not imply that the image quality is not diagnostically acceptable.

The images obtained at the highest ESD of 90.9 µGy (BP5532) were regarded as the best quality image when evaluating both the lung patterns and mediastinum. This is not unexpected as this was a low kV, high mAs technique. The low kV theoretically renders better contrast, however this was shown not always to be true in digital radiography (Chapter 4). The higher mAs of 3.2 mAs compared to the other techniques might have contributed to an image with less noise and therefore the higher dose image was preferred rendering a better image quality ranking compared to the other beam parameter options. However images at an ESD of 50.8 % up to 77.6 % less than current practice was still considered diagnostically acceptable. This raises the question whether observers did not prefer the higher dose option, lower kV technique, because that is the type of images that they are used to report on.

For the evaluation of the diaphragm, the image obtained at BP6020F (Figure 5-10) with an ESD of 32.7 µGy which is 64 % less that current practice was regarded as the best image. A difference in rank position between BP5532 and BP6020F could however not be shown with a 95 % confidence (Table 5.8) but only with a 46 % confidence. When combining information of all three anatomical regions, images obtained with BP6610F was the least preferred for all three anatomical sections evaluated, with a 95 % confidence that these images would result in a different rank compared to the reference of BP5532 (Figure 5-6, Figure 5-8 and Figure 5-10). This can be explained by the high kV and low mAs used for this selection. In Chapter 4 it was shown that that an increase from 55 kV to 60 kV did not have a marked effect on the perceived image contrast, however at 66 kV and higher the contrast decreased slightly.

There appeared to be a large variation in image quality between the standard image and the protocols being investigated for the three anatomical areas. When comparing the overall image quality for neonatal chest x-ray examinations by combining the average rank of the three anatomical areas it can be seen that there is a small difference in average image quality (Figure

5-11, except for BP6610F). The images obtained with BP5532 are still the preferred image with an average rank of 2.8. The image obtained at an ESD 32.7 µGy with average rank of 3.2 is considered as having the second best image quality. It could however not be shown with a 95 % confidence that images acquired with BP5532 and BP6020F will have a different image rank i.e. different image quality. This could only be established with a 68 % confidence. As mentioned previously the fact that a difference in image quality could be observed does not imply that the "lesser" images were regarded as diagnostically unacceptable.

All the images acquired with the six protocols were considered diagnostically acceptable and therefore the results indicate a possible dose reduction of 64 % when using the beam parameters; 60 kV, 2.0 mAs and 2 mm additional Al filtration. This protocol is in agreement with the recommendations by the EC to use 60kV for neonatal AP chest x-ray examinations. This protocol will be recommended as a standard for neonates in the weight group up to 2000 g corresponding to the rabbits used. In a study by Frayre et al., (2012) it was found that the mean dose received by each birth weight group did not significantly differ and therefore it is possible to use the same beam parameters for different neonatal weight groups. Radiographers should use their professional judgement for neonates not within the specified weight category.

The estimated ESD of 32.7 µGy for the proposed protocol for neonatal chest x-ray examinations at UAH are in the same range as reported by Armpilia et al. (2002), Ono et al. (2003), Dougeni et al. (2007), Smans et al. (2008) and Duggan et al. (1999), refer to Table 5-10. These studies mostly used SF instead of CR with no additional filtration and 55 kV or less.

Frayre et al. (2012) investigated ESD for neonatal radiography at institutions using CR systems similar to those used at UAH and found the ESD varying between 40.2 - 242.3 µGy. The lowest level compares well with the results obtained in this study. The large variation in reported ESD values shows the variation in image parameter selection, leading to a variation in ESD, amongst the staff within the same department. This variation might be due to the variation in professional judgement of the individual radiographers based on patient size; however such large variations should be minimized in an effort to maintain good practice with doses below reference levels.

In a study by Jones et al. (2001) also using CR with comparable beam parameters to the suggested protocol (62 kV and 2.0 mAs) an average ESD of 56.7 µGy was reported. The higher ESD might be due to the kV being higher than the 60 kV recommended in this study. No mention of additional filtration was made in their report. As previously discussed the use of an appropriate filter will reduce the ESD without affecting image quality. Although the above mentioned studies focussed separately on either dose (mostly surveys) or image quality, no mention was made of investigating these in combination.

Groenewald and Groenewald (2014a) reported a dose reduction of 63 % when using 57 kV, 2.0 mAs and additional filtration of 0.1 mm Cu + 1 mm Al with an estimated ESD of 16.2 µGy. The lower ESD in their study can be explained in part by the lower kV used in their study with the mAs the same as used in this study. Keeping the mAs constant and reducing the kV will reduce the dose. The different filter combination will also play a large role as the 0.1 mm Cu + 1 mm Al additional filtration is equivalent to 6 mm additional Al compared to the 2 mm Al used in the current study (Groenewald and Groenewald, 2014a). It will therefore result in a lower ESD. The above mentioned study also used CR, a different detector system (which might function better at lower kV technique) was however used and this will affect the beam parameter selection. A similar scoring criteria to that used in the current study was also used by Groenewald and Groenewald (2014a) with the exception of an in-house developed neonatal phantom which might also result in a difference in image quality ratings.

The current study is unique as radiologists evaluated the images in a clinical setup using an image quality score specifically adapted for neonatal chest imaging. It is also known that using higher kV techniques will reduce the dose, however the optimal mAs selection is not known and this should be investigated by each institution with the available additional filtration. The image quality evaluation method used in this study only gives an indication whether differences in image quality caused by a change in beam parameters can be observed. If no change in image quality is observed the dose can be confidently reduced and the process repeated to reduce the dose even further. If differences are however seen the clinical impact must be considered before a further dose reduction can be made.

Although the rabbit phantom image closely resembles clinical neonatal chest images, a limitation of the study is that it was not performed on neonates. This would however not have been feasible in the early stages of experimental exposures which would contribute to the high radiation dose. The clinical questions in the study was limited to general neonatal chest x-ray examinations and therefore the suggested lower dose protocol might not be acceptable for specialised radiographic examinations. This could be an area of further investigation where clinicians and radiologists are interviewed to obtain specific image quality needs for these special examinations. Specialised x-ray examinations are however not requested as frequently and therefore, from a radiation protection point of view consideration was given to the most frequently requested neonatal general x-ray examination namely AP chest.

The limitations of the study includes the involvement of the human factor, observers evaluating the image might get tired and distracted. This was however not considered to influence the results as it gives a close approximation of the situation when the observers evaluate clinical images. The method might also be considered time consuming, but when compared to other subjective evaluation methods it is considered reasonable and the benefit to the patient should be kept in mind.

**Table 5-10: Comparison of parameters and ESD from different studies for neonatal chest radiography**

| Study | kV | mAs | Additional Filtration | Average ESD (µGy) | FFD (cm) | | Approx. Mean weight (g) |
|---|---|---|---|---|---|---|---|
| Current study | 60 | 2.0 | 2 mm Al | 32.7 | 100 | Agfa CR | 2000 |
| (Jones et al., 2001) | 62 | 2.0 | Not specified | 56.7 | 105 | Fuji AC1 CR System | 2500 |
| (Olgar et al., 2008) | 49 (46-51) | 1.9 (1.6-3.5) | Not specified | 67.0 | 100 | Kodak T-mat G/RA film + Kodak Lanex regular screen (400 speed) | 1500 |
| (Faghihi et al., 2012) | 50-70 | 1.0-2.5 | Not specified | 50.0 | 100 | Not specified | 2000 |
| (Ono et al., 2003) | 55 | 1.2 | Not specified | 34 | 90 | Not specified | 2000 |
| (Armpilia et al., 2002) | 53.1 | 2.0 | Not specified | 36 (27.8-49.0) | 100 | Kodak T-mat G/RA film + Kodak Lanex regular screen (400 speed) | Not specified |
| (Dougeni et al., 2007) ≤1000g | 52.5 (45-66) | 1.1 (0.5-2.5) | | 29.8 (16.4-76.9) | 100 | Kodak film + Kodak Lanex regular screen | 2245 |
| 1000-1500g | 52.3 (44-64.5) | 1.2 (0.5-2.0) | | 32.4 (17.8-47.4) | | | |
| 1500-2500g | 52.3 (44-66) | 1.4 (0.5-2.2) | | 37.5 (16.5-57.9) | | | |
| ≥2500g | 54.1 (47-64.5) | 1.6 (0.5-2.6) | | 45.4 (21.1-74.9) | | | |
| (Duggan et al., 1999) | 54 | 1 | Not specified | 35 | 100 | 200 speed system | |
| (Rattan and Cohen, 2013) | 66 | 1 | Not specified | | | | 1500 |
| (Frayre et al., 2012) | 48.9 (43-61) | 1.51 (0.9-2.0) | Not specified | 40.2-242.3 | 70-104 | Agfa CR system | 1158.9 |
| (Smans et al., 2008) | 66 | 0.8 | Not specified | 34 (3-101) | 100 | | 1900 |
| (McParland et al., 1996) | 52-60 | 0.8 | Not specified | 20 | 96.5 | Kodak T-mat G film + Kodak Lanex regular screen (400 speed) | Not specified |
| Groenewald and Groenewald, 2014a | 57 | 2.0 | 0.1 mm Cu + 1 mm Al | 16.2 | 100 | Fuji FCR, Fuji IP CC Cassettes | Not specified |

## 5.5 CONCLUSION

This study showed the marked influence of anatomical noise and the effect of individual opinion of the observers on clinical image quality interpretation. This emphasizes the need for subjective evaluation of clinical image quality in optimization studies. Physical image quality indicators such as contrast and noise have been shown to be an incomplete description of the effect that a change in beam parameters will have on clinical image quality and must therefore be combined with a subjective image quality evaluation. It is also important to select an appropriate phantom, including anatomical features and a likeness to patient images, for clinical image quality evaluation when adjusting the dose.

The rabbit phantom used in this study gives a good indication of clinical structures of interest in neonatal imaging and is cost effective compared to other anthropomorphic phantoms. The multiple rank order method used by Ravenel et al. (2001) was adapted to suit the clinical environment and image quality assessment needs for neonatal imaging at UAH. The method worked well and could be easily adapted for other radiographic imaging applications and executed within a reasonable time period.

The study also showed that a dose reduction of 64 % for general neonatal chest x-ray examinations can be achieved by altering the beam parameters. This reduction will result in an estimated ESD of 32.7 µGy compared to the ESD of 90.9 µGy, by using 60 kV, 2 mAs and 2 mm additional Al filtration as suggested by the European Commission (1996) recommendations for paediatric imaging. Although the ESD is not an indicator of cancer risk a reduction in ESD will minimize the possible stochastic effects and is in agreement with the ALARA principle.

The suggested imaging protocol will be recommended for use in general neonatal chest x-ray examinations. Mobile x-ray units used for neonatal radiography at our institution do not have the option to select additional filtration. It is therefore being recommended to install additional filtration on the x-ray units or motivate that a new unit with a filter tray be purchased for use in neonatal radiography, especially since it is common knowledge that neonates are very sensitive to radiation and reducing the ESD will also reduce the radiation risk

Limited clinical questions were asked in the study as the study only focussed on general neonatal chest x-ray examinations. Further research may include more dose reduction for less demanding investigations such as reviewing the placement of endotracheal tubes and intravenous lines, where the objective is to see if these lines were inserted correctly or if the lines have moved from the intended position. If no other diagnostic information is required, the dose can be reduced further as the diagnostic task is different compared to a general chest x-ray imaging. Radiologists can then evaluate these lower dose images to see if it will fulfil the diagnostic requirement of other more complex clinical conditions requiring more demanding image quality.

In conclusion, the general lack of agreement between the rankings of the different observers is a clear indication that it is very difficult to tell the difference between the images under investigation. The radiation dose resulting from chest x-rays to neonates can therefore be lowered with the appreciation that no clinical information will be lost if the recommended protocol is followed. Taking advantage of the recommended protocol in chest imaging may also pave the way for future dose reduction in other clinical conditions.

# BIBLIOGRAPHY


Armpilia, C.I., Fife, I.A.J., Croasdale, P.L., 2002. *Radiation dose quantities and risk in neonates in a special care baby unit*. Br. J. Radiol., 75, pp. 590–595.

Azevedo, A.C.P., Osibote, O.A., Boechat, M.C.B., 2006. *Paediatric x-ray examinations in Rio de Janeiro*. Phys. Med. Biol,. 51, pp. 3723–3732.

Barrera-Rico, M., López-Rendón, X., Rivera-Ordóñez, C.E., Gamboa-deBuen, I., (2012). *Entrance surface dose in cerebral interventional radiology procedures*, In: AIP Conference Proceedings. Presented at the MEDICAL PHYSICS: Twelfth Mexican Symposium on Medical Physics, AIP Publishing, pp. 76–78.

Båth, M., Håkansson, M., Hansson, J., Månsson, L.G., 2005. *A Conceptual Optimisation Strategy for Radiography in a Digital Environment*. Radiat. Prot. Dosimetry. 114, pp. 230–235.

Blencowe, H., Cousens, S., Oestergaard, M.Z., Chou, D., Moller, A.-B., Narwal, R., Adler, A., Vera Garcia, C., Rohde, S., Say, L., Lawn, J.E., 2012. *National, regional, and worldwide estimates of preterm birth rates in the year 2010 with time trends since 1990 for selected countries: a systematic analysis and implications.* The Lancet, 379, pp. 2162–2172.

Bogdanich, W., Rebelo, K., 2011. *X-rays and unshielded infants*. The New York Times, viewed 8 October 2014, **<** http://www.nytimes.com/2011/02/28/health/28radiation.html>.

Boice, J.D., 1998. *Cancer following irradiation in childhood and adolescence*. Med. Pediatr. Oncol., 27, pp. 29–34.

Borisova, R., Ingilizova, C., Vassileva, J., 2008. *Patient Dosimetry in Paediatric Diagnostic Radiology*. Radiat. Prot. Dosimetry, 129, pp. 155–159.

Burton, E.M., Kirks, D.R., Strife, J.L., Henry, G.C., Kereiakes, J.G., 1988.*Evaluation of a low-dose neonatal chest radiographic system*. AJR, 151, pp. 999-1002.

Bushberg, J.T., Seibert, J.A., Leidholdt, E.M., JR., Boone, J.M., 2011. *The Essential Physics of Medical Imaging*, Third Edition, Lippincott Williams & Wilkins, Philadelphia.

Bushberg, J.T., Seibert, J.A., Leidholdt, E.M., JR., Boone, J.M., 2001. *The Essential Physics of Medical Imaging*. Second edition. Lippincott Williams & Wilkins, Philadelphia .

Chapple, C.L., Faulkner, K., Hunter, E.W., 1994. *Energy imparted to neonates during X-ray examinations in a special care baby unit*. Br. J. Radiol., 67, pp. 366–370.

Dabin, J., Struelens, L., Vanhavere, F., 2014. *Radiation dose to premature new-borns in the Belgian neonatal intensive care units*. Radiat. Prot. Dosimetry, 158, pp. 28-35.

Datz, H., Ben-Shlomo, A., Bader, D., Sadetzki, S., Juster-Reicher, A., Marks, K., Smolkin, T., Zangen, S., Margaliot, M., 2008. *The additional dose to radiosensitive organs caused by using under-collimated X-ray beams in neonatal intensive care radiography*. Radiat. Prot. Dosimetry, 130, pp. 518–524.

Dendy, P.P., Heaton, B., 1999. *Physics for Diagnostic Radiology*, Second Edition. Institute of Physics Publishing, London.

Department of Health Directorate Radiation Control 2014, *Requirements for licence holders with respect to quality control tests for diagnostic x-ray imaging systems*, CODE: DIAGNOSTIC QC Version 8, Department of Health, South Africa.

Don, S., Hildebolt, C.F., Sharp, T.L., Shackelford, G.D., Lau, D.M., Herman, T.E., McAlister, W.H., 1999. *Computed radiography versus screen-film radiography: detection of pulmonary edema in a rabbit model that simulates neonatal pulmonary infiltrates*. Radiology, 213, pp. 455–460.

Dougeni, E.D., Delis, H.B., Karatza, A.A., Kalogeropoulou, C.P., Skiadopoulos, S.G., Mantagos, S.P., Panayiotakis, G.S., 2007. *Dose and image quality optimization in neonatal radiography*. Br. J. Radiol., 80, pp. 807–815.

Duggan, L., Sathiakumar, C., Warren-Forward, H., Symonds, M., McConnell, P., Smith, T., Kron, T., 1999. *Suitability of LiF:Mg,Cu,P and Al2O3:C for Low Dose Measurements in Medical Imaging*. Radiat. Prot. Dosimetry, 85, pp. 425–428.

European Commission, 1996. *European Guidelines on Quality Criteria for Diagnostic Radiographic Images in Paediatrics*, Report EUR 16261, European Commission, Luxembourg.

European Signal Processing Conference (EUSIPCO), 9$^{th}$. 1998. Greece, (1998). A technique for image quality assessment based on a human visual system model, Osberger, W., Maeder, A., Bergmann, N.

Faghihi, R., Mehdizadeh, S., Sina, S., Alizadeh, F.N., Zeinali, B., Kamyab, G.R., Aghevlian, S., Khorramdel, H., Namazi, I., Heirani, M., Moshkriz, M., Mahani, H., Sharifzadeh, M., 2012. *Radiation Dose to Neonates Undergoing X-Ray Imaging in Special Care Baby Units in Iran*. Radiat. Prot. Dosimetry, 150, pp. 55-59.

Frayre, A.S., Torres, P., Gaona, E., Rivera, T., Franco, J., Molina, N., 2012. *Radiation dose reduction in a neonatal intensive care unit in computed radiography*. Appl. Radiat. Isot., 71, Supplement, pp. 57–60.

Gammex, 2008. Physics behind the phantom volume 2, The Neonatal Chest Phantom. Gammex Inc., Middleton, USA, viewed 6 February 2013 <http://www.gammex.com/ace-files/610_Neonatal_Chest_Phantom_WP.pdf>

Gotanda, R., Katsuda, T., Gotanda, T., Tabuchi, A., Yatake, H., Takeda, Y., (2009). *Dose Distribution in Pediatric CT Head Examination: Phantom Study*, In: Sloten, J.V., Verdonck, P., Nyssen, M., Haueisen, J. (Eds.), 4th European Conference of the International

Federation for Medical and Biological Engineering, IFMBE Proceedings. Springer Berlin Heidelberg, pp. 775–779.

Groenewald, A., Groenewald, W. A., 2014. *Reduction of radiation dose and relative risk of cancer induction to neaonates receiving anterior-posterior chest x-rays*. GJSFR, 14, pp. 33-40

Groenewald, A., Groenewald, W. A., 2014. *In-house development of a neonatal chest simulation phantom. Journal of Applied Clinical Medical Physics*, 15, pp. 282-296

Hanson, K.M., (1998) *A Simplified Method of Estimating Noise Power Spectra*. Dobbins, J.T., Boone, J.M. SPIE Proceedings Vol. 3336 Medical Imaging 1998: Physics of Medical Imaging, SPIE.

Hansson, J., Båth, M., Håkansson, M., Grundin, H., Bjurklint, E., Orvestad, P., Kjellström, A., Boström, H., Jönsson, M., Jonsson, K., Månsson, L.G., 2005. *An optimisation strategy in a digital environment applied to neonatal chest imaging*. Radiat. Prot. Dosimetry, 114, pp. 278–285.

Hart, D., Wall, B.F., Schrimpton, P.C., Bungray, D.R., Dance, D.R., 2000. *Reference doses and patient size in paediatric radiology*. National Radiological Protection Board (NRPB), R318, NRPB, United Kingdom.

Hendee, W.R., Ritenour, E.R., 2003. *Medical Imaging Physics*. Fourth Edition, John Wiley & Sons, New Jersey.

Honey, I.D., Mackenzie, A., Evans, D.S., 2005. *Investigation of optimum energies for chest imaging using film-screen and computed radiography*. Br. J. Radiol. 78, pp. 422–427.

International Atomic Energy Agency (IAEA), 2014. *Diagnostic radiology physics: a handbook for teachers and students*, IAEA, Vienna.

ICRP, 2007. International Commission on radiological Protection (ICRP), 2007. *The 2007 recommendations of the international Commission on radiological protection*, Annals of Publication 103, Elsevier, UK.

ICRU, 2005. International Commission on Radiation Units (ICRU), 2005. *Appendix A: backscatter factors*. Journal of the ICRU, 5, Report 74, pp 65-67. Oxford University Press.

IPEM, 2005. Institute of Physics and Engineering in Medicine (IPEM), 2005. *Recommended Standards for Routine Performance Testing of Diagnostic X-ray Imaging Systems*, IPEM Report 91.

Jones, N.F., Palarm, T.W., Negus, I.S., 2001. *Neonatal chest and abdominal radiation dosimetry: a comparison of two radiographic techniques*. Br. J. Radiol., 74, pp. 920–925.

King's centre for the assessment of radiological equipment (KCARE), *CR QA Protocol Draft 8.0,* viewed 11 October 2014, <http://www.scribd.com/doc/91419388/CR-Physics- ProtocolDRAFT8-0#scribd>

Khotle, T., Vos, H. de, Herbst, C.P., Rae, W.I.D., 2009. *Optimization of Exposure Factors and Image Quality for Computed Radiography*, in: Dössel, O., Schlegel, W.C. (Eds.), World Congress on Medical Physics and Biomedical Engineering, September 7 - 12, 2009, Munich, Germany, IFMBE Proceedings. Springer Berlin Heidelberg, pp. 251–254.

Koenig, T.R., Wolff, D., Mettler, F.A., Wagner, L.K., 2001. *Skin injuries from fluoroscopically guided procedures: part 1, characteristics of radiation injury*. AJR Am. J. Roentgenol., 177, pp. 3–11.

Lawn, J.E., Cousens, S., Zupan, J., 2005. *4 million neonatal deaths: When? Where? Why?* The Lancet, 365, pp. 891–900.

Loader, R.J., Gosling, O., Roobottom, C., Morgan-Hughes, G., Rowles, N., 2012. *Practical dosimetry methods for the determination of effective skin and breast dose for a modern CT system, incorporating partial irradiation and prospective cardiac gating*. Br. J. Radiol., 85, pp. 237–248.

Lowe, A., Finch, A., Boniface, D., Chaudhuri, R., Shekhdar, J., 1999. *Diagnostic image quality of mobile neonatal chest X-rays and the radiation exposure incurred*. Br. J. Radiol., 72, pp. 55–61.

Mansilla, W.A., Perkis, A., Ebrahimi, T., 2009. *Exposure effect on experience and visual perception in stereoscopic visual presentations*, In: Proceedings of the International Conference on Advances in Computer Enterntainment Technology, ACE '09. ACM, New York, NY, USA, pp. 332–335.

Månsson, L.G., 2000. *Methods for the evaluation of image quality: a review*. Radiat. Prot. Dosimetry, 90, pp. 89–99.

McParland, B.J., Gorka, W., Lee, R., Lewall, D.B., Omojola, M.F., 1996. *Radiology in the neonatal intensive care unit: dose reduction and image quality*. Br. J. Radiol., 69, pp. 929–937.

Meredith, W.J., Massey, J.B., 1977. *Fundamental Physics of Radiology*. Third Edition, John Wright & Sons Ltd, Bristol.

Mutch, S.J., Wentworth, S.D.P., 2007. *Imaging the neonate in the incubator: an investigation of the technical, radiological and nursing issues.* Br. J. Radiol., 80, pp. 902–910.

Niemann, T., Reisinger, C., Rau, P., Schwarz, J., Ruis-Lopez, L., Bongartz, G., 2010. *Image quality in conventional chest radiography. Evaluation using the postprocessing tool Diamond View*. Eur. J. Radiol., 73, pp. 555–559.

Olgar, T., Onal, E., Bor, D., Okumus, N., Atalay, Y., Turkyilmaz, C., Ergenekon, E., Koc, E., 2008. *Radiation exposure to premature infants in a neonatal intensive care unit in Turkey*. Korean J. Radiol., 9, pp. 416–419.

Ono, K., Akahane, K., Aota, T., Hada, M., Takano, Y., Kai, M., Kusama, T., 2003. *Neonatal doses from X ray examinations by birth weight in a neonatal intensive care unit*. Radiat. Prot. Dosimetry, 103, pp. 155–162.

Rattan, A.S., Cohen, M.D., 2013. *Removal of comfort pads underneath babies: a method of reducing radiation exposure to neonates*. Acad. Radiol., 20, pp. 1297–1300.

Ravenel, J.G., Scalzetti, E.M., Huda, W., Garrisi, W., 2001. *Radiation exposure and image quality in chest CT examinations*. AJR Am. J. Roentgenol., 177, pp. 279–284.

Schneider, K., Kohn, M.M., Ernst, G.E., 1998. *The Derivation of Reference Dose Values to Chest X Rays in Paediatric Radiography*. Radiat. Prot. Dosimetry, 80, pp. 199–202.

Seibert, J.A., 2004. *Computed radiography technology 2004*. Presented at: AAPM Summer School: Specifications, performance evaluation and QA of radiographic and fluoroscopic systems in the digital era, Carnegie Mellon University, Pittsburgh Pennsylvania, viewed on 14 November 2014 <https://www.aapm.org/meetings/04SS/documents/seibert.PDF>

Seifert, H., Jesberger, H.J., Schneider, G., Rein, L., Blass, G., Limbach, H.G., Niewald, M., Sitzmann, F.C., Kramann, B., 1998. *Dose reduction in thorax radiography in simulated neonates with additional filtration and digital luminescence radiography*. Acta Radiol., 39, pp. 514–519.

Servomaa, A., Tapiovaara, M., 1998. *Organ dose calculation in medical x-ray examinations by the program PCXMC*. Radiat. Prot. Dosimetry, 80, pp. 213–219.

Smans, K., Struelens, L., Smet, M., Bosmans, H., Vanhavere, F., 2008. *Patient dose in neonatal units*. Radiat. Prot. Dosimetry, 131, pp. 143–147.

Smans, K., Struelens, L., Smet, M., Bosmans, H., Vanhavere, F., 2010. *Cu filtration for dose reduction in neonatal chest imaging*. Radiat. Prot. Dosimetry, 139, pp. 281–286.

Smans, K., Vandenbroucke, D., Pauwels, H., Struelens, L., Vanhavere, F., Bosmans, H., 2010. *Validation of an image simulation technique for two computed radiography systems: an application to neonatal imaging*. Med. Phys., 37, pp. 2092–2100.

Soliman, K., Alenezi, A., 2013. *Patient entrance surface dose measurements using XR-QA2 Gafchromic films during micturating cystourethrography procedures.* Radiat Prot Dosimetry, 158, pp. 170-174.

Tapiovaara, M.J., 2008. *Review of relationships between physical measurements and user evaluation of image quality.* Radiat. Prot. Dosimetry, 129, pp.244–8.

Tingberg, A., Herrmann, C., Lanhede, B., Alm_, A., J.Besjakov, Mattsson, S., Sund, P., Kheddache, S., Månsson, L.G., 2000. *Comparison of two methods for evaluation of the image quality of lumbar spine radiographs*. Radiat. Prot. Dosimetry, 90, pp. 165–168.

Tomic, N., Quintero, C., Whiting, B.R., Aldelaijan, S., Bekerat, H., Liang, L., DeBlois, F., Seuntjens, J., Devic, S., 2014. *Characterization of calibration curves and energy dependence GafChromic$^{TM}$ XR-QA2 model based radiochromic film dosimetry system*. Med. Phys., 41, pp. 062105

Uffmann, M., Schaefer-Prokop, C., 2009. *Digital radiography: The balance between image quality and required radiation dose.* Eur. J. Radiol., 72, pp. 202–208.

UNSCEAR 2013 Report. United Nations Scientific Committee on the Effects of Atomic Radiation (UNSCEAR), 2013. *Sources, effects and risks of ionizing radiation, Volume 2, Scientific Annex B, Effects of radiation exposure of children*, UNSCEAR, New York, viewed 16 April 2014, <http://www.unscear.org/docs/reports/2013/UNSCEAR2013Report_AnnexB_Children_13-87320_Ebook_web.pdf>

Velaphi, S., Rhoda, N., 2012. *Reducing neonatal deaths in South Africa – are we there yet, and what can be done?* SAJCH., 6, pp. 67-71.

Wall B.F., (1996). *How to assess the dose to the patient in diagnostic radiology*. Presented at: The International Congress on Radiation Protection (IRPA), 14-19 April 1996, Vienna, Austria.

Wang, Z., Bovik, A.C., Sheikh, H.R., Simoncelli, E.P., 2004. *Image quality assessment: from error visibility to structural similarity*. IEEE Trans. Image Process., 13, pp. 600–612.

Willis, C.E., 2009. *Optimizing digital radiography of children*. Eur. J. Radiol., 72, pp. 266–273.

Wraith, C.M., Martin, C.J., Stockdale, E.J., McDonald, S., Farquhar, B., 1995. *An investigation into techniques for reducing doses from neo-natal radiographic examinations*. Br. J. Radiol., 68, pp. 1074–1082.

Yaffe, M.J., Rowlands, J.A., 1997. *X-ray detectors for digital radiography*. Phys. Med. Biol., 42, pp. 1-39.

Zaiontz, C. n.d. *Intraclass Correlation Real Statistics Using Excel*, viewed 11 July 2014, <http://www.real-statistics.com/reliability/intraclass-correlation>

# SUMMARY


**Introduction**

Neonates who are ill at birth often require a large number of radiographs during the period of hospitalization. Radiography refers to the imaging of body parts using x-rays and plays an important role in the diagnosis and follow-up of patients suffering from various medical conditions.

X-rays fall into the category of ionizing radiation which has the potential to cause cell damage and therefore are associated with a radiation risk. The radiation risk to these neonates is higher than in adults. Therefore the dose should be kept as low as reasonable achievable (ALARA) while still rendering images that comply with the diagnostic task.

Large variations have been found with respect to the beam parameters used to acquire neonatal anterior posterior (AP) chest x-ray images, emphasizing the need for optimization. Changing the beam parameters will not only influence the radiation dose, but also the image quality. Although physical image quality metrics such as contrast, resolution and noise can be used to quantify image quality these metrics do not give an indication of the diagnostic image requirements. Subjective image evaluation using appropriate phantoms is therefore also required.

**Aim**

The aim of this phantom study was to reduce neonatal radiation dose while maintaining diagnostically adequate image quality for neonatal radiography.

**Methods**

Entrance surface doses (ESD) and exit doses were determined for the beam parameters (55 kV, 2 mAs no additional filtration) used to acquire neonatal AP chest x-rays at Universitas Academic Hospital (UAH). Beam parameter combinations, reducing the ESD by 50 % or more compared to

the current practice, were then selected keeping the dose to the Computed Radiography imaging plate (detector) constant. The effect of using different beam parameters on the image quality was investigated, using a chicken corpse as a phantom to simulate the neonatal chest. The contrast as well as contrast to noise ratios were determined. Ten observers comprising radiographers, radiologists and a medical physicist were then tasked to evaluate the overall subjective image quality using a multiple rank order method.

Based on the image quality ranking the beam parameters delivering acceptable image quality were then used to image five living (sedated) rabbits with a weight of approximately 2000g, simulating the neonatal chest with a heart and lungs. Eight radiology registrars gave their opinion on the diagnostic quality of the images using a five-point scale. These radiologists then evaluated the image quality subjectively using the multiple rank order method with the focus on three anatomical regions namely the lung patterns, the heart borders and the diaphragm.

**Results and Discussion**

The contrast and contrast to noise ratio stayed constant in the range 55 – 66 kV, indicating the influence of post processing on digital images. Large variation in observer opinion of image quality was seen for both the chicken and rabbit phantom images obtained with different beam parameters (different dose values). Even amongst a single observer large variation in their opinion was seen when evaluating images of different rabbits at the same beam parameters.

All the images were regarded as being diagnostically acceptable. This indicates that a lower dose option could be selected without compromising the diagnostic value of the images.

**Conclusion**

The chicken phantom proved to be a good simulation of the neonatal chest; however when one needs to investigate clinical features the rabbit phantom would be recommended. This study shows a possible dose reduction of 64 % when using beam parameters 60 kV, 2.0 mAs and 2 mm Al additional filtration.

**KEYWORDS**

*Neonate*

*Computed radiography*

*Chest x-ray*

*Dose reduction*

*Subjective image quality evaluation*

*kV*

*mAs*

*Additional filtration*

*Chicken phantom*

*Rabbit phantom*

# OPSOMMING

**Inleiding**

Siek neonate benodig ‘n groot aantal x-straal beelde tydens hospitalisasie. X-straal beelde val in die kategorie van ioniserende straling en hou dus ‘n stralingsrisiko in. Hierdie stralingsrisiko is hoër in neonate as in volwassenes. Dit is om hierdie rede belangrik om te verseker dat die laagste moontlike stralings dosis gebruik word.

Die variasie in bundel parameters (kV, mAs en filtrasie) wat gebruik word vir neonatale anterior posterior borskas x-straal beelding dui op die noodsaaklikheid van optimalisering. ‘n Verandering in die bundel parameters beinvloed nie die stralings dosis alleenlik nie, maar ook die beeld kwaliteit.

Alhoewel beeldkwalitiet parameters soos kontras, resolusie en geruis gebruik word om die beeld kwaliteit te kwantifiseer gee die parameters egter nie ‘n aanduiding of die beeld aan die diagnostiese vereistes voldoen nie. Vir hierdie doel is subjektiewe evaluasie van beeldkwaliteit met gebruik van die geskikte fantome genoodsaak.

**Doel**

Die doel van die fantoom studie was om die neonatale stralings dosis te verminder sonder om die diagnostiese beeldkwaliteit te verlaag.

**Metodes**

Die ingangsdosis en uitgangsdosis was bepaal vir die bundel parameters (55 kV, 2 mAs en geen addisionele filtrasie) huidiglik in gebruik by die Universitas Akademiese Hospitaal (UAH).

Bundel parameter kombinasies wat die ingangs dosis met 50 % of meer verminder het, terwyl die detektor dosis konstant gehou is, is gebruik. ‘n Hoender fantoom is gebruik om die neonatale borskas te simuleer in ‘n poging om die effek van die gekose bundel parameters op die beeldkwalitiet te ondersoek.

Die kontras en kontras-tot-geruis vehoudings is bepaal. Tien waarnemers wat radiograwe, radioloë en ‘n mediese fisikus insluit, het die beelde geëvalueer op grond van algemene beeldkwaliteit mbv. ‘n veelvuldige rangorde metode.

Die bundel parameters wat aanvaarbare beeldkwaliteit gelewer het, is gebruik om x-straal beelde van vyf lewendige (gesedeerde) konyne, met ‘n massa van ongeveer 2000g, te verkry. Die konyne is gebruik om die neonatale borskas met ‘n hart en longe te simuleer.

Agt radiologie kliniese assistente het die konyn beelde geëvalueer m.b.v. ‘n vyf-punt skaal. Die beeldkwaliteit is ook subjektief geëvalueer mbv. die veelvuldige rangorde metode met die fokus op drie anatomiese dele naamlik die long patrone, hart rande en diafragmas.

**Resultate en Bespreking**

Die kontras en kontras-tot-geruis verhoudings het konstant gebly in die reeks 55 – 66 kV. Dit gee ‘n aanduiding van die invloed wat “post” verwerking op die digitale beeld het. Groot variasies in waarnemer opinie van beeldkwaliteit is waargeneem, in beide die hoender en konyn fantoom beelde, met die gebruik van verskillende beeld parameters. Die verskille was selfs waargeneem vir ‘n enkele waarnemer tydens die evaluasie van die vyf konyn beelde by ‘n bundel parameter kombinasie.

Al die beelde was van aanvaarbare diagnostiese kwaliteit wat aandui dat ‘n bundel parameter kombinasie met ‘n laer stralings dosis gebruik kan word.

**Gevolgtrekking**

Die hoender fantoom het die neonatale borskas goed verteenwoordig. Die konyn fantoom word egter aanbeveel wanneer gedetaileerde kliniese strukture evalueer moet word. Die studie bewys dat ‘n dosis vermindering van 64 % moontlik is met die gebruik van bundel parameters 60 kV, 2.0 mAs en 2 mm Al addissionele filtrasie.

**SLEUTELWOORDE**

*Neonate*

*Digitale radiografie*

*Borskas x-straal beeld*

*Stralings dosis vermindering*

*Subjektiewe beeldkwaliteit evalueering*

*kV*

*mAs*

*Addisionele filtrasie*

*Hoender fantoom*

*Konyn fantoom*